5-2007

The Differential Effects of Two Critical Osteoclastogenesis Stimulating Factors on Bone Biomechanics

Yuyu Yuan
Clemson University, yyuan@clemson.edu

THE DIFFERENTIAL EFFECTS OF TWO CRITICAL OSTEOCLASTOGENESIS STIMULATING FACTORS ON BONE BIOMECHANICS

A Dissertation
Presented to
the Graduate School of
Clemson University

In Partial Fulfillment
of the Requirements for the Degree
Doctor of Philosophy
Bioengineering

---

by
Yuyu Yuan
May 2007

Accepted by:
Dr. Ted Bateman, Committee Chair
Dr. Karen Burg
Dr. Sarah Harcum
Dr. Dan Simionescu
Dr. Naren Vyavahare

ABSTRACT

Many skeletal diseases, such as osteoporosis and malignant bone metastases, are generally osteolytic and associated with increased bone resorption and decreased bone strength. Within a complex cytokine environment, the proteins RANKL and M-CSF are critical for osteoclast differentiation and activation, and thus fundamental effectors of osteolytic disorders. Previous studies showed that M-CSF stimulates the proliferation and early differentiation of osteoclast progenitors to osteoclast lineage, while RANKL targets the later stages of fusion and activation, and stimulates the formation of functional active osteoclasts. However, impacts of artificially elevated levels of these proteins on the skeleton system have not been fully characterized.

In this project, we amplified the circulating levels of RANKL and M-CSF by injections or continuous administrations and examined the effects on bone volume and quality. We hypothesized that while M-CSF and RANKL can both stimulate osteoclastogenesis, the differences in activation stages targeted by these two cytokines would result in distinct responses on bone biomechanics. RANKL would directly stimulate osteoclast activity and increase bone resorption, while M-CSF would act anabolically through coupling between osteoblast development and the promoted osteoclastogenesis at the early stage, and promote bone formation indirectly.

Data obtained in this project demonstrated that *in vivo* administration of RANKL and M-CSF induced general opposing effects on bone volume, architecture, mineralization and strength. RANKL directly stimulated bone resorption and reduceed bone biomechanical properties. The destructive skeleton induced by RANKL could serve

as a novel animal model that exhibits a series of skeletal complications similar to those observed in osteolytic skeletal diseases, such as osteoporosis. Alternately, administrations of M-CSF markedly stimulated trabecular bone formation and had less of an influence on cortical bone. These changes demonstrated the potential of M-CSF as an anabolic agent for osteoporosis.

This project has further examined the *in vivo* characteristics and functional effects of RANKL and M-CSF on the skeleton system. Findings in this project, such as the creation of RANKL induced bone loss model and characterization of the anabolic potential of M-CSF on the skeleton, could provide useful information and tools for further explorations on human skeletal diseases.

DEDICATION

This work is dedicated to my wife and my parents. I like to express my most sincere appreciations for their love and support through the course of my studies. This dissertation would not have been possible without their help and encouragement.

ACKNOWLEDGMENTS

First, I would like to thank my advisor Dr. Ted Bateman for his guidance, support, and encouragement throughout the course of my Ph. D study. Especially, I thank him for giving me the opportunity to conduct research in this exciting field and to collaborate with the world's most famous biotech companies such as Amgen and Chiron, governmental agencies like National Aeronautics and Space Administration (NASA) and other national laboratories. Being a part of a new research group and starting a new research area, Dr. Bateman has provided me with crucial lessons and experience from the very beginning, which will be beneficial to me for my future careers.

I would also like to thank all of my advisory committee members, Dr. Karen Burg, Dr. Sarah Harcum, Dr. Jiro Nagatomi, Dr. Dan Simionescu and Dr. Naren Vyavahare for their great support and invaluable advice in my research.

I am grateful to all the current and past members of the Osteoporosis Biomechanics Laboratory for their suggestions and assistance in my research. I really enjoyed their friendship and kindness, which have been my great wealth during the period of my graduate education.

I am also indebted to the faculty members, staff and fellow students in the Department of Bioengineering, for their various help during my study at Clemson University.

In addition, I would also like to thank Godley Snell Research Center for their help in my animal studies. I enjoyed very much the time working with them in the animal center.

Finally, I would like to acknowledge the funding support from National Space Biomedical Research Institute through NASA NCC 9-58, Amgen Inc., Chiron Inc., and BioServe Space Technologies (through NASA NCC8-242).

TABLE OF CONTENTS

Table of Contents (Continued)

Page

Table of Contents (Continued)

Table of Contents (Continued)

LIST OF TABLES

LIST OF FIGURES

List of Figures (Continued)

List of Figures (Continued)

CHAPTER 1

INTRODUCTION

1.1 General Bone Biology

1.1.1 Component and Function

Bone is a specialized connective tissue composed of cells and extracellular matrix. Bone matrix is formed by collagen fibers (type I, 90% of the total protein), noncollagenous proteins, and inorganic minerals. Collagen fibers are oriented in specific directions and contribute to the flexibility and the great tensile strength of bone (Viguet-Carrin, Garnero et al. 2006). Mineral crystals (primarily hydroxyapatite, accounting for 65% of bone mass) surround and attach to the collagen fibers using the noncollagenous proteins, allowing bone to resist compression with its exceptional hardness (Buckwalter and Cooper 1987).

Two primary types of bones make up the skeletal system (Figure 1.1). Cortical bone is the hard, outer shell that comprises 80% of the skeletal system (by mass). It exhibits advanced mineralization and has a slow turnover rate. Mature cortical bone consists of small units called osteons, which are organized in concentric layers of bone that surround a vascular channel. The other type of bone is trabecular bone (also known as cancellous or spongy bone). Trabecular bone is a network of small, connected struts that is weaker than cortical bone and located at the epiphyses of long bones and throughout the interior of short bones. Cancellous bone has a much higher turnover rate than cortical bone; therefore it is typically less mineralized (Heaney 2003).

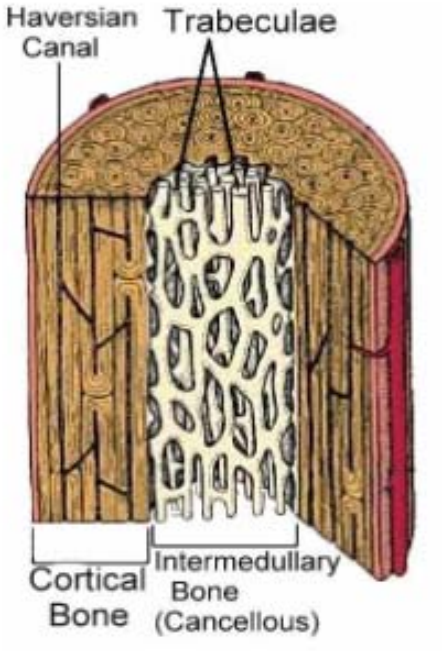

Figure 1.1 Diagram showing basic bone structure (http://www.abdn.ac.uk/orthopaedics)

Bone, together with cartilage, makes up the skeletal system and provides several essential functions to life. First, bones connect to each other by ligaments and provide both the framework of the body and mechanical support for movement (Kell, Bell et al. 2001). Skeletal muscles attach to bones via tendons, and use bones as levers to move the body. Second, bones provide protection for the vital organs. For instance, the central nervous system is protected by the skull, and ribs protect the cardiovascular organs. The third function of bone is to serve as a reservoir for vital minerals (primarily calcium and phosphate). Calcium is an essential element that maintains and regulates a number of physiological activities; approximately 99% of the body's calcium is stored in the skeleton in the form of hydroxyapatite and can be released into the blood stream for distribution to body parts when needed (Specker 1996). Finally, the marrow cavities in

certain bones (i.e. long bones) provide the microenvironment for blood cell formation (hematopoiesis).

1.1.2 Bone Remodeling

Bone is a dynamic tissue. In a mature skeleton, bone is continuously being broken down (bone resorption) and reformed (bone formation), allowing for the maintenance of bone tissue. This coordinated process is called bone remodeling. Bone remodeling is directed by the actions of the two major bone cells: osteoclasts (cells responsible for bone resorption) and osteoblasts (cells responsible for bone formation) (Parfitt 1984). The sequence of bone remodeling is always with resorption occurring first via active osteoclasts, followed by formation to form new bone tissue and resolve the defect (Ljunggren, Ljunghall et al. 1995).

1.1.2.1 Bone Resorption by Osteoclasts

Osteoclasts are giant multinucleated cells that differentiate from hematopoietic precursors of the monocyte/macrophage lineage (Udagawa, Takahashi et al. 1990). They are typically located in contact with a calcified bone surface or within a lacuna (Howship's lacunae), usually with one or two in each resorption site (Vaananen, Hentunen et al. 1988). A most important feature of osteoclasts is the ruffled borders formed by deep foldings of plasma membranes in the area facing bone matrix (Figure 1.2): The ruffled border is centrally located and surrounded by a ring of actin that serves to attach the cell to the bone surface, thus sealing off the bone resorbing compartment (Vaananen, Zhao et al. 2000).

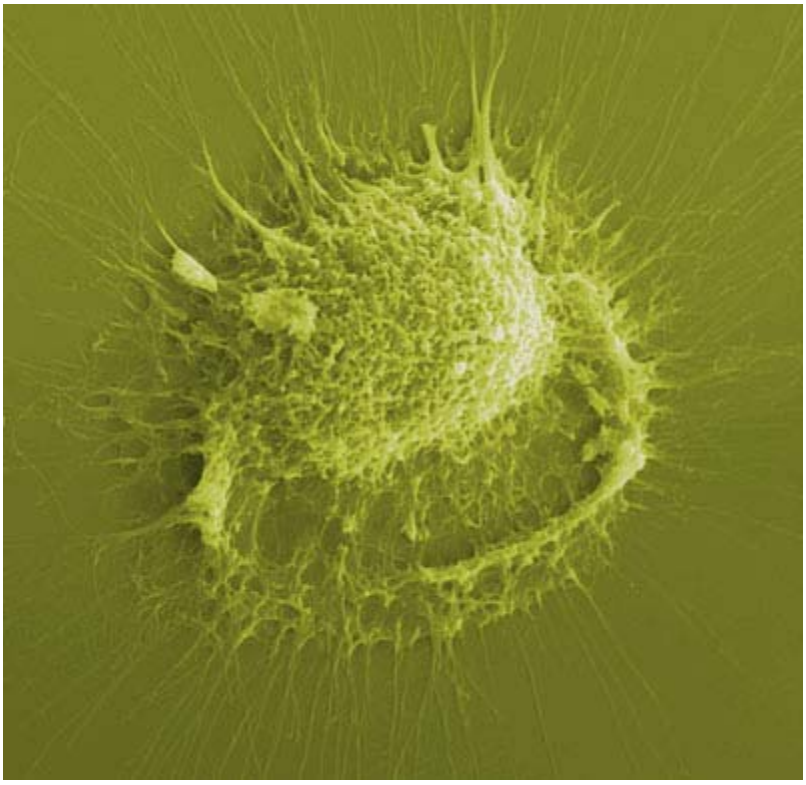

Figure 1.2 Scanning electron micrograph showing an active osteoclast (Bone Research Society, www. brsoc.org.uk)

When bone matrix is undergoing bone resorption by osteoclasts, lysosomal enzymes (Tartrate Resistant Acid Phosphatase, cathepsin K, etc.) are secreted into the extracellular bone resorbing compartment through the ruffled border (Zaidi, Pazianas et al. 1993). Since this compartment is sealed from the surrounding marrow cavity, enzymes are able to reach a high concentration. Accompanied with the lysosomal enzymes, protons are secreted by osteoclasts using proton pumps and across the ruffled border, thus causing an increase in the acidity of the extracellular compartment (Vaananen, Zhao et al. 2000). Therefore, the extracellular bone resorbing compartment is functionally equivalent to a lysosome with low pH, high concentration lysosomal enzymes, and the substrate (bone matrix, figure 1.3). Resorption starts with the hydroxyapatite crystals being

mobilized by digestion of their links (the non-collagenous proteins) with collagen and dissolved by the acid environment. Then, the residual collagen fibers are digested either by the activation of collagenase or by the action of cathepsins at low pH. Residues from this extracellular digestion are internalized, transported through the cell and released at the basolateral domain, or released during the periods of relapse of the sealing zone (Lerner 2000).

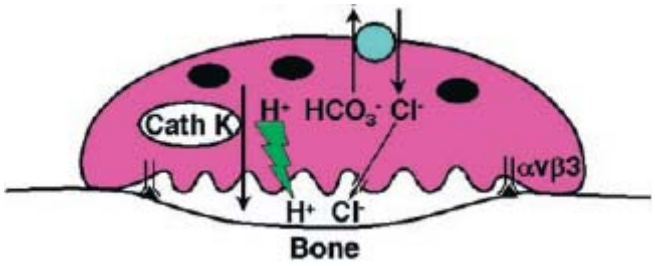

Figure 1.3 Picture illustrating osteoclastic bone resorption. The differentiated osteoclast polarizes on the bone surface, which involves matrix-derived signals transmitted by the αvβ3 integrin. After formation of the ruffled membrane, the osteoclast acidifies an extracellular microenvironment by means of an electrogenic proton pump. Intracellular pH is maintained by HCO_3^-/Cl^- exchange at the cell's antiresorptive surface. Cl^- ions pass through a ruffled membrane-residing anion channel into the resorptive microenvironment, which achieves a pH approximating 4.5. The acidic milieu mobilizes the mineral phase of bone and provides an optimal environment for organic matrix degradation by cathepsin K (Teitelbaum 2000).

1.1.2.2 Bone Formation by Osteoblasts

Osteoblasts are bone lining cells that are responsible for the production of bone matrix (collagens and ground substance). Osteoblasts originate from bone marrow stromal stem cells and connective tissue mesenchymal stem cells; under the regulation of a series of growth factors and cytokines, osteoblast progenitors proliferate and differentiate into preosteoblasts and then mature osteoblasts (Lian and Stein 1995). On bone surfaces, osteoblasts connect to each other via adhering junctions and enable intercellular communications; they function in clusters of around 100-400 cells along

each bone forming site (Stains and Civitelli 2005). When they receive signals from bone matrix, osteoblasts lay down osteoid (new bone matrix before it is mineralized) into bone resorption sites. In humans, the osteoid exists for approximately 10 days before mineralization is initiated, and the mineralized bone matrix is formed (Anderson 1989). Osteocytes are osteoblasts and bone-lining cells that were trapped within the matrix during the mineralization of bone. They are in direct communication with each other and with surface osteoblasts through their cellular processes. These intercellular communications have been indicated to play an important role in both the mineralization of bone and the detection and response to mechanical forces within bone matrix (Rodan 1992).

1.1.2.3 Bone Remodeling Process

The process of bone remodeling can be divided into five stages (Parfitt 1984): quiescence, activation, resorption, reversal, formation and then back to quiescence (Figure 1.4). Quiescence refers to the resting state of bone surface. In this stage, the bone surface is surrounded by elongated osteoblasts called bone lining cells (LC, Figure 1.4). When bone remodeling is initiated, bone lining cells retract from the activated bone surface and the exposed mineralized surface attracts circulating preosteoclasts (POC, Figure 1.4) to aggregate, then fuse into multinucleated osteoclasts (activation phase). Afterwards, osteoclasts (OC, Figure 1.4) become activated and start to resorb the mineralized bone matrix during the resorption stage. In the reversal phase, cellular activities on the resorbed bone surface switch from resorption by osteoclasts to recruitment of osteoblasts. Osteoblasts aggregate on the bone resorption sites and then start to deposit new bone matrix (formation phase).

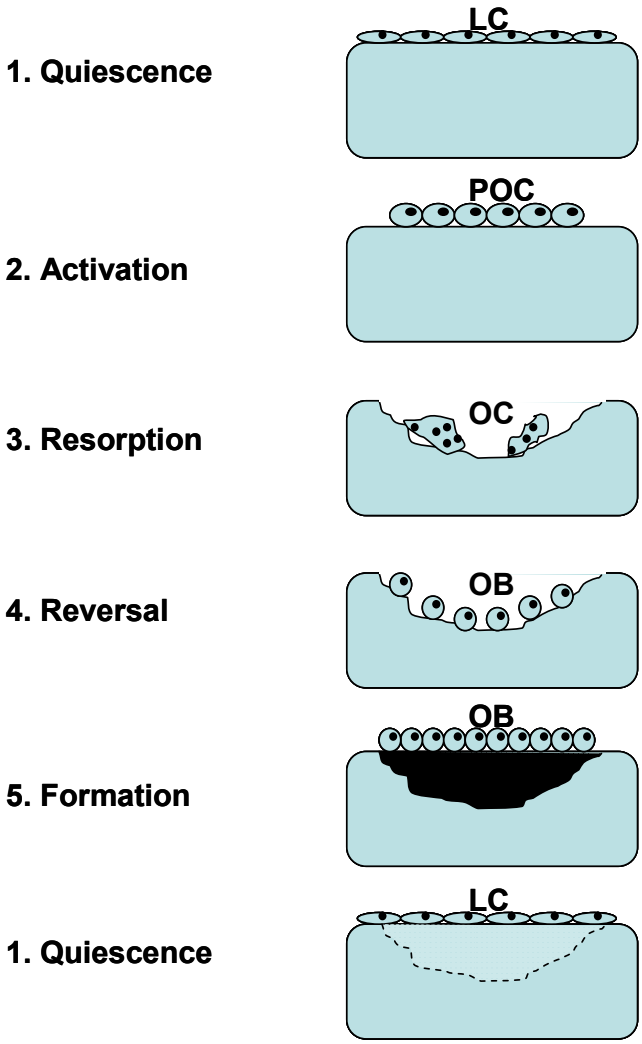

Figure 1.4 Bone remodeling phases. LC refers to bone lining cells (elongated osteoblasts), POC refers to preosteoclasts, OC refers to osteoclasts, and OB refers to osteoblasts.

Bone remodeling is the result of interactions among multiple elements, including osteoblasts, osteoclasts, hormones, growth factors, and cytokines (Mundy 1993). In a healthy skeleton, activities of bone resorption and formation are coupled, meaning that bone formation always occurs following the previous bone resorption, as the bone remodeling process describes. The phenomena is largely related to the signals initiated during bone matrix resorption and then transferred to osteoblasts and pre-osteoblasts via

local regulatory network (Howard, Bottemiller et al. 1981; Locklin, Khosla et al. 2003). Accordingly, a series of factors which can promote or inhibit osteoclastic bone resorption result in similar stimulation or inhibition of osteoblast activation and bone formation (Manolagas and Jilka 1995). Under normal conditions bone remodeling is a balanced process that allows a renewal of 5-10% of bone volume each year (Fernandez-Tresguerres-Hernandez-Gil, Alobera-Gracia et al. 2006). However, this balanced network can be disrupted in some pathological conditions, leading to the onset of skeletal diseases, including osteoporosis, osteopetrosis, Paget's disease, and bone malignant metastasis (Manolagas and Jilka 1995; Blair, Zhou et al. 2006).

1.1.3 Bone Biomechanics

As described at the beginning of this chapter, bone serves four major functions, the first two relate to bone's biomechanical role in the body. First, bones serve as levers against muscle contractions and support body movement; second, bones shield vital organs from trauma. Bone fragility, or bone strength, is used to indicate the biomechanical status of bone, representing bone's susceptibility to fracture (Turner 2002). Bone strength has many determinants, including the intrinsic properties of bone tissue (bone material properties), bone mass (also referred as bone volume in preclinical studies), and bone structural properties, such as bone size, cortical thickness, porosity, and architecture (Turner 2002; Ammann and Rizzoli 2003; Burr 2004). Clinically, bone strength is generally estimated by bone mineral density (BMD) using dual-energy X-ray absorptiometry (DXA). DXA measures the amount of minerals (calcium) present in bone and compares with normal data from specific age and race to predict fracture risk; it is the most commonly used tool to clinically diagnose osteoporosis. However, as BMD itself

only accounts for 60-70% of bone strength, many important factors cannot be captured by DXA (Friedman 2006; Turner 2006). For instance, the fracture risk in a 75-year-old woman is 4-7 times as that in a 45-year-old woman with identical BMD (Hui, Slemenda et al. 1988). These important bone strength determinants, other than BMD, can be broadly defined as bone quality (Burr 2004). Bone quality is mainly comprised of the material properties of bone tissue and bone structural properties, and is also largely influenced by bone turnover rates.

1.1.3.1 Material Properties of Bone

Bone tissue is a composite material composed mostly of type I collagen and minerals. Type I collagen has little influence on the stiffness of bone, particularly in compression, but has a profound effect on its toughness (Burr 2002; Wang, Shen et al. 2002). Regulated by the nature of applied stress on bone, collagen fibers grow in preferential orientations (Martin and Ishida 1989) and contribute to the tensile strength of bone (Riggs, Vaughan et al. 1993; Takano, Turner et al. 1999). Collagen fibers can also enhance bone's toughness by increasing the amount of cross-linking (Zioupos, Currey et al. 1999). Studies have shown that the decreased extent of collagen fiber crosslinking with aging reduces bone's energy to failure, leading to increased fracture risk (Zioupos, Currey et al. 1999). On the other hand, minerals contribute largely to bone's stiffness and resistance to compressive force due to its hardness. Most bone minerals exist in the form of hydroxyapatite crystals: $Ca_{10}(PO_4)_6(OH)_2$. These calcium phosphate crystals have spindle- or plate-like shapes and connect to collagen fibers via the non-collagenous proteins (anionic complexes with high ion-binding capacities).

In healthy bones, minerals and collagen fibers maintain a ratio that lead to biomechanical properties sufficient to withstand normal loading of bone, but this ratio varies in other conditions, leading to increased fracture risk (Currey, Brear et al. 1996). For instance, bones from osteopetrotic patients (bone minerals over-accumulate, hypermineralization) are very stiff, but also very brittle and result in reduced energy to failure. In contrast, patients with osteomalacia have high turnover, less mineralized bone (hypomineralization), which are ductile and can undergo large deformation without breaking but are poorly mineralized and weak. Both hypo- and hypermineralization reduce bone mechanical properties (Currey 1975; Currey, Brear et al. 1996).

1.1.3.2 Structural Properties of Bone

The structural properties of bone depend on mass distribution throughout the structure. From the macroscopic perspective, bone size is an important component. With the same cross-sectional area, bones with a larger diameter are stronger in resisting bending stress than smaller bones with thicker cortical walls. Distribution of bone materials further from the neutral axis of bone contributes to a higher polar moment of inertia (pMOI, which is used to predict object's ability to resist torsion, and also widely used in bone engineering to predict cortical geometry and the ability to resist bending load).

Besides bone size, intrinsic bone geometry also determines bone structural properties and strength. Trabecular bone geometry is an important component of bone structural properties. Trabecular bones exist at the ends of long bones and throughout the inside of short bones. The small plate-like structures (individual trabeculae) of trabecular bone are connected to each other to appropriately distribute forces throughout the shaft.

In osteoporotic conditions, loss of trabecular connectivity decreases the capability of the trabecular meshwork to effectively distribute forces. Without a great change in bone mineral density, bone strength can be largely decreased due to the loss of connectivity between trabeculae struts. This can be demonstrated by antiresorptive therapies on osteoporosis patients: One-year treatment of bisphosphonates (a category of antiresorptive treatment) decreased fracture risk by 50-60% with only 5% increase in bone mineral density (Burr 2004).

Besides trabecular geometry, cortical bone geometry also contributes to the structural properties of bone. Bone geometry change induced by anabolic treatments of osteoporosis is a common example. Parathyroid hormone (Teriparatide, PTH I-34) stimulates new bone formation at the periosteal (outside) surface and lowers fracture risk in osteoporotic patients. At the same time, PTH also induces an increase in cortical porosity and partly counteracts the positive effects on bone strength (Burr, Hirano et al. 2001). It is the deposition of bone at the periosteal surface, having a greater contribution to torsional and bending moments of inertia, that more than compensates for this greater porosity

1.1.3.3 Influence of Turnover on Bone Biomechanics

Bone turnover, which represents the rate bone is remodeled, is an important determinant of bone quality (Heaney 2003). Normal bone turnover rates in healthy individuals ensure the balance between old bone removal and new bone formation. Variations in bone turnover interrupt bone remodeling balance and result in direct changes in bone material and structural properties, as seen in aged people or patients with

skeletal disease (Parfitt 2002). High or low bone turnover rate cause different changes in bone material and structural properties, but both compromise bone biomechanics.

An abnormally high bone turnover results in increased bone resorption rates, decreased bone mass, decreased bone mineralization, and decreased bone strength (Heaney 2003). An extreme example with pathologically high bone turnover rates is Paget's disease. Symptoms of Paget's disease include the presence of large, woven, less mineralized bone and skeletal abnormity, bones are ductile and weak (Raisz 1999; Siris 1999; Whyte 2006). As described above, PTH as an anabolic agent increases overall bone remodeling speed (turnover rate), resulting in increased cortical porosity (Turner 2002; Burr 2005).

In contrast, an unusually low turnover rate leads to microdamage accumulation and hypermineralization of bone matrix, resulting in brittle bone and increased risk of fracture. Osteopetrosis is an extreme example of low bone turnover induced by defects in osteoclast formation and function. In the skeletons of osteopetrosis patients, defects in bone resorption induce accumulation of microdamage; bones are thick and dense but brittle and abnormal (Tolar, Teitelbaum et al. 2004). Decreased bone turnover is usually associated with antiresorptive therapy of osteoporosis (i.e. bisphosphonates). Bisphosphonates stimulate osteoclast apoptosis, inhibit osteoclastic bone resorption, and decrease bone turnover. However, bisphosphonates also compromise the removal of microdamaged bone and enable the accumulation of microfractures, thus degrade bone quality. Potential long-term negative effects induced by bisphosphonates have attracted much debate and concern recently; details will be discussed later in this chapter (Sibilia

and Netti 1996; Rodan, Reszka et al. 2004; Iwamoto, Takeda et al. 2006; Liberman 2006).

1.2 Osteoclastogenesis

Osteoclasts are multinucleated giant cells responsible for bone resorption. They maintain bone homeostasis by resorbing the old, damaged bones and initiate bone remodeling. Among the various skeletal diseases known to occur in humans, the majority of them are triggered by abnormalities in osteoclast development or function. These osteoclast abnormalities can be divided into two distinct situations. First, the loss of function in osteoclasts, due to problems in differentiation or abnormal apoptosis, leads to osteopetrosis with little or no osteoclasts activity and a dense but brittle skeleton (Marks 1987; Tolar, Teitelbaum et al. 2004). On the other hand, excessive number and activity of osteoclasts initiate osteolytic bone diseases, including osteoporosis, rheumatoid arthritis and malignant bone metastases, resulting in bone loss, deterioration in architecture, and decrease bone biomechanical properties (Teitelbaum 1996; Boyce, Xing et al. 2003). Osteolytic bone diseases are most common (Rodan and Martin 2000), and are induced by excessive level of osteoclastogenesis due to abnormalities in regulation signals that are released into the bone microenvironment. Osteoclastogenesis regulation is a complicated process, with many cells, hormones, and cytokines involved; exact mechanisms in various situations are still unclear. Therefore, to better understand the skeletal diseases, it is important to understand the osteoclastogenesis pathway and its regulation system.

1.2.1 Origin of Osteoclasts

In the 1980s, significant debate and confusion existed on the origin of osteoclasts. The classic concept was that osteoclasts originated from connective tissue cells, while others hypothesized that it originated from mature hematopoietic cells, particularly from monocyte or macrophage cells (Hanaoka, Yabe et al. 1989). In 1990, researchers using an *in vitro* cell coculture system demonstrated that macrophages could differentiate into osteoclasts with the presence of bone marrow stromal cells and their osteoblast progenitors (Udagawa, Takahashi et al. 1990). This proved for the first time the concept that osteoclasts are derived from haematopoietic stem cells of the monocyte/macrophage lineage in the bone marrow.

Hematopoietic stem cell precursors first undergo a phase of determination to acquire the potential of becoming either osteoclasts or macrophages. After proliferation, committed precursors differentiate to become either cell type. Studies have shown that the transcription factor PU.1 is critical for the initial commitment or determination phase: Its deletion results in osteopetrosis without either osteoclasts or macrophages (Tondravi, McKercher et al. 1997).

1.2.2 Regulation of Osteoclastogenesis

Under a series of regulations, hematopoietic stem cells experience several processes, including proliferation, differentiation, fusion, and activation, and become functional active osteoclasts (Figure 1.5). The active osteoclasts eventually have the capability to resorb bone. Breakthroughs have occurred in this field during the past decade and have increased people's understanding in osteoclast biology. It is now clear that cells required for *in vitro* osteoclast culture, osteoblasts and stromal cells, express

two essential molecules that are necessary and sufficient to promote osteoclastogenesis: macrophage colony-stimulating factor (M-CSF) and receptor activator of nuclear kappa B (RANK) ligand (RANKL) (Teitelbaum 2000). *In vitro* osteoclast development could be achieved by pure macrophages exposed to M-CSF and RANKL (Lacey, Timms et al. 1998), indicating the indispensable role of osteoblasts/stromal cells in osteoclastogenesis through the release of these two cytokines. Different numbers and activities of osteoclasts can be modulated by varying the concentrations and ratio of these two proteins in the culture media (Lacey, Tan et al. 2000).

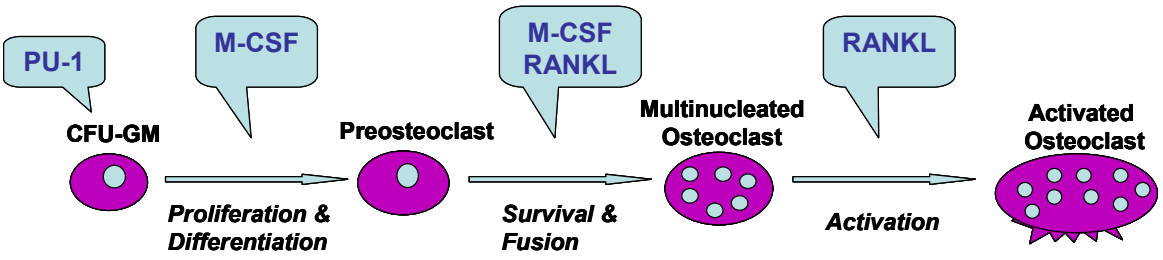

Figure 1.5 Osteoclastogenesis regulation. The transcription factor PU.1 is critical for the initial commitment or determination phase. M-CSF is necessary for proliferation and differentiation, as well as the survival of osteoclast progenitors. RANKL is the key regulator for the latter stages, primarily the fusion of preosteoclasts and the final activation phase.

M-CSF is a cytokine expressed by osteoblasts and stromal cells. It binds to its receptor *c-fms* on early osteoclast precursors, thus stimulating early stage osteoclastogenesis, particularly proliferation and differentiation (Kodama, Nose et al. 1991; Corboz, Cecchini et al. 1992; Felix, Halasy-Nagy et al. 1996). The important role of M-CSF in osteoclastogenesis has been confirmed *in vivo* using M-CSF-deficient osteopetrotic (*op/op*) mice: Mice with a specific knock-out of the M-CSF gene developed profound osteopetrotic phenotype with little or no osteoclast activity (Wiktor-Jedrzejczak, Bartocci et al. 1990; Yoshida, Hayashi et al. 1990). Subsequent studies

showed that systemic administration of recombinant human M-CSF to *op/op* mice increased the number of osteoclasts and led to partial or complete resolution of the osteopetrotic defect (Kodama, Yamasaki et al. 1991; Sundquist, Jackson et al. 1995; Abboud, Woodruff et al. 2002). However, no evidence was found that indicate M-CSF plays a role in the activation phase of osteoclastogenesis. In contrast, a few studies indicated that high concentration of M-CSF could potentially inhibit osteoclast activity by inhibiting osteoclast activation (Perkins and Kling 1995; Abboud, Ghosh-Choudhury et al. 2003). Detailed mechanisms of M-CSF will be discussed later in this chapter.

RANKL was discovered in 1998 and has been proven to be an important mediator for osteoclastogenesis, which stimulates the latter stages of osteoclastogenesis: fusion, survival, and activation (Figure 1.5). RANKL binds to its receptor RANK on the surface of osteoclasts and their precursors, stimulates the activation of pre-osteoclasts to functionally mature osteoclasts, and induces bone resorption (Lacey, Timms et al. 1998; Yasuda, Shima et al. 1998). Osteoprotegerin (OPG) is the decoy receptor for RANKL. It competes with RANK for the binding of RANKL, therefore decreasing RANKL-RANK interaction and inhibiting bone resorption (Simonet, Lacey et al. 1997; Tsuda, Goto et al. 1997). Transgenic mice over-expressing RANKL, and OPG-knockout mice ($OPG^{-/-}$) developed severe osteoporosis symptoms including increased osteoclast numbers and activities, low bone-mineral density, and high bone turnover (Kostenuik and Shalhoub 2001; Mizuno, Kanno et al. 2002). Detailed mechanisms of RANKL/OPG and their roles in osteoclastogenesis will be discussed in the next section.

M-CSF and RANKL do not function alone to regulate osteoclastogenesis. Certain hormones and cytokines produced in distant organs can also influence osteoclastogenesis

(Figure 1.6). It has been shown that pro-resorptive factors, including tumor necrosis factor α (TNF-α), interleukin 1β (IL-1β), interleukin 6 (IL-6), $1,25(OH)_2$ vitamin D_3, prostaglandin E2 (PGE2), parathyroid hormone (PTH), and PTH-related peptide (PHTrP), can upregulate RANKL expression by osteoblasts, consequently stimulating osteoclastogenesis and inducing bone resorption (Udagawa, Takahashi et al. 2000; Schoppet, Preissner et al. 2002). On the other hand, antiresorptive factors can inhibit osteoclastogenesis by decreasing RANKL expression or increasing OPG release. This category of factors includes calcitonin, oetrogens, transforming growth factor β (TGF-β), TPO, IL-17, interferon γ (INF-γ), and Platelet-derived growth factor (PDGF) (Nakashima, Kobayashi et al. 2000; Boyle, Simonet et al. 2003).

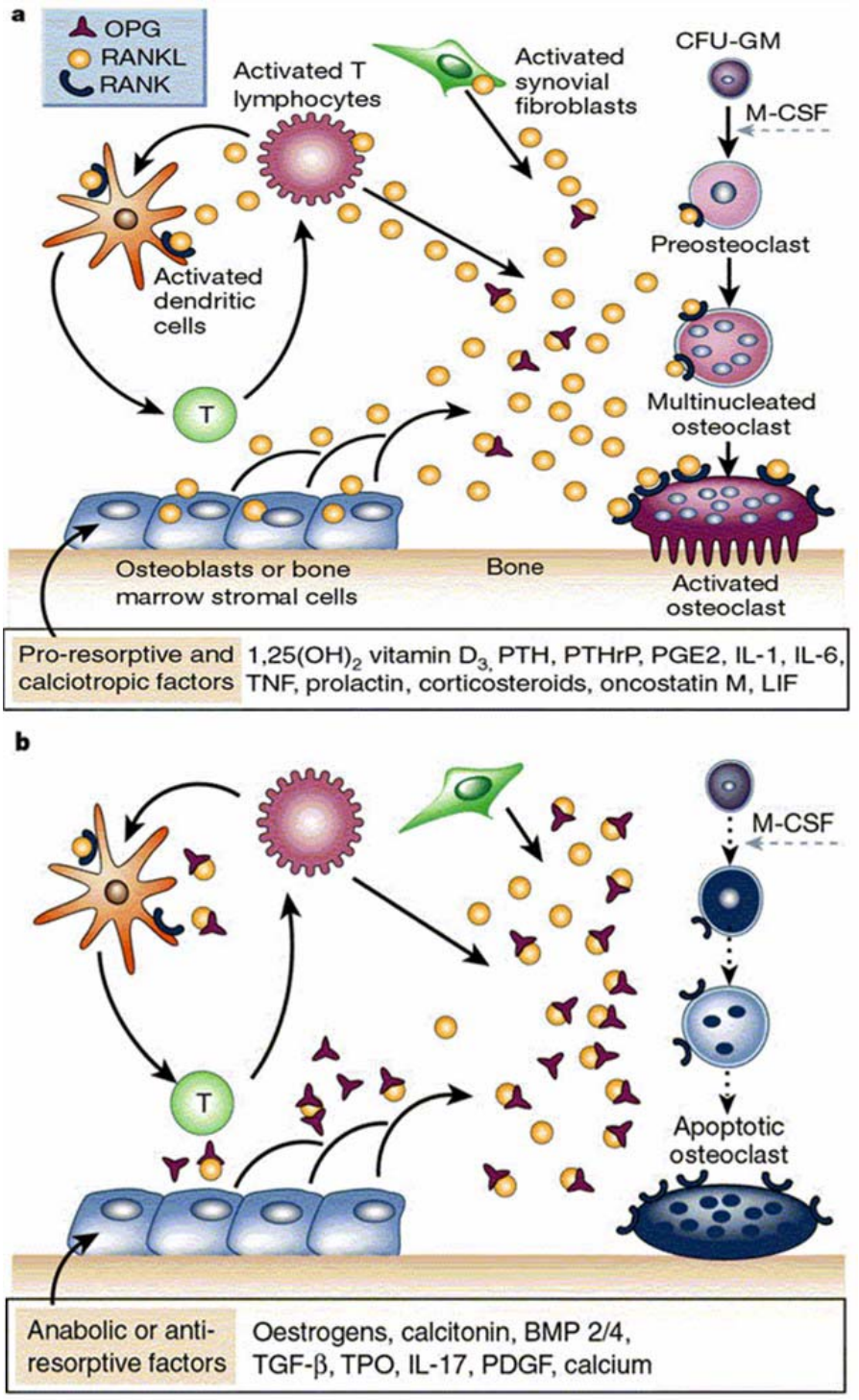

Figure 1.6 Hormonal regulations systems on osteoclastogenesis (Boyle, Simonet et al. 2003). PTH: Parathyroid hormone; PTHrP: PTH related peptide; PGE2: Prostaglandin E2; IL: Interleukin; TNF: Tumor necrosis factor; LIF: Leukemia inhibitory factor; BMP: Bone morphogenetic protein; TGF-β: Transforming growth factor β; TPO: Thrombopoietin; PDGF: Platelet-derived growth factor.

1.3 RANK/RANKL/OPG System

Over the past two decades, the largest breakthroughs in bone biology have been triggered by the identification and characterization of the RANK/RANKL/OPG system (Simonet, Lacey et al. 1997; Tsuda, Goto et al. 1997; Lacey, Timms et al. 1998; Yasuda, Shima et al. 1998).

As first noted in 1990, preosteoblasts and stromal cells regulate osteoclast differentiation both by producing soluble factors and signaling to osteoclast progenitors through cell-cell interaction (Udagawa, Takahashi et al. 1990; Suda, Takahashi et al. 1992). However, the critical factor produced by these cells mediating osteoclastogenesis remained unknown for the next several years; bone biologists performed searches trying to identify this mediator, and finally in 1997 and 1998, the identification of RANK/RANKL/OPG system as the critical and final mediator of osteoclastogenesis ended this obscurity (Simonet, Lacey et al. 1997; Tsuda, Goto et al. 1997; Lacey, Timms et al. 1998; Yasuda, Shima et al. 1998). Osteoprotegerin (OPG) was first identified as a TNF superfamily soluble member that inhibits osteoclastogenesis (Simonet, Lacey et al. 1997). Overexpression of OPG in the livers of transgenic mice resulted in osteopetrosis (Simonet, Lacey et al. 1997); in contrast, disruption of the OPG gene ($OPG^{-/-}$ mice) produced a high bone turnover osteoporotic phenotype (Bucay, Sarosi et al. 1998). Subsequently, RANKL was identified to be the molecule, present in both membrane-bound and soluble forms, that was blocked by OPG and functions as the key mediator of osteoclastogenesis (Lacey, Timms et al. 1998; Yasuda, Shima et al. 1998). These seminal papers have initiated numerous studies on the RANK/RANKL/OPG system.

1.3.1 Osteoprotegerin

OPG is a glycoprotein secreted by osteoblasts and stromal cells in the bone microenvironment and binds to RANKL as a decoy receptor inhibiting osteoclastogenesis. OPG was discovered in 1997 by two groups in two different ways (Simonet, Lacey et al. 1997; Tsuda, Goto et al. 1997). In a project focused on identifying TNF receptor-related molecules that potentially have therapeutic utility, the Amgen Inc. group found a particular cDNA in the rat intestine. Overexpression of this gene in a mouse resulted in an osteopetrotic phenotype accompanied by a profound decrease in osteoclasts (Simonet, Lacey et al. 1997). Later studies found that transgenic mice with OPG gene knockout showed less bone mineral density and other severe osteoporosis symptoms (Mizuno, Amizuka et al. 1998) (Figure 1.7). This study first discovered OPG and indicated that it plays an important role in osteoclastogenesis. A month later, the Snow Brand Milk Group in Japan reported a novel cytokine from the conditioned medium of human embryonic lung fibroblasts cultures that inhibited osteoclastogenesis (Tsuda, Goto et al. 1997). This factor, termed osteoclastogenesis inhibitory factor (OCIF), later proved to be identical to OPG (Yasuda, Shima et al. 1998).

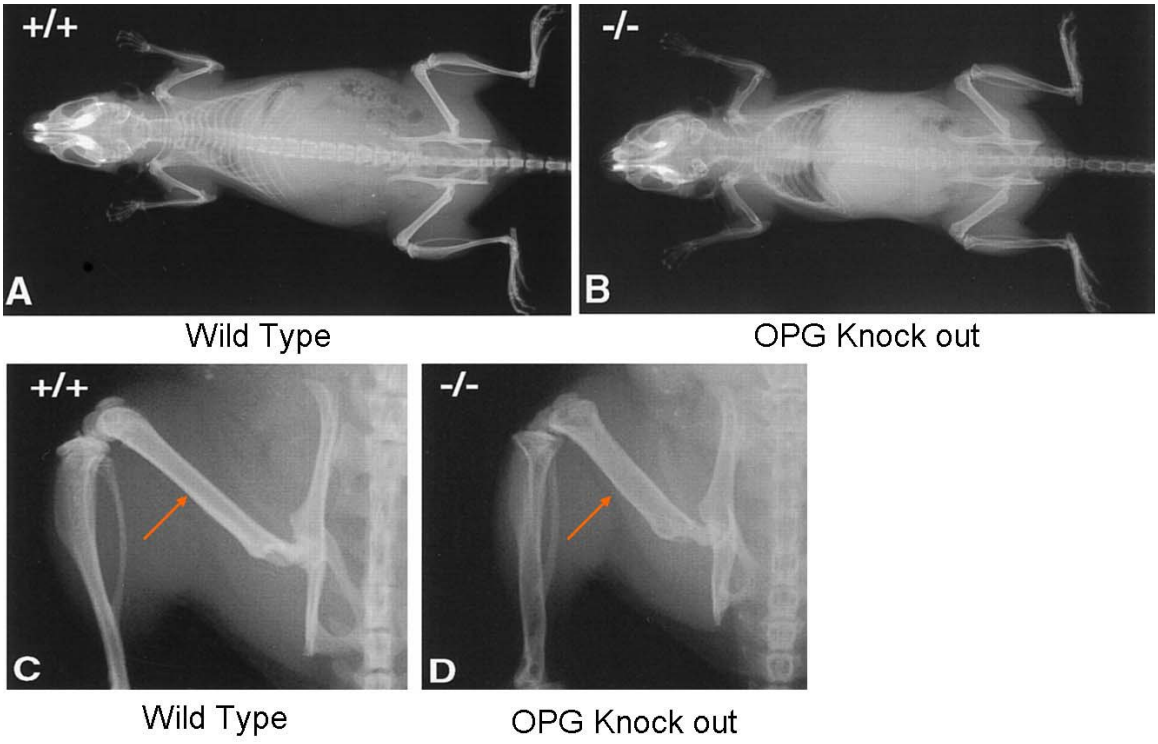

Figure 1.7 Transgenic mice with OPG knockout showed severe osteoporosis symptoms (Mizuno, Amizuka et al. 1998).

In contrast to other TNF receptor superfamily members, OPG lacks transmembrane and cytoplasmic domains and is therefore secreted as a soluble protein with 380 amino acids. OPG mRNA is expressed in many tissues, including bone, lung, heart, kidney, liver, stomach, intestine, brain spinal cord, and thyroid gland (Simonet, Lacey et al. 1997; Yasuda, Shima et al. 1998). In addition to severe osteoporosis, mice with the OPG gene knock-out also developed calcification in large aortas (Bucay, Sarosi et al. 1998; Mizuno, Amizuka et al. 1998); studies have shown that OPG may be important for the survival of endothelial cells (Malyankar, Scatena et al. 2000). These findings indicate that the RANK/RANKL/OPG system might be involved in the regulation mechanism of the cardiovascular system. For this reason, vascular calcification

induced by RANKL was examined in an *in vivo* study of this project (see Chapter 4 for details).

1.3.2 RANKL and RANK

RANKL was identified by both Amgen and the Snow Brand Milk Group using expression cloning with OPG as a probe, this time with the Japanese group reporting their results first (Lacey, Timms et al. 1998; Yasuda, Shima et al. 1998). This protein was initially termed OPG ligand (OPGL) and osteoclast differentiation factor (ODF), which later turned out to be identical with two previous known members of the TNF ligand family: TNF-related activation induced cytokine (TRANCE) and RANKL, a factor known to stimulate dendritic cells (Anderson, Maraskovsky et al. 1997; Wong, Rho et al. 1997). This protein was eventually termed RANKL.

RANKL is a 317-amino acid family peptide that belongs to the TNF superfamily of cytokines. RANKL exists in two forms: a 40- to 45-kDa membrane-bound form and a 31kDa soluble form derived by cleavage of the full-length form at position 140 or 145 (Lacey, Timms et al. 1998). RANKL mRNA is expressed in various tissues, with highest levels in bone and bone marrow, as well as in lymphoid tissues (Anderson, Maraskovsky et al. 1997; Wong, Rho et al. 1997; Lacey, Timms et al. 1998; Yasuda, Shima et al. 1998). Although RANKL was originally identified as a dendritic cell survival factor produced by activated T cells, subsequent studies have established the role of RANKL being the primary mediator and final effector of osteoclastogenesis. Its role and importance to the immune system is still being identified, while its critical role in osteoclastogenesis is established (Figure 1.8).

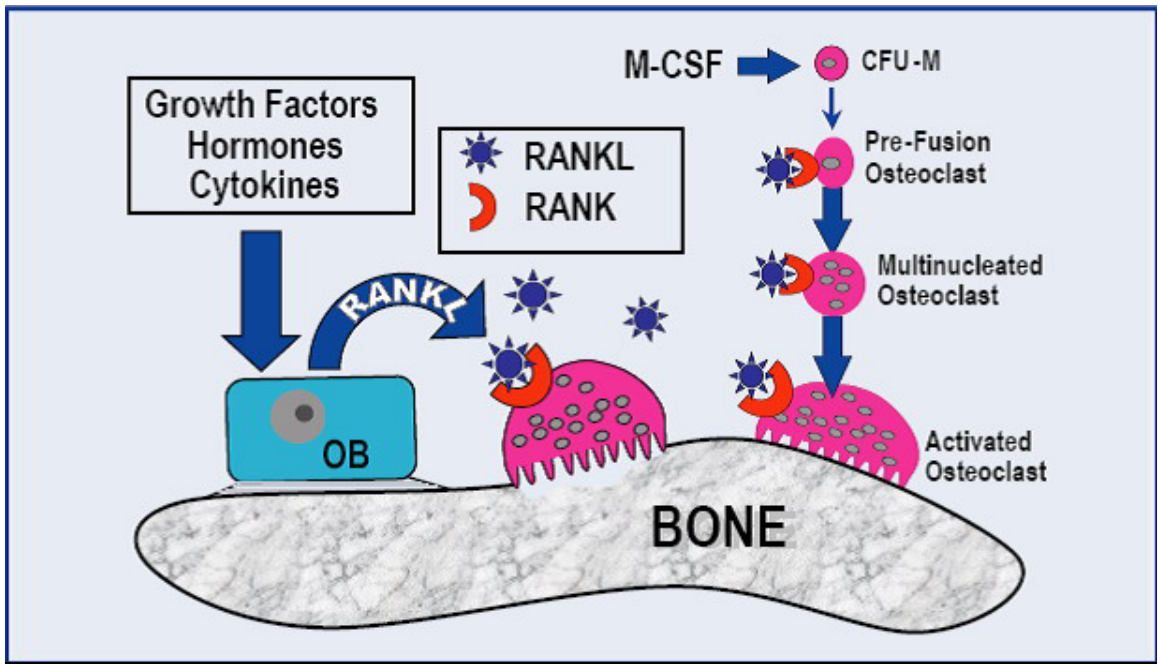

Figure 1.8 Mechanism of action of RANKL (Amgen Inc., Thousand oaks, CA). OB: Osteoblast; CFU-M: Colony forming unit- macrophage.

RANK, the receptor of RANKL, belongs to the TNF receptor superfamily (Anderson, Maraskovsky et al. 1997). RANK mRNA is highly expressed in osteoclast progenitors and mature osteoclasts (Hsu, Lacey et al. 1999). RANK knock-out transgenic mice showed profound osteopetrosis due to the lack of osteoclasts (Li, Sarosi et al. 2000), demonstrating RANK as the sole receptor for RANKL during osteoclastogenesis. RANKL interacts with the RANK receptor to recruit TNF receptor–associated factor 6 (TRAF-6), a member of TNF family signal transducers (Theill, Boyle et al. 2002). TRAF-6 binds to one or more of four binding sites in the intracellular domain of the RANK receptor and then signals downstream through several signaling cascades, most notably those involving NF-κB, mitogen-activated protein (MAP) kinases (extracellular

signal-regulated kinase [Erk], Janus N-terminal kinase [JNK], and p38), and Akt-2 (Theill, Boyle et al. 2002).

1.3.3 RANK/RANKL/OPG System in Skeletal Diseases

The RANKL to OPG ratio has been suggested to represent a potentially important determinant of bone remodeling, and an increased RANKL:OPG ratio is evident in various bone diseases (Blair, Zhou et al. 2006). These disorders range from traditional causes for osteoporosis to localized inflammatory conditions leading to osteolysis and include cancer, particularly when metastasized to bone.

Estrogen deprivation in postmenopausal women stimulates the production of a variety of regulatory cytokines, such as IL-1β, IL-6, TNF-α, and M-CSF, which promote RANKL production and stimulate osteoclast formation and activation (Suda, Takahashi et al. 1999; Eghbali-Fatourechi, Khosla et al. 2003). In a study targeting postmenopausal osteoporosis patients, RANKL concentration was shown to correlate with the bone resorption markers, serum C-terminal telopeptide and urine N-telopeptide of type I collagen, indicating RANKL as the final effector of osteoclastogenesis (Eghbali-Fatourechi, Khosla et al. 2003).

In an inflammatory environment, such as in rheumatoid arthritis, cytokines released by the immune cells (IL-1, TNF-α, IL-6) increase the RANKL:OPG ratio and lead to joint destruction and bone loss (Kong, Feige et al. 1999; Lubberts, van den Bersselaar et al. 2003; Stolina, Adamu et al. 2005). Additionally, RANKL also plays an important role in malignant diseases, such as multiple myeloma and osteolytic bone metastases. Myeloma cells enhance RANKL release and down-regulate OPG expression, thereby increasing bone resorption while inhibiting bone formation, which uncouples

bone remodeling and leads to accelerated bone loss (Giuliani, Bataille et al. 2001; Standal, Seidel et al. 2002). In osteolytic bone metastases, such as breast and lung cancer, tumor cells directly express RANKL and/or indirectly increase RANKL levels through expression of PTH related peptide (PTHrP), resulting in bone lesions (Michigami, Ihara-Watanabe et al. 2001; Mundy 2002).

1.4 Macrophage Colony Stimulating Factor

As a known key regulator for the proliferation and differentiation stages of osteoclastogenesis, M-CSF (also known as colony stimulating factor-I [CSF-I]) was originally defined by its ability to stimulate the preferential growth of macrophage colonies from bone marrow precursors (Stanley, Guilbert et al. 1983). Subsequent studies found that M-CSF is a haematopoietic growth factor that stimulates the survival, proliferation, differentiation and functions of cells from the mononuclear phagocytic lineage (Rettenmier and Sherr 1989) (Figure 1.9). M-CSF is primarily produced by connective tissue cells (including osteoblasts) and exists in both soluble and membrane-bound forms. The membrane-bound form is expressed as an integral transmembrane glycoprotein, whereas the soluble form is rapidly secreted into the circulation as a glycoprotein or chondroitin sulfate-containing proteoglycan. Both isoforms act on the target cells through a specific cell surface tyrosine kinase receptor encoded by the *c-fms* proto-oncogene. M-CSF receptor (CSF-1R) contains an extracellular ligand-binding domain, a transmembrane domain, and an intracellular tyrosine domain. M-CSF is a disulfide-linked homodimer that, by binding to CSF-1R, stabilizes CSF-1R dimerization to activate the receptor through autophosphorylation, thereby initiating a series of membrane-proximal tyrosine phosphorylation cascades, leading to rapid stimulation of

cytoskeletal remodeling, gene transcription, and protein translation (Yeung and Stanley 2003).

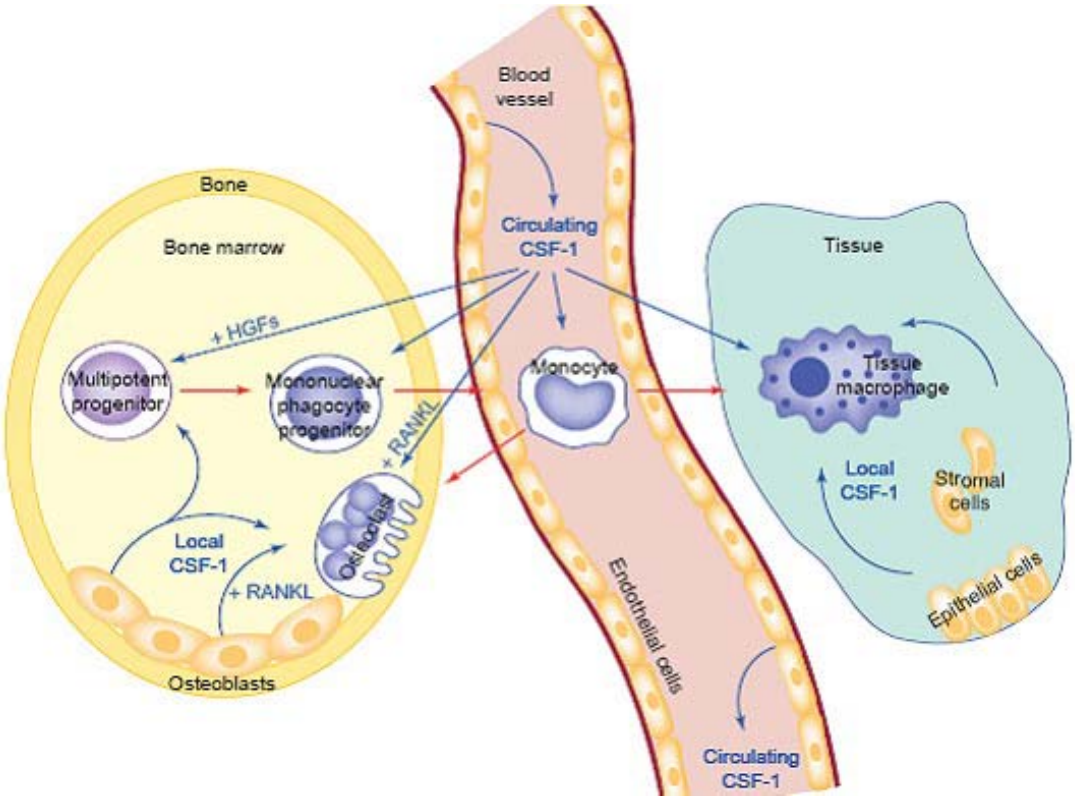

Figure 1.9 M-CSF action in bone and other tissues. M-CSF (CSF-1) synergizes with hematopoietic growth factors (HGFs) to generate mononuclear progenitor cells from multipotent progenitors, and with RANKL to generate osteoclasts from mononuclear phagocytes. Red arrows indicate cell differentiation steps; blue arrows indicate cytokine regulation (Pixley and Stanley 2004).

1.4.1 The Central Role of M-CSF in Osteoclastogenesis

Numerous *in vitro* and *in vivo* studies have been done to prove that M-CSF is a critical regulator of osteoclastogenesis. Takahashi et al. demonstrated that M-CSF is central for the proliferation of osteoclast progenitors derived from committed granulocyte-macrophage progenitors (CFU-GM) (Takahashi, Udagawa et al. 1991). Pretreatment of bone marrow cells with M-CSF in the culture media for 6 days before incubation with normal osteoblasts resulted in the formation of numerous osteoclast-like

multinucleated cells in the presence of vitamin D3. Subsequently, Tanaka et al. demonstrated that M-CSF was required for both the proliferation and differentiation of osteoclast progenitors (Tanaka, Takahashi et al. 1993). Spleen cells are a source of osteoclasts; when co-cultured with mouse osteoblasts and incubated with either anti-M-CSF or *c-fms* antibody during the proliferation and differentiation phases, osteoclast formation that was induced by 1,25(OH)3D3 was inhibited. The ability of M-CSF to stimulate osteoclast development and function *in vivo* has been confirmed using the M-CSF deficient osteopetrotic (*op/op*) mouse model (Wiktor-Jedrzejczak, Bartocci et al. 1990; Yoshida, Hayashi et al. 1990). Systemic administration of recombinant human soluble M-CSF to *op/op* mice had been shown to increase the number of osteoclasts and led to partial or complete resolution of the osteopetrotic defect (Kodama, Yamasaki et al. 1991; Wiktor-Jedrzejczak, Urbanowska et al. 1991; Sundquist, Cecchini et al. 1995).

1.4.2 The Antiresorptive Potential of M-CSF

The action of M-CSF on bone is complex. Though being a potent promoter of osteoclast proliferation and differentiation, M-CSF inhibits mature osteoclasts activity thus decreasing bone resorption. In a study using ST-2 stromal cell and murine bone marrow coculture, exogenous M-CSF caused a 98% dose-dependent decrease in tartrate-resistant acid phosphatase (TRAP) positive multinucleated cells (Perkins and Kling 1995). In studies using isolated mature rat osteoclasts, Hattersley et al. demonstrated that M-CSF, though enhanced osteoclast survival by preventing apoptosis, acted as a chemotactic agent and inhibited bone resorption (Hattersley, Dorey et al. 1988; Fuller, Owens et al. 1993). *In vivo*, transgenic mice selectively over-expressed soluble M-CSF in

bone and showed increased cortical thickness in the femoral diaphysis caused by new bone formation along the endocortical surface (Abboud, Ghosh-Choudhury et al. 2003).

As a summary, these findings indicated that M-CSF is a key determinant for osteoclastogenesis both *in vitro* and *in vivo*. M-CSF exhibits bi-polar effects: it promotes osteoclast proliferation and differentiation while inhibiting osteoclast activation. However, the precise biological effects of M-CSF on bone formation, geometry, structure, and bone biomechanics remain unclear. Therefore, we performed *in vivo* studies with M-CSF to explore these unknown effects on bone biomechanics. Details will be presented in Chapter 5 of this project.

1.5 Skeletal Diseases

Under most conditions, osteoblast and osteoclast activities are closely coupled: a direct increase or decrease in the activity level of one cell type will lead to an indirect change in the other cell type in the same direction through cytokine signaling. There are, however, some skeletal pathologies characterized by uncoupled osteoclast and osteoblast activity, mostly exhibiting excessive osteoclast activity. This excessive osteolysis is an important clinical problem in many common lesions, including osteoporosis, cancer metastases in bone, inflammatory joint diseases, and implanted joint prosthesis failure. The following paragraphs will focus on osteoporosis and malignant bone metastases, which are the most common osteolytic diseases triggered by the abnormally activated osteoclasts.

1.5.1 Osteoporosis

Osteoporosis is currently defined as a systemic skeletal disorder characterized by low bone mass and bone microarchitecture deterioration (Figure 1.10), with a consequent increase in bone fragility and susceptibility to fracture (Consensus Development Conference, 1993). Clinically, osteoporosis is recognized by the occurrence of characteristic low trauma fractures, which typically arise at the hip, spine, and wrist. It is also a disease that increases in severity with age of the patient. The clinical diagnosis of osteoporosis is made if a bone densitometry scan demonstrates a bone mineral density (BMD) that is 2.5 standard deviations below the mean peak bone mass of young adult. Osteopenia ('at risk', low bone mass) is defined at BMD 1.0 standard deviations below normal (National Osteoporosis Foundation, www.nof.org).

Osteoporosis is a major public health problem. According to the International Osteoporosis Foundation, osteoporosis affects an estimated 75 million people in Europe, USA and Japan. Overall 30%-50% women and 15%-30% of men will suffer a fracture related to osteoporosis in their lifetime. Because hip fracture incidence rates increase exponentially with age, the number of hip fractures worldwide will rise from 1.3 million in 1990 to an estimated 2.3 million in 2020 (L Joseph Melton, et al. 2004). Treatments for osteoporosis related fractures are normally invasive surgeries, such as hip replacement. This substantial number of hip surgeries, in addition to the other fractures associated with osteoporosis, could have a devastating effect on patient costs and quality of life for the elderly population.

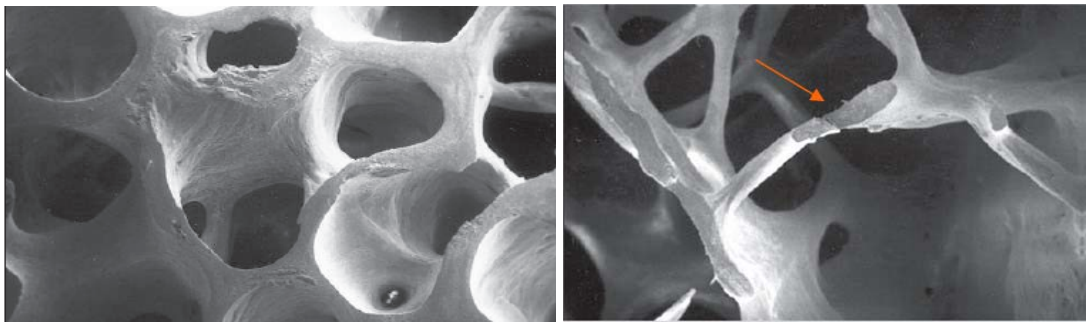

Figure 1.10. Normal (left) and osteoporotic (right) human trabecular bone (Marx 2004).

1.5.1.1 Mechanism of Osteoporosis

Osteoporosis can be triggered by many factors, such as menopause, glucocorticoid therapies, and aging. Among these factors, estrogen deficiency in menopausal states is the most common cause. Estrogen is an important regulator of bone remodeling; it protects against bone loss. Studies have shown that estrogen deficiency is the cause of both the early and the late forms of osteoporosis in post-menopausal women and contributes to the development of osteoporosis in aging men (Khosla, Melton et al. 2002; Riggs, Khosla et al. 2002). Estrogen deficiency is associated with an increase in bone resorption over bone formation, leading to excessive and sustained bone loss. The increase in bone resorption is due both to increased osteoclastogenesis and to decreased osteoclast apoptosis (Manolagas 2000). The mechanism of estrogen deficiency induced bone loss, though not fully understood, is largely related to the RANK/RANKL/OPG system by increasing RANKL/OPG ratio.

Studies have shown that estrogen deprivation in postmenopausal women led to increased production of a variety of regulatory cytokines, such as IL-1β, IL-6, TNF-α and M-CSF, which boost RANKL production and thus osteoclast formation and activation

(Suda, Takahashi et al. 1999; Eghbali-Fatourechi, Khosla et al. 2003). In a study using fluorescent-activated cell sorting to isolate osteoblast precursor cells from premenopausal women, women in early menopause without any treatment, and estrogen-treated postmenopausal women, researchers found that the cells from the untreated postmenopausal women carried much higher levels of RANKL than those from the women in the other two groups (Eghbali-Fatourechi, Khosla et al. 2003). In this study, the RANKL concentration also correlated with the bone resorption markers serum C-terminal telopeptide and urine N-telopeptide of type I collagen, indicating RANKL as the final effector of osteoclastogenesis (Eghbali-Fatourechi, Khosla et al. 2003). By up-regulating RANKL production, estrogen deficiency has several functional effects, including: increased bone turnover rates, deep resorption cavities, trabecular plate perforation, wide separation and disconnection of trabeculae, and enlargement and coalescence of sub-endocortical spaces.

Besides estrogen deficiency, incidence of osteoporosis increases with age. In aging skeletons, the number of osteoblasts that are recruited to erosion surfaces and osteoblast functional activity are decreased, resulting in a decreased rate of bone formation. Estrogen deficiency also suppresses survival of osteocytes and impairs the response of osteoblasts to mechanical stimuli and detection of microdamage, and therefore the repair of aged bone (Manolagas 2000). With increasing age in women as well as in men, microdamage accumulates more rapidly than intrinsic processes can repair, resulting in microarchitectural deterioration and decreased bone strength (Schaffler, Choi et al. 1995).

1.5.1.2 Osteoporosis Therapies

Current therapies for osteoporosis can be classified to two major categories: antiresorptive and anabolic. Antiresorptive therapies target osteoclasts, either decreasing osteoclastogenesis or increasing osteoclast apoptosis. Over the past decades, most osteoporosis patients have been treated with antiresorptive agents such as estrogen and bisphosphonates. Researchers have long known that estrogen deficiency is the major cause of osteoporosis, however, the most obvious therapeutic strategy, hormone replacement therapy (HRT), had been implicated in increasing the risk of both breast cancer and cardiovascular diseases (Couzin 2003). Therefore antiresorptive therapies, namely bisphosphonates, have been used most extensively due to their safety and potent efficacies on inhibiting bone resorption.

Bisphosphonates are a class of pyrophosphate analogues that bind with high affinity to the hydroxyapatite bone matrix, internalized by osteoclasts through endocytosis during bone resorption (Coxon, Thompson et al. 2006). This internalization leads to osteoclast apoptosis by inhibition of farnesyl diphosphate synthase, a key enzyme of the mevalonate pathway (Coxon, Thompson et al. 2006). Several bisphosphonates have been approved by FDA for treatment of osteoporosis, including as alendronate (ALN), risedronate (RIS), zoledronate (ZLN), and ibandronate (IBN) (Chapurlat and Delmas 2006). Clinical use of these drugs has been shown to improve patients' bone mineral density, trabecular bone connectivity and decrease the risk of fracture. However, due to the coupling of bone resorption and bone formation, bisphosphonates can inhibit or reduce bone formation. After binding with bone matrix, bisphosphonate molecules can remain in the skeletal system for many years.

Accumulation of bisphosphonates due to long-term therapies can potentially over-suppress bone turnover, impairing bone's natural recovering ability and increasing fracture risk (Rodan, Reszka et al. 2004).

Recombinant human parathyroid hormone (rhPTH, I-34) was approved by FDA in 2002 as an anabolic agent to treat osteoporosis through stimulating new bone growth. This anabolic bone-active agent stimulates osteoclasts to form new bone, primarily by stimulating new formation on quiescent bone surface that is not simultaneously undergoing remodeling. In a large clinical trial performed by Neer and colleagues, postmenopausal women patients receiving rhPTH increased BMD by 9-13% in the lumbar spine and 3% in the femoral neck (Neer, Arnaud et al. 2001). The anabolic effects of rhPTH have been demonstrated to be most pronounced in the trabecular bone, evidenced by increased trabecular number and connectivity (Dempster, Cosman et al. 2001). Compared to the patients receiving placebo control, risk of new vertebral fractures was reduced by 65% and nonvertebral fractures reduced by 35% (Neer, Arnaud et al. 2001). However, rhPTH is not an ideal treatment for osteoporosis. First, compare to the common weekly oral doses of bisphosphonates, it requires daily injection, which is inconvenient and limits compliance. Second, rhPTH injection also stimulates the production of osteoclast stimulating cytokines, primary RANKL and IL-6, thus increasing bone resorption simultaneously with bone formation and partly counteracts its positive effects on bone strength (Fu, Jilka et al. 2002). Furthermore, as an anabolic agent, rhPTH can potentially stimulate the growth of tumor cells and increase the risk of tumor incidence and metastasis. Therefore, to limit the risk of tumor initiation, current rhPTH therapy was approved for use for a maximum of two years.

In recent years, many studies have shown great potential in using RANK/RANKL/OPG system as a therapeutic target for osteoporosis. Strategies include: suppression of RANKL expression using 17 β-estradiol (Eghbali-Fatourechi, Khosla et al. 2003); RANKL blockage by soluble RANK fusion proteins, OPG fusion proteins, or RANKL antibodies (Min, Morony et al. 2000; Oyajobi, Anderson et al. 2001; Bekker, Holloway et al. 2004); and stimulation of OPG production (Onyia, Galvin et al. 2004). A clinical trial reported that a single dose of AMG 162, a RANKL antibody developed by Amgen (Thousand Oaks, CA), decreased bone resorption for up to 6 months when given to postmenopausal women. The drugs effect in blocking bone resorption was at least comparable to bisphosphonates (Bekker, Holloway et al. 2004).

1.5.2 Osteolytic Bone Metastasis

Cancerous cells can remain in the particular organ of origin (primary cancer) or metastasize to other organs and tissues (metastatic cancer). Due to the highly vascularized structure and the cytokine and growth factor environment, the skeleton is the most common organ to be affected by metastatic cancer. Common tumors, such as breast, lung, and prostate frequently metastasize to bone. Bone metastases are often classified as either osteolytic or osteoblastic. The majority of malignant bone metastases are osteolytic, including breast and lung cancer, as well as those bone lesions found in multiple myeloma. These osteolytic bone metastases can result in severe bone pain, decreased bone mineral density, reduced bone strength, pathological fractures, and hypercalcemia (Mundy 2002; Blair, Zhou et al. 2006). On the other hand, prostate cancer bone metastases, as well as some other bone metastases, are osteoblastic. In these lesions, excess bone tissue is deposited in a disorganized woven structure, bones are weak and

pathological fractures frequently occur (Mundy 2002; Blair, Zhou et al. 2006). Due to the coupling between bone resorption and bone formation, there is no absolute osteolytic or osteoblastic cancers, most bone metastases show mixed patterns with the dominant lesion being osteolytic or osteoblastic, symptoms of the other lesion are usually evident. Osteolytic bone metastases induce abnormalities in bone remodeling primarily through stimulations on osteoclastogenesis. Studies have indicated that RANK/RANKL/OPG systems play an important role in this regulation process.

1.5.2.1 Mechanisms of Osteolytic Metastases

Among many regulation factors, PTH related peptide (PTHrP) is a key mediator of bone destruction in osteolytic cancers (Southby, Kissin et al. 1990; Powell, Southby et al. 1991; Miki, Yano et al. 2000; Bryden, Hoyland et al. 2002). It is well known that osteolytic breast cancer tumor cells can express PTHrP *in vivo*. Previous studies also show that PTHrP expression is greater when the tumor cells metastasize to bone than when they are present in soft tissue sites or in the breast (Southby, Kissin et al. 1990; Powell, Southby et al. 1991). In the bone microenvironment, the overproduction of PTHrP, as well as cytokines such as IL-1 and IL-6, stimulates osteoclast activity by stimulating RANKL production by osteoblasts and stromal cells. RANKL binds to RANK and triggers the intracellular signal transduction, leading to differentiation of osteoclast progenitors into mature osteoclasts (Figure 1.11). Moreover, PTHrP can decrease the production of OPG, thus further increasing the RANKL/OPG ratio. Some researchers also reported that RANKL can be released directly by the tumor cells that migrated to the bone microenvironment (Zhang, Dai et al. 2001).

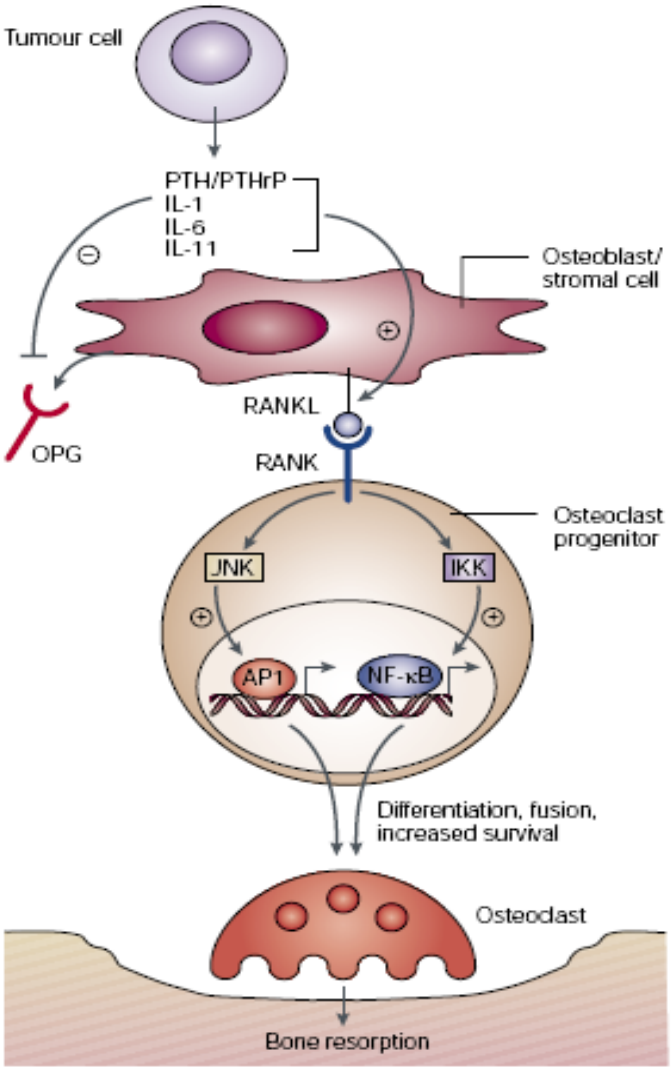

Figure 1.11 The RANK/RANKL/OPG system in osteolytic bone metastases. Cytokines such as PTH or PTH-related peptide, interleukin (IL)-1, IL-6 and IL-11 stimulate production of RANKL by osteoblasts and stromal cells. Signaling through RANK in osteoclast progenitors activates transcription factors such as AP1 (activated by JUN N-terminal kinase (JNK), or JUN) and NF-κB (activated by inhibitor of κB kinase (IKK)), leading to the differentiation of osteoclast progenitors into mature osteoclasts. These osteoclasts mediate bone resorption (Mundy 2002).

Interaction between tumor cells and osteoclasts not only cause osteolytic bone destruction, but may also contribute to tumor proliferation. Active growth factors released during bone resorption, including primary insulin-like growth factor 1 (IGF-1) and TGF-β, together with the elevated extracellular calcium concentrations, can stimulate

the differentiation and growth of tumor cells (Yin, Selander et al. 1999; Yu and Rohan 2000). The increased number and activity of tumor cells thus release more PTHrP into the bone microenvironment, inducing bone destruction through stimulating RANKL expression. Increased RANKL will result in an increase in active growth factors levels via increased resorption, thus further stimulating tumor cell growth. Therefore, a vicious cycle exists in the mechanism pathway of osteolytic metastases (Figure 1.12). This cycle supports the growth of tumor cells metastasized to bone and their interrelations with bone remodeling, further contributing to the high frequency of the skeleton as a cancer metastatic site.

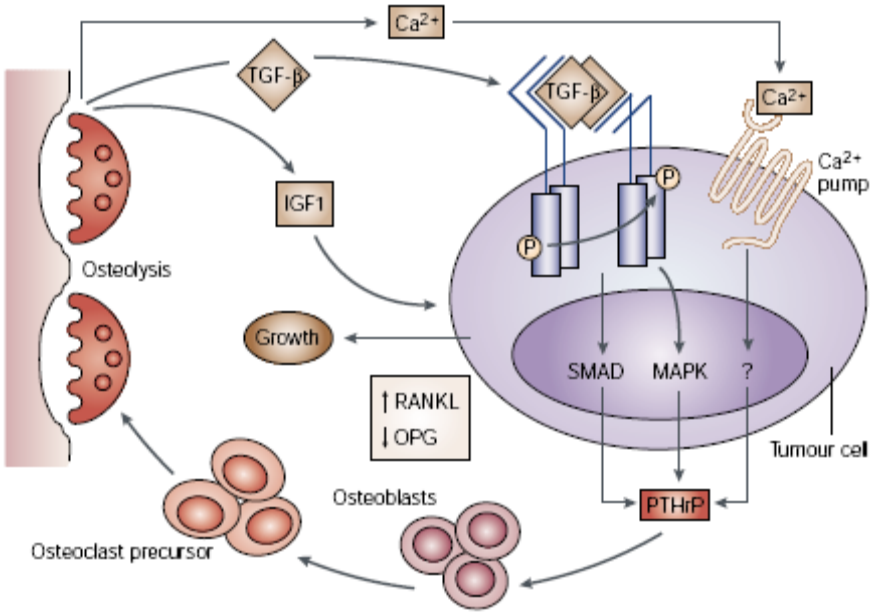

Figure 1.12 The cycle of osteolytic metastases not only cause bone destruction, but also initiates a feedback loop that promotes tumor proliferation and therefore additional bone destruction (Mundy 2002).

1.5.2.2 Therapeutic Approaches

Currently, bisphosphonates are widely used to treat osteolytic bone metastases through inhibiting bone resorption. These antiresorptive agents can interrupt the cycle by stimulating osteoclast apoptosis, thus decreasing the bone tumor burden and stimulating tumor cell apoptosis (Diel, Solomayer et al. 1998; Powles 1999). Recent studies show that the new generation of bone resorption inhibitors, such as OPG and RANKL antibody (AMG 162) which directly targets RANKL, might be more effective than bisphosphonates (Oyajobi, Anderson et al. 2001). Clinical studies have shown that OPG causes a rapid, sustained, dose-dependent decrease in bone resorption marker levels in multiple myeloma and breast cancer patients (Body, Greipp et al. 2003; Body, Facon et al. 2006).

1.5.3 Animal Models for Skeletal Diseases

Laboratory animals have played a major role in the enhanced understanding of skeletal diseases. Animals contributed to the knowledge of the etiology of osteoporosis and are essential for the preclinical evaluation of efficacy and safety in the discovery of therapies. The goal of setting up an animal model is to successfully predict an outcome in humans. However, perfect models for any disease rarely exist; weaknesses are present in each well-established model currently being used for skeletal disorders.

Because of the low costs, fast growth, and the well-characterized skeletons, rats have historically been used as the most used laboratory animal for studies of osteoporosis. A study performed in 1985 observed that acute ovarian estrogen deficiency leads to dramatically increased cancellous bone turnover (Wronski, Lowry et al. 1985). Subsequent studies showed that ovariectomy (OVX) resulted in cortical and trabecular

bone loss, leading to the wide adoption of this model (Turner, Riggs et al. 1994). OVX rats trigger a series of cytokine reactions that mimic the postmenopausal status, thus stimulate bone resorption and lead to bone loss. Detailed mechanisms of estrogen deficiency had been described earlier (1.5.1.1 Mechanism of osteoporosis). However, the OVX model requires a complicated surgical procedure on each subject, which increases the cost and limits the practicality of this model. Besides the OVX models, rats had been also used as a model for disuse osteoporosis, which could be induced by unilateral sciatic nerve damage, tendonotomy, unilateral limb casting, hindlimb suspension or spaceflight (Morey and Baylink 1978; Turner and Bell 1986; Bateman, Zimmerman et al. 1998). All disuse models require surgery or other complicated procedures.

Recent improvements on transgenic technology allow the purposeful manipulation of targeted gene expression, which had made mice another popular model for skeletal diseases. Many studies had used the techniques of specific knock-out or over-expression of targeted genes in transgenic mice and greatly improved understanding of the mechanisms of bone remodeling and skeletal diseases. The roles of a series of key regulators in the skeletal system, such as M-CSF, RANKL, OPG, PTHrP, and PU-1, were either discovered or confirmed using transgenic mice (Felix, Cecchini et al. 1990; Lanske, Karaplis et al. 1996; Simonet, Lacey et al. 1997). However, drawbacks also exist while use transgenic mice as a disease model: Genes being specifically knocked-out or over-expressed are usually important in other systems besides the skeleton, thus many growth defects accompanied the skeletal abnormality in transgenic mice, which makes it difficult to mimic the pathological states. Furthermore, the development of a new transgenic mice model usually takes a long period of time.

Therefore, there is a need to develop novel animal models for skeletal diseases. Due to the unique role and functions of RANK/RANKL/OPG system in osteoclastogenesis, we have targeted RANKL, the final effector of osteoclastogenesis, as a specific agent for developing novel bone loss models. Study details will be presented in Chapter 4 of this project.

1.6 References

Abboud, S. L., N. Ghosh-Choudhury, et al. (2003). "Osteoblast-specific targeting of soluble colony-stimulating factor-1 increases cortical bone thickness in mice." J Bone Miner Res **18**(8): 1386-94.

Abboud, S. L., K. Woodruff, et al. (2002). "Rescue of the osteopetrotic defect in op/op mice by osteoblast-specific targeting of soluble colony-stimulating factor-1." Endocrinology **143**(5): 1942-9.

Ammann, P. and R. Rizzoli (2003). "Bone strength and its determinants." Osteoporos Int **14 Suppl 3**: S13-8.

Anderson, D. M., E. Maraskovsky, et al. (1997). "A homologue of the TNF receptor and its ligand enhance T-cell growth and dendritic-cell function." Nature **390**(6656): 175-9.

Anderson, H. C. (1989). "Mechanism of mineral formation in bone." Lab Invest **60**(3): 320-30.

Bateman, T. A., R. J. Zimmerman, et al. (1998). "Histomorphometric, physical, and mechanical effects of spaceflight and insulin-like growth factor-I on rat long bones." Bone **23**(6): 527-35.

Bekker, P. J., D. L. Holloway, et al. (2004). "A single-dose placebo-controlled study of AMG 162, a fully human monoclonal antibody to RANKL, in postmenopausal women." J Bone Miner Res **19**(7): 1059-66.

Blair, J. M., H. Zhou, et al. (2006). "Mechanisms of disease: roles of OPG, RANKL and RANK in the pathophysiology of skeletal metastasis." Nat Clin Pract Oncol **3**(1): 41-9.

Body, J. J., T. Facon, et al. (2006). "A study of the biological receptor activator of nuclear factor-kappaB ligand inhibitor, denosumab, in patients with multiple myeloma or bone metastases from breast cancer." Clin Cancer Res **12**(4): 1221-8.

Body, J. J., P. Greipp, et al. (2003). "A phase I study of AMGN-0007, a recombinant osteoprotegerin construct, in patients with multiple myeloma or breast carcinoma related bone metastases." Cancer **97**(3 Suppl): 887-92.

Boyce, B. F., L. Xing, et al. (2003). "Regulation of bone remodeling and emerging breakthrough drugs for osteoporosis and osteolytic bone metastases." Kidney Int Suppl(85): S2-5.

Boyle, W. J., W. S. Simonet, et al. (2003). "Osteoclast differentiation and activation." Nature **423**(6937): 337-42.

Bryden, A. A., J. A. Hoyland, et al. (2002). "Parathyroid hormone related peptide and receptor expression in paired primary prostate cancer and bone metastases." Br J Cancer **86**(3): 322-5.

Bucay, N., I. Sarosi, et al. (1998). "osteoprotegerin-deficient mice develop early onset osteoporosis and arterial calcification." Genes Dev **12**(9): 1260-8.

Buckwalter, J. A. and R. R. Cooper (1987). "Bone structure and function." Instr Course Lect **36**: 27-48.

Burr, D. B. (2002). "The contribution of the organic matrix to bone's material properties." Bone **31**(1): 8-11.

Burr, D. B. (2004). "Bone quality: understanding what matters." J Musculoskelet Neuronal Interact **4**(2): 184-6.

Burr, D. B. (2005). "Does early PTH treatment compromise bone strength? The balance between remodeling, porosity, bone mineral, and bone size." Curr Osteoporos Rep **3**(1): 19-24.

Burr, D. B., T. Hirano, et al. (2001). "Intermittently administered human parathyroid hormone(1-34) treatment increases intracortical bone turnover and porosity without reducing bone strength in the humerus of ovariectomized cynomolgus monkeys." J Bone Miner Res **16**(1): 157-65.

Chapurlat, R. D. and P. D. Delmas (2006). "Drug insight: Bisphosphonates for postmenopausal osteoporosis." Nat Clin Pract Endocrinol Metab **2**(4): 211-9; quiz following 238.

Corboz, V. A., M. G. Cecchini, et al. (1992). "Effect of macrophage colony-stimulating factor on in vitro osteoclast generation and bone resorption." Endocrinology **130**(1): 437-42.

Couzin, J. (2003). "Estrogen research. The great estrogen conundrum." Science **302**(5648): 1136-8.

Coxon, F. P., K. Thompson, et al. (2006). "Recent advances in understanding the mechanism of action of bisphosphonates." Curr Opin Pharmacol **6**(3): 307-12.

Currey, J. D. (1975). "The effects of strain rate, reconstruction and mineral content on some mechanical properties of bovine bone." J Biomech **8**(1): 81-6.

Currey, J. D., K. Brear, et al. (1996). "The effects of ageing and changes in mineral content in degrading the toughness of human femora." J Biomech **29**(2): 257-60.

Dempster, D. W., F. Cosman, et al. (2001). "Effects of daily treatment with parathyroid hormone on bone microarchitecture and turnover in patients with osteoporosis: a paired biopsy study." J Bone Miner Res **16**(10): 1846-53.

Diel, I. J., E. F. Solomayer, et al. (1998). "Reduction in new metastases in breast cancer with adjuvant clodronate treatment." N Engl J Med **339**(6): 357-63.

Eghbali-Fatourechi, G., S. Khosla, et al. (2003). "Role of RANK ligand in mediating increased bone resorption in early postmenopausal women." J Clin Invest **111**(8): 1221-30.

Felix, R., M. G. Cecchini, et al. (1990). "Macrophage colony stimulating factor restores in vivo bone resorption in the op/op osteopetrotic mouse." Endocrinology **127**(5): 2592-4.

Felix, R., J. Halasy-Nagy, et al. (1996). "Synthesis of membrane- and matrix-bound colony-stimulating factor-1 by cultured osteoblasts." J Cell Physiol **166**(2): 311-22.

Fernandez-Tresguerres-Hernandez-Gil, I., M. A. Alobera-Gracia, et al. (2006). "Physiological bases of bone regeneration II. The remodeling process." Med Oral Patol Oral Cir Bucal **11**(2): E151-7.

Friedman, A. W. (2006). "Important determinants of bone strength: beyond bone mineral density." J Clin Rheumatol **12**(2): 70-7.

Fu, Q., R. L. Jilka, et al. (2002). "Parathyroid hormone stimulates receptor activator of NFkappa B ligand and inhibits osteoprotegerin expression via protein kinase A activation of cAMP-response element-binding protein." J Biol Chem **277**(50): 48868-75.

Fuller, K., J. M. Owens, et al. (1993). "Macrophage colony-stimulating factor stimulates survival and chemotactic behavior in isolated osteoclasts." J Exp Med **178**(5): 1733-44.

Giuliani, N., R. Bataille, et al. (2001). "Myeloma cells induce imbalance in the osteoprotegerin/osteoprotegerin ligand system in the human bone marrow environment." Blood **98**(13): 3527-33.

Hanaoka, H., H. Yabe, et al. (1989). "The origin of the osteoclast." Clin Orthop Relat Res(239): 286-98.

Hattersley, G., E. Dorey, et al. (1988). "Human macrophage colony-stimulating factor inhibits bone resorption by osteoclasts disaggregated from rat bone." J Cell Physiol **137**(1): 199-203.

Heaney, R. P. (2003). "Is the paradigm shifting?" Bone **33**(4): 457-65.

Howard, G. A., B. L. Bottemiller, et al. (1981). "Parathyroid hormone stimulates bone formation and resorption in organ culture: evidence for a coupling mechanism." Proc Natl Acad Sci U S A **78**(5): 3204-8.

Hsu, H., D. L. Lacey, et al. (1999). "Tumor necrosis factor receptor family member RANK mediates osteoclast differentiation and activation induced by osteoprotegerin ligand." Proc Natl Acad Sci U S A **96**(7): 3540-5.

Hui, S. L., C. W. Slemenda, et al. (1988). "Age and bone mass as predictors of fracture in a prospective study." J Clin Invest **81**(6): 1804-9.

Iwamoto, J., T. Takeda, et al. (2006). "Efficacy and safety of alendronate and risedronate for postmenopausal osteoporosis." Curr Med Res Opin **22**(5): 919-28.

Kell, R. T., G. Bell, et al. (2001). "Musculoskeletal fitness, health outcomes and quality of life." Sports Med **31**(12): 863-73.

Khosla, S., L. J. Melton, 3rd, et al. (2002). "Clinical review 144: Estrogen and the male skeleton." J Clin Endocrinol Metab **87**(4): 1443-50.

Kodama, H., M. Nose, et al. (1991). "Essential role of macrophage colony-stimulating factor in the osteoclast differentiation supported by stromal cells." J Exp Med **173**(5): 1291-4.

Kodama, H., A. Yamasaki, et al. (1991). "Congenital osteoclast deficiency in osteopetrotic (op/op) mice is cured by injections of macrophage colony-stimulating factor." J Exp Med **173**(1): 269-72.

Kong, Y. Y., U. Feige, et al. (1999). "Activated T cells regulate bone loss and joint destruction in adjuvant arthritis through osteoprotegerin ligand." Nature **402**(6759): 304-9.

Kostenuik, P. J. and V. Shalhoub (2001). "Osteoprotegerin: a physiological and pharmacological inhibitor of bone resorption." Curr Pharm Des **7**(8): 613-35.

Lacey, D. L., H. L. Tan, et al. (2000). "Osteoprotegerin ligand modulates murine osteoclast survival in vitro and in vivo." Am J Pathol **157**(2): 435-48.

Lacey, D. L., E. Timms, et al. (1998). "Osteoprotegerin ligand is a cytokine that regulates osteoclast differentiation and activation." Cell **93**(2): 165-76.

Lanske, B., A. C. Karaplis, et al. (1996). "PTH/PTHrP receptor in early development and Indian hedgehog-regulated bone growth." Science **273**(5275): 663-6.

Lerner, U. H. (2000). "Osteoclast formation and resorption." Matrix Biol **19**(2): 107-20.

Li, J., I. Sarosi, et al. (2000). "RANK is the intrinsic hematopoietic cell surface receptor that controls osteoclastogenesis and regulation of bone mass and calcium metabolism." Proc Natl Acad Sci U S A **97**(4): 1566-71.

Lian, J. B. and G. S. Stein (1995). "Development of the osteoblast phenotype: molecular mechanisms mediating osteoblast growth and differentiation." Iowa Orthop J **15**: 118-40.

Liberman, U. A. (2006). "Long-term safety of bisphosphonate therapy for osteoporosis: a review of the evidence." Drugs Aging **23**(4): 289-98.

Ljunggren, O., S. Ljunghall, et al. (1995). "[Continuous remodeling of the skeleton. Growth factors and cytokines direct the activity]." Lakartidningen **92**(20): 2094-6, 2099-100.

Locklin, R. M., S. Khosla, et al. (2003). "Mediators of the biphasic responses of bone to intermittent and continuously administered parathyroid hormone." J Cell Biochem **89**(1): 180-90.

Lubberts, E., L. van den Bersselaar, et al. (2003). "IL-17 promotes bone erosion in murine collagen-induced arthritis through loss of the receptor activator of NF-kappa B ligand/osteoprotegerin balance." J Immunol **170**(5): 2655-62.

Malyankar, U. M., M. Scatena, et al. (2000). "Osteoprotegerin is an alpha vbeta 3-induced, NF-kappa B-dependent survival factor for endothelial cells." J Biol Chem **275**(28): 20959-62.

Manolagas, S. C. (2000). "Birth and death of bone cells: basic regulatory mechanisms and implications for the pathogenesis and treatment of osteoporosis." Endocr Rev **21**(2): 115-37.

Manolagas, S. C. and R. L. Jilka (1995). "Bone marrow, cytokines, and bone remodeling. Emerging insights into the pathophysiology of osteoporosis." N Engl J Med **332**(5): 305-11.

Marks, S. C., Jr. (1987). "Osteopetrosis--multiple pathways for the interception of osteoclast function." Appl Pathol **5**(3): 172-83.

Martin, R. B. and J. Ishida (1989). "The relative effects of collagen fiber orientation, porosity, density, and mineralization on bone strength." J Biomech **22**(5): 419-26.

Marx, J. (2004). "Coming to grips with bone loss." Science **305**(5689): 1420-2.

Michigami, T., M. Ihara-Watanabe, et al. (2001). "Receptor activator of nuclear factor kappaB ligand (RANKL) is a key molecule of osteoclast formation for bone metastasis in a newly developed model of human neuroblastoma." Cancer Res **61**(4): 1637-44.

Miki, T., S. Yano, et al. (2000). "Bone metastasis model with multiorgan dissemination of human small-cell lung cancer (SBC-5) cells in natural killer cell-depleted SCID mice." Oncol Res **12**(5): 209-17.

Min, H., S. Morony, et al. (2000). "Osteoprotegerin reverses osteoporosis by inhibiting endosteal osteoclasts and prevents vascular calcification by blocking a process resembling osteoclastogenesis." J Exp Med **192**(4): 463-74.

Mizuno, A., N. Amizuka, et al. (1998). "Severe osteoporosis in mice lacking osteoclastogenesis inhibitory factor/osteoprotegerin." Biochem Biophys Res Commun **247**(3): 610-5.

Mizuno, A., T. Kanno, et al. (2002). "Transgenic mice overexpressing soluble osteoclast differentiation factor (sODF) exhibit severe osteoporosis." J Bone Miner Metab **20**(6): 337-44.

Morey, E. R. and D. J. Baylink (1978). "Inhibition of bone formation during space flight." Science **201**(4361): 1138-41.

Mundy, G. R. (1993). "Cytokines and growth factors in the regulation of bone remodeling." J Bone Miner Res **8 Suppl 2**: S505-10.

Mundy, G. R. (2002). "Metastasis to bone: causes, consequences and therapeutic opportunities." Nat Rev Cancer **2**(8): 584-93.

Nakashima, T., Y. Kobayashi, et al. (2000). "Protein expression and functional difference of membrane-bound and soluble receptor activator of NF-kappaB ligand: modulation of the expression by osteotropic factors and cytokines." Biochem Biophys Res Commun **275**(3): 768-75.

Neer, R. M., C. D. Arnaud, et al. (2001). "Effect of parathyroid hormone (1-34) on fractures and bone mineral density in postmenopausal women with osteoporosis." N Engl J Med **344**(19): 1434-41.

Onyia, J. E., R. J. Galvin, et al. (2004). "Novel and selective small molecule stimulators of osteoprotegerin expression inhibit bone resorption." J Pharmacol Exp Ther **309**(1): 369-79.

Oyajobi, B. O., D. M. Anderson, et al. (2001). "Therapeutic efficacy of a soluble receptor activator of nuclear factor kappaB-IgG Fc fusion protein in suppressing bone resorption and hypercalcemia in a model of humoral hypercalcemia of malignancy." Cancer Res **61**(6): 2572-8.

Parfitt, A. M. (1984). "The cellular basis of bone remodeling: the quantum concept reexamined in light of recent advances in the cell biology of bone." Calcif Tissue Int **36 Suppl 1**: S37-45.

Parfitt, A. M. (2002). "High bone turnover is intrinsically harmful: two paths to a similar conclusion. The Parfitt view." J Bone Miner Res **17**(8): 1558-9; author reply 1560.

Perkins, S. L. and S. J. Kling (1995). "Local concentrations of macrophage colony-stimulating factor mediate osteoclastic differentiation." Am J Physiol **269**(6 Pt 1): E1024-30.

Pixley, F. J. and E. R. Stanley (2004). "CSF-1 regulation of the wandering macrophage: complexity in action." Trends Cell Biol **14**(11): 628-38.

Powell, G. J., J. Southby, et al. (1991). "Localization of parathyroid hormone-related protein in breast cancer metastases: increased incidence in bone compared with other sites." Cancer Res **51**(11): 3059-61.

Powles, T. J. (1999). "Re: Tamoxifen for prevention of breast cancer: report of the National Surgical Adjuvant Breast and Bowel Project P-1 Study." J Natl Cancer Inst **91**(8): 730.

Raisz, L. G. (1999). "Physiology and pathophysiology of bone remodeling." Clin Chem **45**(8 Pt 2): 1353-8.

Rettenmier, C. W. and C. J. Sherr (1989). "The mononuclear phagocyte colony-stimulating factor (CSF-1, M-CSF)." Hematol Oncol Clin North Am **3**(3): 479-93.

Riggs, B. L., S. Khosla, et al. (2002). "Sex steroids and the construction and conservation of the adult skeleton." Endocr Rev **23**(3): 279-302.

Riggs, C. M., L. C. Vaughan, et al. (1993). "Mechanical implications of collagen fibre orientation in cortical bone of the equine radius." Anat Embryol (Berl) **187**(3): 239-48.

Rodan, G., A. Reszka, et al. (2004). "Bone safety of long-term bisphosphonate treatment." Curr Med Res Opin **20**(8): 1291-300.

Rodan, G. A. (1992). "Introduction to bone biology." Bone **13 Suppl 1**: S3-6.

Rodan, G. A. and T. J. Martin (2000). "Therapeutic approaches to bone diseases." Science **289**(5484): 1508-14.

Schaffler, M. B., K. Choi, et al. (1995). "Aging and matrix microdamage accumulation in human compact bone." Bone **17**(6): 521-25.

Schoppet, M., K. T. Preissner, et al. (2002). "RANK ligand and osteoprotegerin: paracrine regulators of bone metabolism and vascular function." Arterioscler Thromb Vasc Biol **22**(4): 549-53.

Sibilia, V. and C. Netti (1996). "Current therapies and future directions in osteoporosis management." Pharmacol Res **34**(5-6): 237-45.

Simonet, W. S., D. L. Lacey, et al. (1997). "Osteoprotegerin: a novel secreted protein involved in the regulation of bone density." Cell **89**(2): 309-19.

Siris, E. S. (1999). "Goals of treatment for Paget's disease of bone." J Bone Miner Res **14 Suppl 2**: 49-52.

Southby, J., M. W. Kissin, et al. (1990). "Immunohistochemical localization of parathyroid hormone-related protein in human breast cancer." Cancer Res **50**(23): 7710-6.

Specker, B. L. (1996). "Evidence for an interaction between calcium intake and physical activity on changes in bone mineral density." J Bone Miner Res **11**(10): 1539-44.

Stains, J. P. and R. Civitelli (2005). "Cell-cell interactions in regulating osteogenesis and osteoblast function." Birth Defects Res C Embryo Today **75**(1): 72-80.

Standal, T., C. Seidel, et al. (2002). "Osteoprotegerin is bound, internalized, and degraded by multiple myeloma cells." Blood **100**(8): 3002-7.

Stanley, E. R., L. J. Guilbert, et al. (1983). "CSF-1--a mononuclear phagocyte lineage-specific hemopoietic growth factor." J Cell Biochem **21**(2): 151-9.

Stolina, M., S. Adamu, et al. (2005). "RANKL is a marker and mediator of local and systemic bone loss in two rat models of inflammatory arthritis." J Bone Miner Res **20**(10): 1756-65.

Suda, T., N. Takahashi, et al. (1992). "Modulation of osteoclast differentiation." Endocr Rev **13**(1): 66-80.

Suda, T., N. Takahashi, et al. (1999). "Modulation of osteoclast differentiation and function by the new members of the tumor necrosis factor receptor and ligand families." Endocr Rev **20**(3): 345-57.

Sundquist, K. T., M. G. Cecchini, et al. (1995). "Colony-stimulating factor-1 injections improve but do not cure skeletal sclerosis in osteopetrotic (op) mice." Bone **16**(1): 39.

Sundquist, K. T., M. E. Jackson, et al. (1995). "Osteoblasts from the toothless (osteopetrotic) mutation in the rat are unable to direct bone resorption by normal osteoclasts in response to 1,25-dihydroxyvitamin D." Tissue Cell **27**(5): 569-74.

Takahashi, N., N. Udagawa, et al. (1991). "Role of colony-stimulating factors in osteoclast development." J Bone Miner Res **6**(9): 977-85.

Takano, Y., C. H. Turner, et al. (1999). "Elastic anisotropy and collagen orientation of osteonal bone are dependent on the mechanical strain distribution." J Orthop Res **17**(1): 59-66.

Tanaka, S., N. Takahashi, et al. (1993). "Macrophage colony-stimulating factor is indispensable for both proliferation and differentiation of osteoclast progenitors." J Clin Invest **91**(1): 257-63.

Teitelbaum, S. I. (1996). "The osteoclast and osteoporosis." Mt Sinai J Med **63**(5-6): 399-402.

Teitelbaum, S. L. (2000). "Bone resorption by osteoclasts." Science **289**(5484): 1504-8.

Theill, L. E., W. J. Boyle, et al. (2002). "RANK-L and RANK: T cells, bone loss, and mammalian evolution." Annu Rev Immunol **20**: 795-823.

Tolar, J., S. L. Teitelbaum, et al. (2004). "Osteopetrosis." N Engl J Med **351**(27): 2839-49.

Tondravi, M. M., S. R. McKercher, et al. (1997). "Osteopetrosis in mice lacking haematopoietic transcription factor PU.1." Nature **386**(6620): 81-4.

Tsuda, E., M. Goto, et al. (1997). "Isolation of a novel cytokine from human fibroblasts that specifically inhibits osteoclastogenesis." Biochem Biophys Res Commun **234**(1): 137-42.

Turner, C. H. (2002). "Biomechanics of bone: determinants of skeletal fragility and bone quality." Osteoporos Int **13**(2): 97-104.

Turner, C. H. (2006). "Bone strength: current concepts." Ann N Y Acad Sci **1068**: 429-46.

Turner, R. T. and N. H. Bell (1986). "The effects of immobilization on bone histomorphometry in rats." J Bone Miner Res **1**(5): 399-407.

Turner, R. T., B. L. Riggs, et al. (1994). "Skeletal effects of estrogen." Endocr Rev **15**(3): 275-300.

Udagawa, N., N. Takahashi, et al. (1990). "Origin of osteoclasts: mature monocytes and macrophages are capable of differentiating into osteoclasts under a suitable microenvironment prepared by bone marrow-derived stromal cells." Proc Natl Acad Sci U S A **87**(18): 7260-4.

Udagawa, N., N. Takahashi, et al. (2000). "Osteoprotegerin produced by osteoblasts is an important regulator in osteoclast development and function." Endocrinology **141**(9): 3478-84.

Vaananen, H. K., T. Hentunen, et al. (1988). "Mechanism of osteoclast mediated bone resorption." Ann Chir Gynaecol **77**(5-6): 193-6.

Vaananen, H. K., H. Zhao, et al. (2000). "The cell biology of osteoclast function." J Cell Sci **113 (Pt 3)**: 377-81.

Viguet-Carrin, S., P. Garnero, et al. (2006). "The role of collagen in bone strength." Osteoporos Int **17**(3): 319-36.

Wang, X., X. Shen, et al. (2002). "Age-related changes in the collagen network and toughness of bone." Bone **31**(1): 1-7.

Whyte, M. P. (2006). "Paget's disease of bone and genetic disorders of RANKL/OPG/RANK/NF-kappaB signaling." Ann N Y Acad Sci **1068**: 143-64.

Wiktor-Jedrzejczak, W., A. Bartocci, et al. (1990). "Total absence of colony-stimulating factor 1 in the macrophage-deficient osteopetrotic (op/op) mouse." Proc Natl Acad Sci U S A **87**(12): 4828-32.

Wiktor-Jedrzejczak, W., E. Urbanowska, et al. (1991). "Correction by CSF-1 of defects in the osteopetrotic op/op mouse suggests local, developmental, and humoral requirements for this growth factor." Exp Hematol **19**(10): 1049-54.

Wong, B. R., J. Rho, et al. (1997). "TRANCE is a novel ligand of the tumor necrosis factor receptor family that activates c-Jun N-terminal kinase in T cells." J Biol Chem **272**(40): 25190-4.

Wronski, T. J., P. L. Lowry, et al. (1985). "Skeletal alterations in ovariectomized rats." Calcif Tissue Int **37**(3): 324-8.

Yasuda, H., N. Shima, et al. (1998). "Identity of osteoclastogenesis inhibitory factor (OCIF) and osteoprotegerin (OPG): a mechanism by which OPG/OCIF inhibits osteoclastogenesis in vitro." Endocrinology **139**(3): 1329-37.

Yasuda, H., N. Shima, et al. (1998). "Osteoclast differentiation factor is a ligand for osteoprotegerin/osteoclastogenesis-inhibitory factor and is identical to TRANCE/RANKL." Proc Natl Acad Sci U S A **95**(7): 3597-602.

Yeung, Y. G. and E. R. Stanley (2003). "Proteomic approaches to the analysis of early events in colony-stimulating factor-1 signal transduction." Mol Cell Proteomics **2**(11): 1143-55.

Yin, J. J., K. Selander, et al. (1999). "TGF-beta signaling blockade inhibits PTHrP secretion by breast cancer cells and bone metastases development." J Clin Invest **103**(2): 197-206.

Yoshida, H., S. Hayashi, et al. (1990). "The murine mutation osteopetrosis is in the coding region of the macrophage colony stimulating factor gene." Nature **345**(6274): 442-4.

Yu, H. and T. Rohan (2000). "Role of the insulin-like growth factor family in cancer development and progression." J Natl Cancer Inst **92**(18): 1472-89.

Zaidi, M., M. Pazianas, et al. (1993). "Osteoclast function and its control." Exp Physiol **78**(6): 721-39.

Zhang, J., J. Dai, et al. (2001). "Osteoprotegerin inhibits prostate cancer-induced osteoclastogenesis and prevents prostate tumor growth in the bone." J Clin Invest **107**(10): 1235-44.

Zioupos, P., J. D. Currey, et al. (1999). "The role of collagen in the declining mechanical properties of aging human cortical bone." J Biomed Mater Res **45**(2): 108-16.

CHAPTER 2

PROJECT RATIONALE

2.1 General Hypothesis

As described in detail in Chapter One, previous studies have demonstrated the important role of M-CSF and RANKL on osteoclastgenesis. M-CSF stimulates the proliferation and early differentiation of osteoclast progenitors to osteoclast lineage, while RANKL targets the later stages of fusion and activation, and stimulates the formation of functional active osteoclasts (Figure 2.1). In this project, **we hypothesized that while M-CSF and RANKL can both stimulate osteoclastogenesis, the differences in activation stages targeted by these two cytokines would result in distinct responses on bone biomechanics.** RANKL would act as the final effector of osteoclastogenesis by directly stimulating osteoclast activity and increasing bone resorption. Alternately, M-CSF promotes the proliferation and differentiation of osteoclast progenitors but not the activation of mature osteoclasts, thus it has less influence on bone resorption but stimulates osteoblast development through the coupling of osteoclast-osteoblast cells, and may promote bone formation and increase bone biomechanical properties.

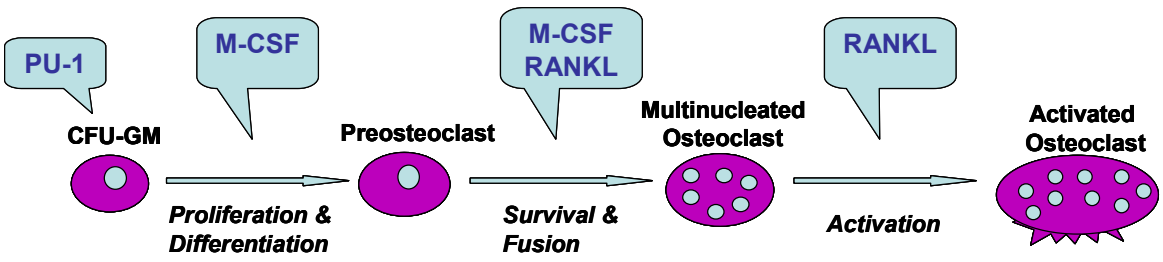

Figure 2.1 Osteoclastogenesis regulation

2.2 Specific Aims

Aim 1: Examine the basic functional and biomechanical effects of RANKL administration on mouse bone density and quality. **Hypothesis:** Artificial RANKL administration is destructive to bone biomechanics. **Approach:** Mice received two different dosages of RANKL by twice daily injections for 10 days. Femora and tibiae were collected at sacrifice. Cortical and trabecular bone volume, bone mineral content, bone strength, and bone turnover markers were analyzed to evaluate the functional changes on bone induced by direct soluble RANKL injection. These experimental results are presented in Chapter 3.

Aim 2: Develop a RANKL-induced bone destructive model for high-turnover osteolytic bone diseases. **Hypothesis:** Continuous infusion of metabolically relevant doses of RANKL in a mature rat model mimics deleterious skeletal changes in many osteolytic skeletal diseases. **Approach:** Six-month old rats received long term (28 days) RANKL infusion via osmotic pumps to create a skeletally mature bone loss model. Blood was collected at predetermined time points to examine changes in bone turnover markers rates by ELISA. Femurs and tibias were collected at sacrifice to evaluate the changes in volume, mineral content, geometry and strength. Aortas were also collected to evaluate the correlation of vascular calcification and RANKL induced bone loss. These experimental results are presented in Chapter 4.

Aim 3: Characterize the effects of artificial M-CSF administration on the skeleton and determine its potential as an anabolic agent for bone biomechanics. **Hypothesis:** Activation of osteoclasts early in the differentiation cycle will have an anabolic, rather than catabolic, effect on skeletal properties. **Approach:** High dosages M-CSF were

administered to seven-week old mice for 3 weeks. Serum was collected at sacrifice to examine bone turnover markers levels. Femora and tibias were collected to evaluate the changes in volume, mineral content, geometry and strength. These experimental results are presented in Chapter 5.

2.3 Clinical Significance

Many skeletal diseases, such as osteoporosis, malignant bone metastases, and rheumatoid arthritis are generally osteolytic and associated with increased bone turnover rates and bone remodeling towards excessive resorption. Equilibrium of the regulation network is interrupted in these disease states, resulting in excessive osteoclast activity, bone loss, inferior bone architecture, and increased fracture risk. Within the complex cytokine environment, RANKL and M-CSF are critical for osteoclast differentiation and activation. RANKL is the final effector of osteoclast activation and bone resorption. Skeletal complications in osteolytic diseases are generally triggered by up-regulation of RANKL expression levels in the bone local environment. M-CSF plays an indispensable role in early osteoclast development. Mice with M-CSF gene knockout developed profound osteoporosis-opposite (osteopetrotic) phenotype with little or no osteoclast activity.

It is evident that both RANKL and M-CSF are necessary for osteoclastogenesis. However, the impact of excessive levels of these two cytokines, resulting in activations of osteoclastogenesis at different stages, has not been fully characterized. The goal of this project is to further investigate the mechanism of critical cytokine regulation on osteoclastogenesis and subsequent biomechanical changes. Studies in this project have demonstrated the deleterious effects of elevated RANKL levels to bone biomechanics,

and suggested a novel bone loss animal model induced by RANKL for osteolytic skeletal disease research. Aim 3 of this project showed that M-CSF increased bone formation through coupled stimulating early osteoclastogenesis and osteoblast development, and indicated the potential of M-CSF as a novel anabolic agent for osteoporosis. Finally, Chapter 6 presents the conclusions and recommendation for future work. Data from this study could provide fundamental tools and information for future exploration on skeletal diseases.

.

CHAPTER 3

EXAMINATION OF RANKL AS A CRITICAL OSTEOCLASTOGENESIS STIMULATOR AND ITS FUNCTIONAL EFFECTS ON BONE DENSITY AND QUALITY

Data related to this chapter has been submitted as a manuscript to *Bone.* Contents presented here are the manuscript formatted following dissertation requirements.

3.1 Introduction

Bone strength is determined by bone mass and bone quality (Ammann and Rizzoli 2003; Heaney 2003). Bone mass reflects the balance between bone formation and bone resorption, which involves regulation of osteoblast and osteoclast numbers and activity at the cellular level. Moreover, bone formation and resorption is a coupled process: osteoblasts regulate the recruitment and activity of osteoclasts through expression of RANKL and OPG (Simonet, Lacey et al. 1997; Lacey, Timms et al. 1998). Balanced RANKL/OPG levels are critical for maintaining bone remodeling in a precise manner (Simonet, Lacey et al. 1997; Lacey, Timms et al. 1998; Hofbauer and Heufelder 2001; Khosla 2001). Bone quality is determined by a number of variables, including bone turnover, microarchitecture, microdamage, and degree of mineralization. Of these many determinants of bone quality, bone turnover is particularly important. Unnecessarily high bone turnover markedly degrades bone quality by disrupting the normal bone remodeling cycle (Turner 2002; Heaney 2003). For example, Paget's disease in humans is

characterized by high bone turnover, rapid remodeling of woven bone, skeletal deformity, and fractures (Roodman and Windle 2005).

RANKL (Receptor Activator of NF-κB Ligand), expressed by stromal cells and osteoblasts, is an essential mediator of osteoclast formation, activation, and survival (Lacey, Timms et al. 1998). RANKL binds to its receptor RANK on the surface of osteoclasts and their precursors; stimulates differentiation of osteoclastic precursors into mature osteoclasts; activates mature osteoclasts; and induces bone resorption (Lacey, Timms et al. 1998; Suda, Takahashi et al. 1999; Takahashi, Udagawa et al. 1999; Lacey, Tan et al. 2000). Osteoprotegerin (OPG), a member of the tumor necrosis factor-receptor superfamily, is a soluble decoy receptor for the ligand and blocks RANKL/RANK interactions (Simonet, Lacey et al. 1997; Kostenuik and Shalhoub 2001). Previous studies confirm this important role of the RANKL/OPG system. Transgenic mice overexpressing RANKL, and OPG-knockout mice ($OPG^{-/-}$) each develop severe osteoporosis accompanied by increased osteoclast differentiation and activation, low bone mineral density, and high bone turnover (Lacey, Timms et al. 1998; Kostenuik and Shalhoub 2001; Mizuno, Kanno et al. 2002). As these studies indicate, the amount of bone resorbed during the bone remodeling process is dictated by the balance between the expression of RANKL and its inhibitor, OPG.

RANKL exists in both soluble and membrane-bound forms. Membrane-bound RANKL has been found to be a member of membrane-associated tumor necrosis factor family, expressed on the osteoblast/stromal cell surface (Lacey, Timms et al. 1998; Hofbauer and Heufelder 2001). Membrane-bound RANKL mediates bone resorption by binding to its receptor RANK through direct cell-to-cell interaction between osteoblasts

and osteoclasts (Yasuda, Shima et al. 1998). In cell co-culture systems, this cell-cell interaction appears to be essential for osteoclastogenesis and activation (Yasuda, Shima et al. 1998). However, soluble RANKL also induces osteoclastogenesis and bone resorption in cell culture systems (Lacey, Timms et al. 1998). In addition to its membrane-bound form, RANKL can be directly secreted from cells (Suzuki, Ikeda et al. 2004), and can also be released from the surface of activated T cells (Mizuno, Kanno et al. 2002; Kanamaru, Iwai et al. 2004). Although previous *in vitro* studies suggest that membrane-bound RANKL is more potent than the soluble form in osteoclastogenesis development (Yasuda, Shima et al. 1998; Nakashima, Kobayashi et al. 2000), the contribution of each form on regulation of bone remodeling remains largely unknown. We hypothesized that the direct injection of soluble recombinant RANKL would recapitulate many of the skeletal changes that have been described in mice that lack the OPG gene, including deleterious effects on bone volume, geometry, density, and strength, and serve as an accelerated model for high-turnover bone disease such as post-menopausal osteoporosis.

3.2 Materials and Methods

3.2.1 Study design

Thirty-six female C57BL/6J mice (Jackson Laboratory, Bar Harbor, ME) aged 10 weeks were assigned to one of three groups: VEH (placebo control, phosphate buffered saline, n=12), LOW (0.4 mg/kg/day RANKL injection, n=12), HI (2 mg/kg/day RANKL injection, n=12). The form of human RANKL used in all studies comprised amino acids 143-317, a region that includes the entire active ligand moiety distal to the extracellular cleavage site, as previously described (Lacey, Timms et al. 1998). This construct, which

lacks transmembrane and intracellular domains, was expressed in Chinese Hamster Ovary (CHO) cells and purified at Amgen. The purified protein had a molecular weight of 27 kD. All mice received twice daily subcutaneous injections (0.2ml per injection) for 10 days. Body weights were monitored every two days, and drug concentrations were adjusted accordingly. Calcein (20 mg/kg) was injected (*i.p.*) as a fluorescent label at Day 2 to monitor new bone growth. At Day 10, animals were anesthetized with isoflurane and euthanized by exsanguination followed by cervical dislocation. Both hind limbs were removed and cleaned of all nonosseous tissue. All procedures performed throughout the experiment conformed to the guidelines of Clemson University's Institutional Animal Care and Use Committee (Figure 3.1).

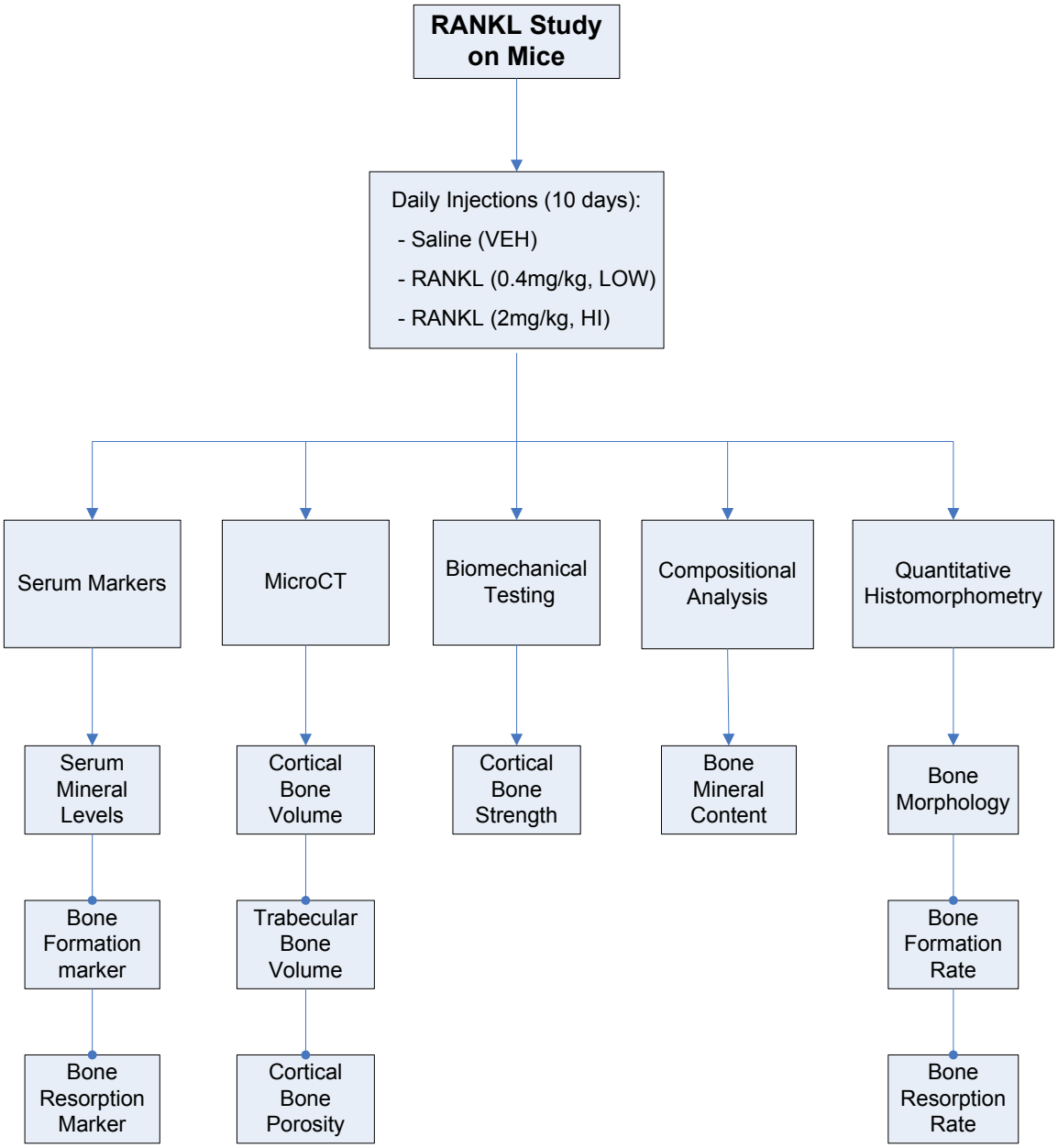

Figure 3.1 Flowchart illustrating study design of the *in vivo* characterization of RANKL on bone biomechanics.

3.2.2 Serum bone-turnover markers

Serum was obtained at sacrifice, and markers for bone formation and resorption were measured. Serum alkaline phosphatase (ALP) and total calcium levels were measured by an automated chemistry analyzer (Hitachi) as markers of bone formation and hypercalcemia, respectively. As a bone resorption marker, serum TRAP-5b was measured by ELISA (SBA Science/IDS Inc.).

3.2.3 Micro CT

Microcomputed tomography analysis (*μCT20*, Scanco Medical AG, Bassersdorf, Switzerland) with a voxel size of 9 μm in all three spatial dimensions was used to obtain both cortical and trabecular parameters (Ruegsegger, Koller et al. 1996; Dufresne 1998). Right femora were air-dried prior to the scan. Cortical bone parameters were obtained by scanning an 8 mm section of the femoral diaphysis (Figure 3.2), the same span length examined by mechanical testing. A total of 81 slices were analyzed, with 100μm increment lengths between slices. To determine bone volume and polar moment of inertia, contours were traced at the periosteal surface and calculated by Scanco IPL-Moment software. To quantify the porosity of femoral cortical bone, two contours were traced on the periosteal and endocortical surfaces of each slice and evaluated by Scanco software. During evaluation, femur diaphysis was separated into three sections: proximal diaphysis (2.5mm in length, slices taken from the third trochanter), mid-diaphysis (3mm long), and distal diaphysis (2.5mm long, slices taken from the metaphysis). Porosity data were obtained from each of these sections.

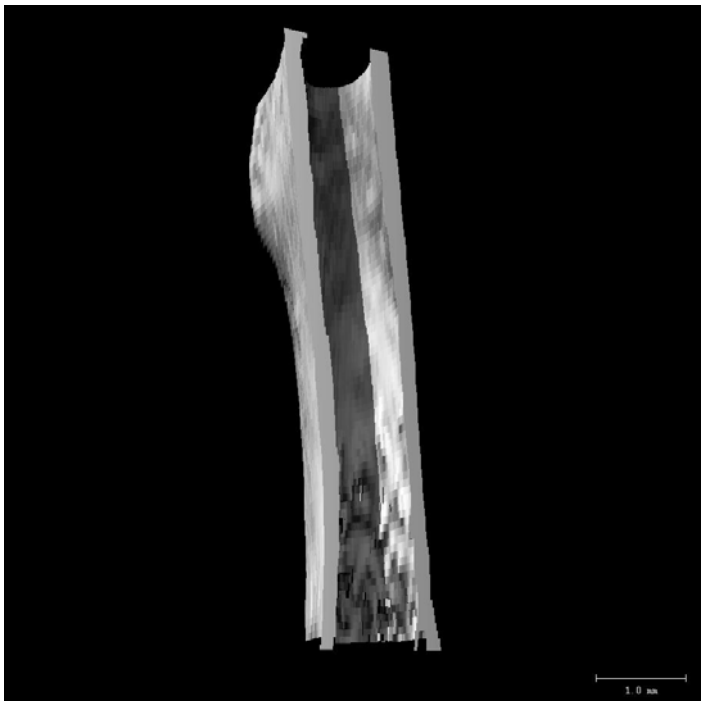

Figure 3.2 3D microCT picture of an 8-mm long femur diaphysis

Right tibiae were fixed in 10% neural buffered formalin for 2 days, rinsed with distilled water, and stored in 70% ethanol. Trabecular bone parameters were obtained by microCT scan of 0.9 mm sections of trabecular bone at the proximal end of the tibia, immediately distal to the growth plate (Figure 3.3). These parameters included trabecular bone volume (BV), total volume (TV), percent connectivity of trabecular struts, and trabecular volume fraction (BV/TV).

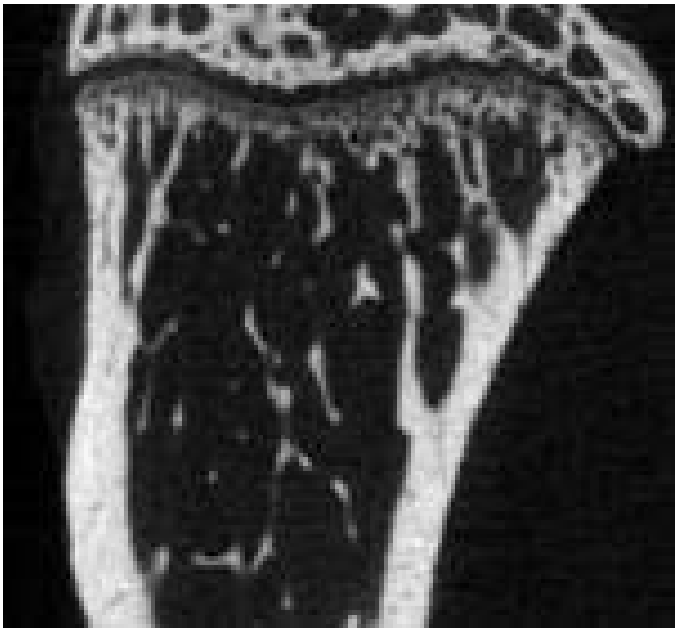

Figure 3.3 2-D cross-sectional picture on mouse proximal tibia showing the growth plate and trabecular bones

3.2.4 Biomechanical testing

Mechanical properties of right femora were tested following microCT analysis. All bones were rehydrated in phosphate-buffered saline (PBS) for 1.5 hours prior to mechanical testing to simulate *in vivo* properties (Broz, Simske et al. 1993). Three-point bending tests were performed using an Instron 5582 (Merlin, Series IX software). Femora were tested to failure with an 8 mm span length and deflection rate of 5mm/min (Figure 3.4). Force (N) and deflection (mm) were measured at the elastic limit (P_e, δ_e), maximum force, and failure for all mechanically tested bones. Stiffness (S) was calculated from P_e/δ_e.

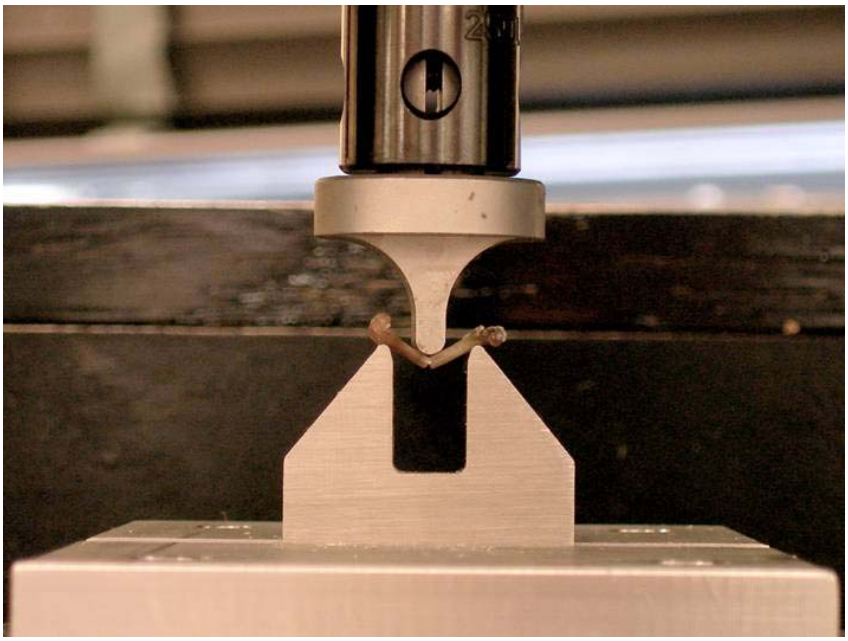

Figure 3.4 Three point bending test on mid-femur with 8 mm span length

3.2.5 Mineral content analysis

Mineral content analysis was performed on the fractured femur. Prior to analysis, epiphyses at both proximal and distal ends were separated. Mineral-content data were obtained separately from epiphysis and diaphysis. Dry mass (Dry-M) was measured after heating the bones for 24 h at 105ºC. Mineral mass (Min-M) was measured after the bones had been ashed by baking for another 24 h at 800ºC. Percent mineralization (%Min) was calculated by the formula % Min = Min-M/Dry-M * 100%.

3.2.6 Quantitative histomorphometry

Left femora were placed in 10% neutral-buffered formalin for 48 hours and then stored in ethanol after being rinsed with distilled water. Bones were then allowed to air-dry and embedded with noninfiltrating Epo-Kwick epoxy (Buehler, Lake Bluff, IL). The formed disks were sectioned with a low-speed saw (Buehler, 12.7cm x 0.5mm diamond

blade) at the mid-diaphysis of the femur. The sections were wheel-polished to a flat, smooth surface using 600-, 800-, and 1200-grit carbide paper followed by polishing with a cloth impregnated with 6 μm diamond paste. This allowed micrographs at 50X magnification to be taken of the bone cross-sections under a far blue light (400 nm). Green calcein labels were visualized, indicating the bone formation sites during the period of the study (Figure 3.5). Quantitative histomorphometric analysis was performed using these photographs and SigmaScan Pro software (SPSS, San Rafael, CA).

Measurements of bone morphology (Parfitt, Drezner et al. 1987) included total bone area (T.Ar) enclosed by periosteal perimeter and endocortical area (Ec.Ar). Cortical area was calculated as T.Ar – Ec.Ar. A calcein label was injected at Day 2 of the study; the area between the labels and the cortical perimeter was measured as bone formation area (BFA), and linear content of the labeled perimeter was defined as active mineralizing perimeter (aMPm). Bone-formation rates were calculated as BFR = BFA/8 days and mineral apposition rate as MAR = BFR/aMPm separately in the periosteal (Ps.BFR, Ps.MAR) and endocortical (Ec.BFR, Ps.MAR) areas. Endocortical-bone resorption perimeter (Ec.Rs.Pm) was also measured by quantifying the portion of the nonlabeled surface with rough/ruffled border.

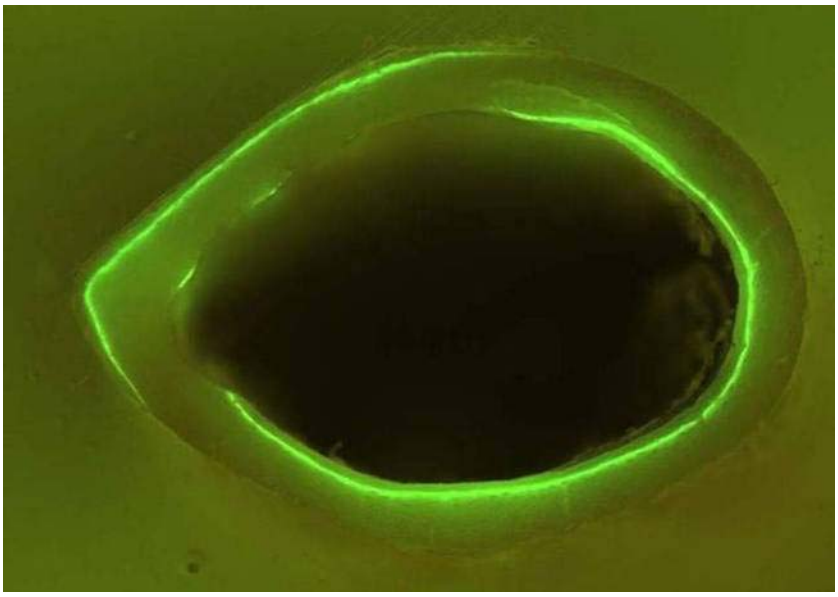

Figure 3.5 2 D cross-sectional picture on mouse mid-femur showing fluorescent calcein labels under Ultraviolet (UV) microscope

3.2.7 Statistics

Statistical comparisons were performed using repeated measures of analysis of variance (ANOVA) with SigmaStat software. One-way ANOVAs, with a Tukey test for follow-up comparisons, were used. A 95% level of significance (type I error) was used for each of these tests. The correlation between serum TRAP-5b levels and bone strength was obtained from Pearson Product Moment Correlation test with SigmaStat. Data are presented as mean $\pm$ standard error (SE).

3.3 Results

3.3.1 Weight loss and hypercalcemia

Mice treated with saline or 0.4 mg/kg RANKL maintained normal body mass and blood calcium levels during the 10-day study. In HI group, an 11% weight loss was observed at the day of sacrifice ($p<0.001$, Figure 3.6); this was accompanied by

hypercalcemia symptoms, such as lethargy. Total serum calcium levels increased by 15.7 % in HI group ($p<0.001$ vs. VEH), while a 20.3% increase was observed in serum phosphorus levels for HI group ($p<0.001$) compared to VEH, while those in LOW group remained unchanged (Figure 3.7).

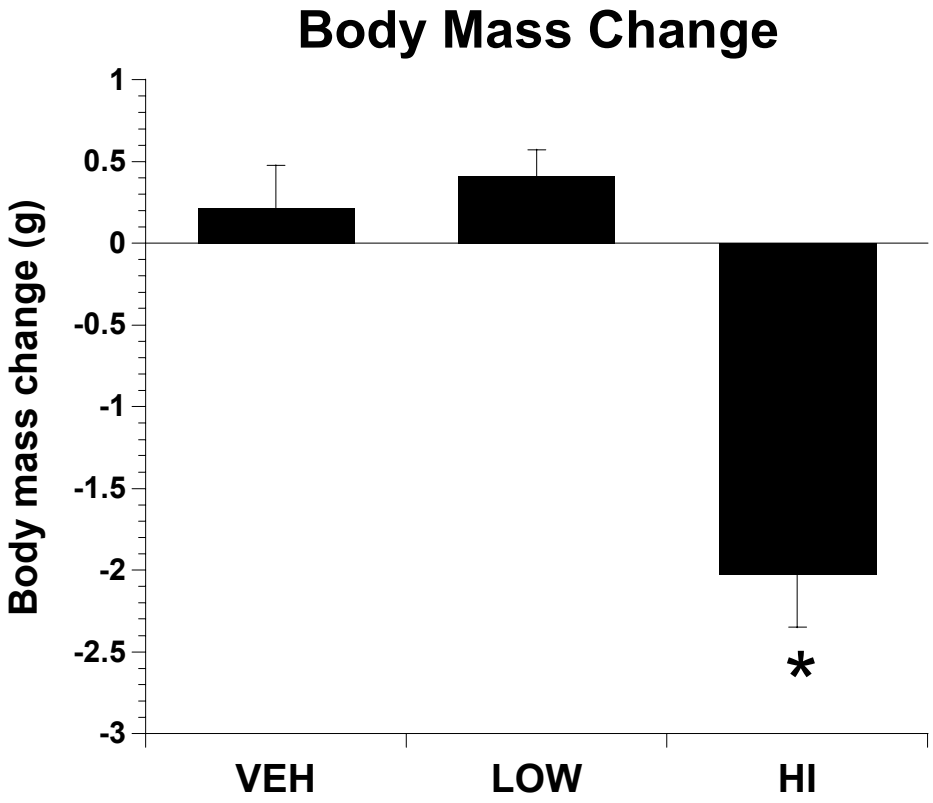

Figure 3.6 Body mass in the HI group decreased by 11% at sacrifice when compared to body mass at Day 0 ($p< 0.001$).

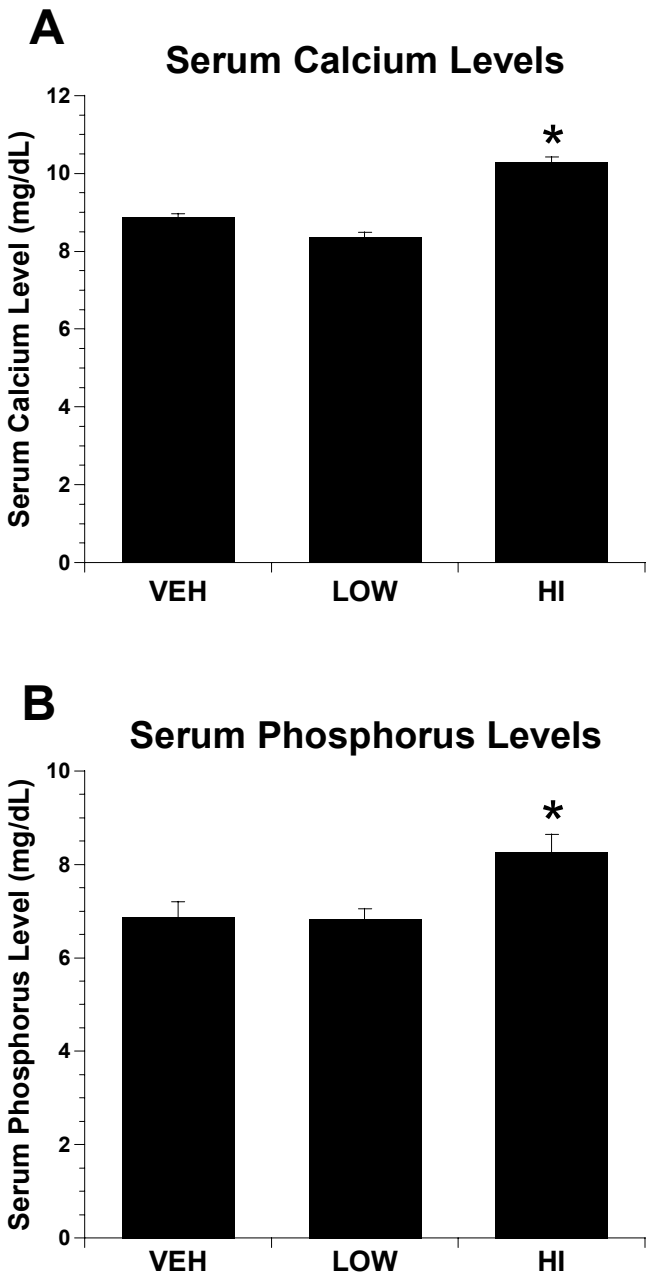

Figure 3.7 Total serum calcium levels (A) increased by 15.7 % in HI group ($p<0.001$ vs. VEH). A 20.3% increase was observed in serum phosphorus levels (B) for HI group ($p<0.001$) compared to VEH, while those in LOW group remained unchanged.

3.3.2 Bone turnover

Bone turnover rates were greatly accelerated by 10-day treatment of RANKL in both doses. The bone formation marker serum alkaline phosphatase levels (ALP) increased 224% and 321% in mice treated with low- and high-dose RANKL, respectively ($p<0.001$) vs. VEH. The bone resorption marker serum TRAP-5b was increased by 83.8% and 49.2% ($p<0.05$) in LOW and HI group mice, respectively, relative to VEH (Figure 3.8).

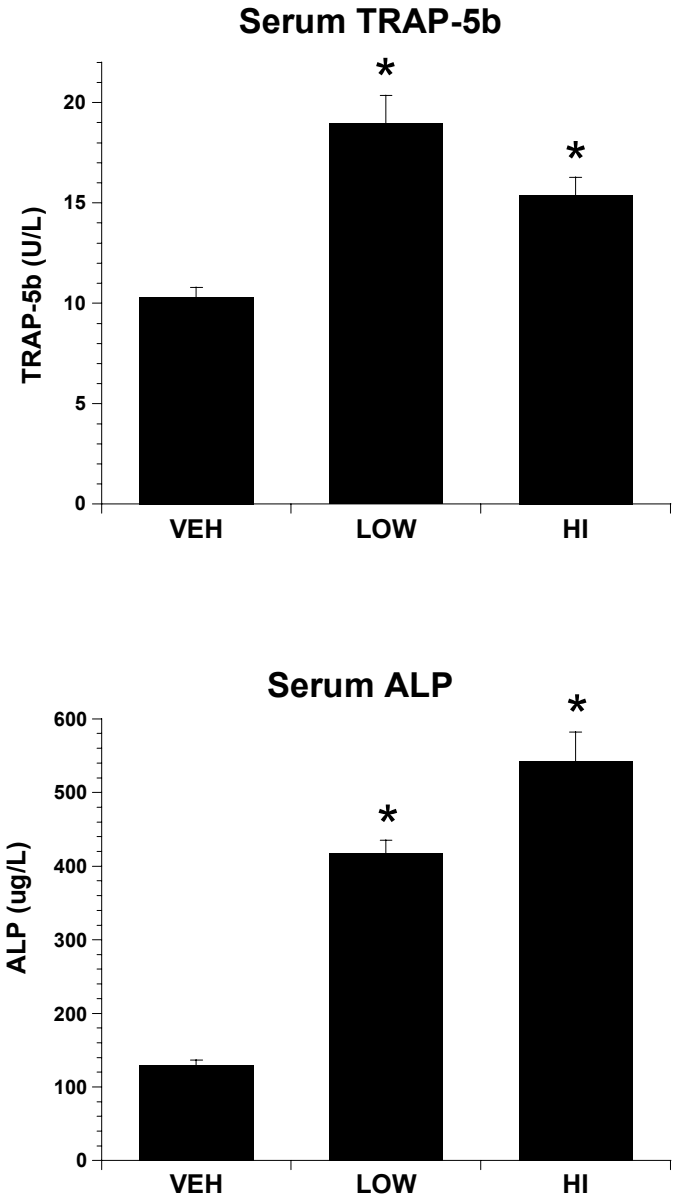

Figure 3.8 RANKL increased bone turnover rates. (A) Serum TRAP-5b levels were accelerated by 83.8% and 49.2% in low-and high-dose RANKL mice ($p<0.05$ vs. VEH). (B) Serum alkaline phosphatase levels increased 3-fold in 0.4mg/kg RANKL (LOW) and 4-fold in 2.0mg/kg RANKIL (HI) mice after 10 days of twice daily injections ($p<0.001$ vs. VEH). Data are presented as the mean ± SE. * = significantly different from VEH.

3.3.3 Cortical bone strength

Both doses of RANKL reduced femur maximum strength, fracture strength, and stiffness. Maximum bending loads of femoral diaphyses were reduced by 25% (LOW) and 19% (HI), while structural stiffness was decreased by 38.5% (LOW) and 37.4% (HI) vs. VEH ($p<0.001$, Figure 3.9). In the HI group, serum TRAP-5b levels showed a negative correlation with maximum strength of the femur ($r= -0.74$, $p=0.01$, Figure 3.10A), while serum ALP levels showed a positive correlation with maximum strength ($r= 0.68$, $p=0.02$, Figure 3.10B).

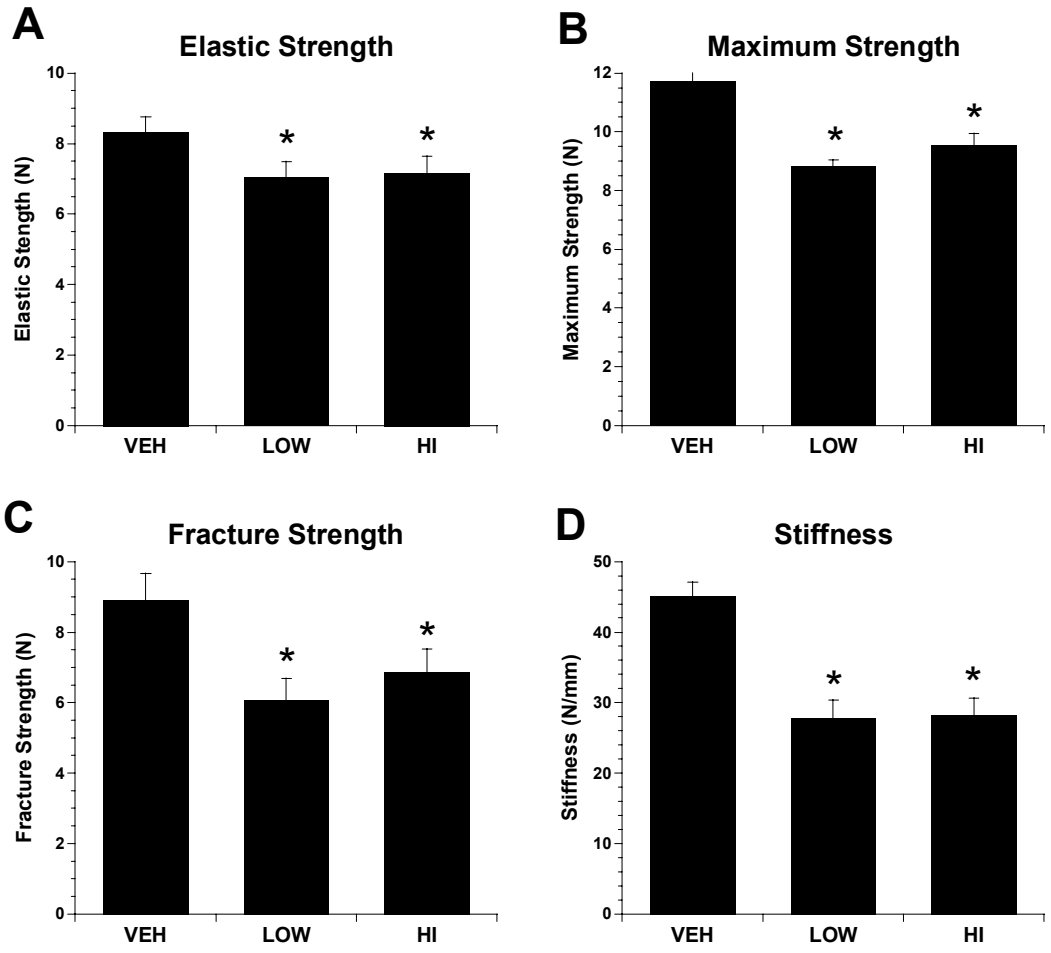

Figure 3.9 Bone maximum bending strength was significantly reduced in RANKL groups, by 19% to 25% (B), after 10 days of RANKL treatment ($p<0.001$). Femur stiffness (D) was decreased by 38.5% and 37.4% in low-and high-RANKL groups ($p<0.001$), respectively. In both RANKL treatment groups, there is a decreasing trend in elastic force ($p=0.098$, A) and fracture force (C, $p=0.014$ Low, $p=0.102$ in high dose group) compared to VEH. Data are presented as the mean ± SE. * = $p<0.001$, # = $p<0.05$ vs. VEH.

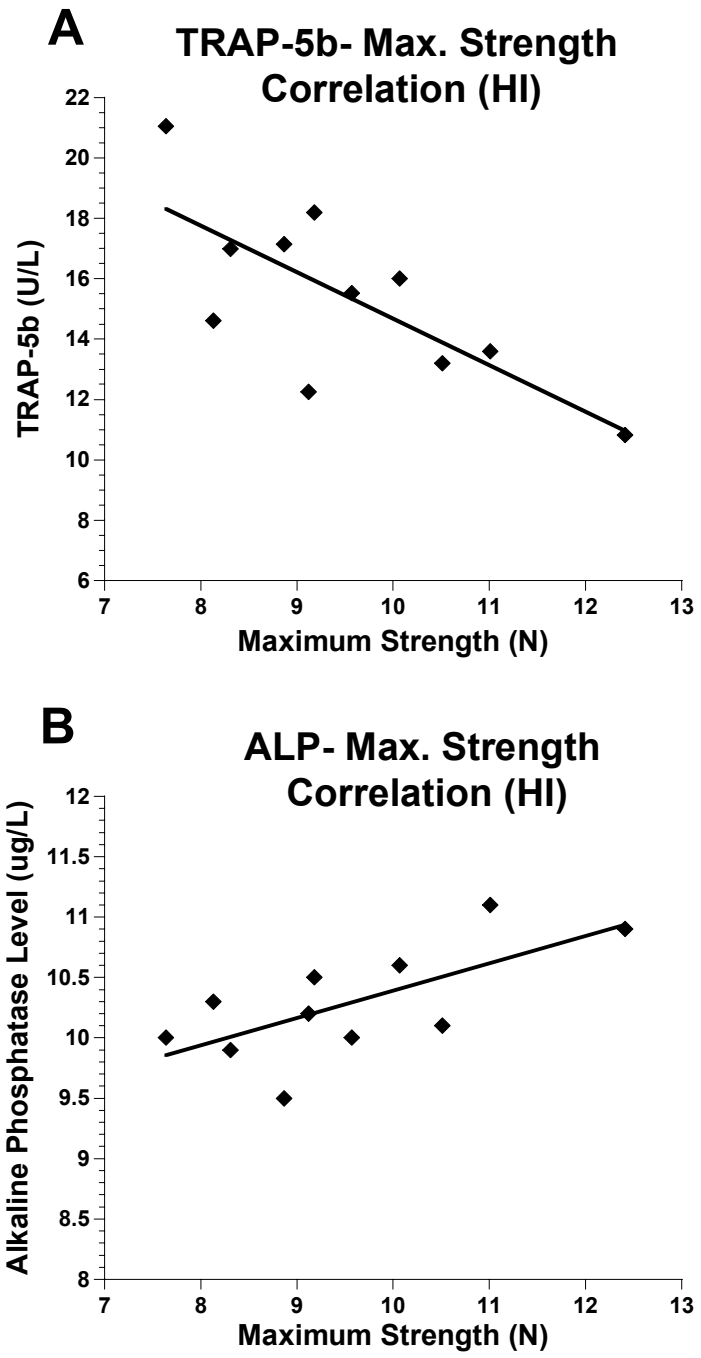

Figure 3.10 Serum TRAP-5b levels (A) negatively correlated to femur maximum strength with correlation coefficient r= -0.74 (p=0.01), while serum ALP levels (B) showed a positive correlation with maximum strength (r= 0.68, p=0.02).

3.3.4 Bone mineral content

Whole femur dry mass measured from LOW and HI groups were significantly lower than VEH (12.2% and 15.9% respectively; $p<0.001$). The reduction in BMC at the epiphysis was greater than in the diaphysis. In the femoral epiphyses, reduction of dry mass in HI group was 9.9% greater than LOW ($P<0.05$)**.** The outcome observed in mineral mass was similar. A dose-dependent decrease in femoral epiphyses was observed in LOW and HI groups. As a result, femur total percent mineralization was decreased by 5.9% and 6.8% ($p<0.05$ vs. VEH), while the decrease in femur epiphyses was 8.9% and 12.5% in LOW and HI groups relative to VEH, respectively ($p<0.001$, Figure 3.11).

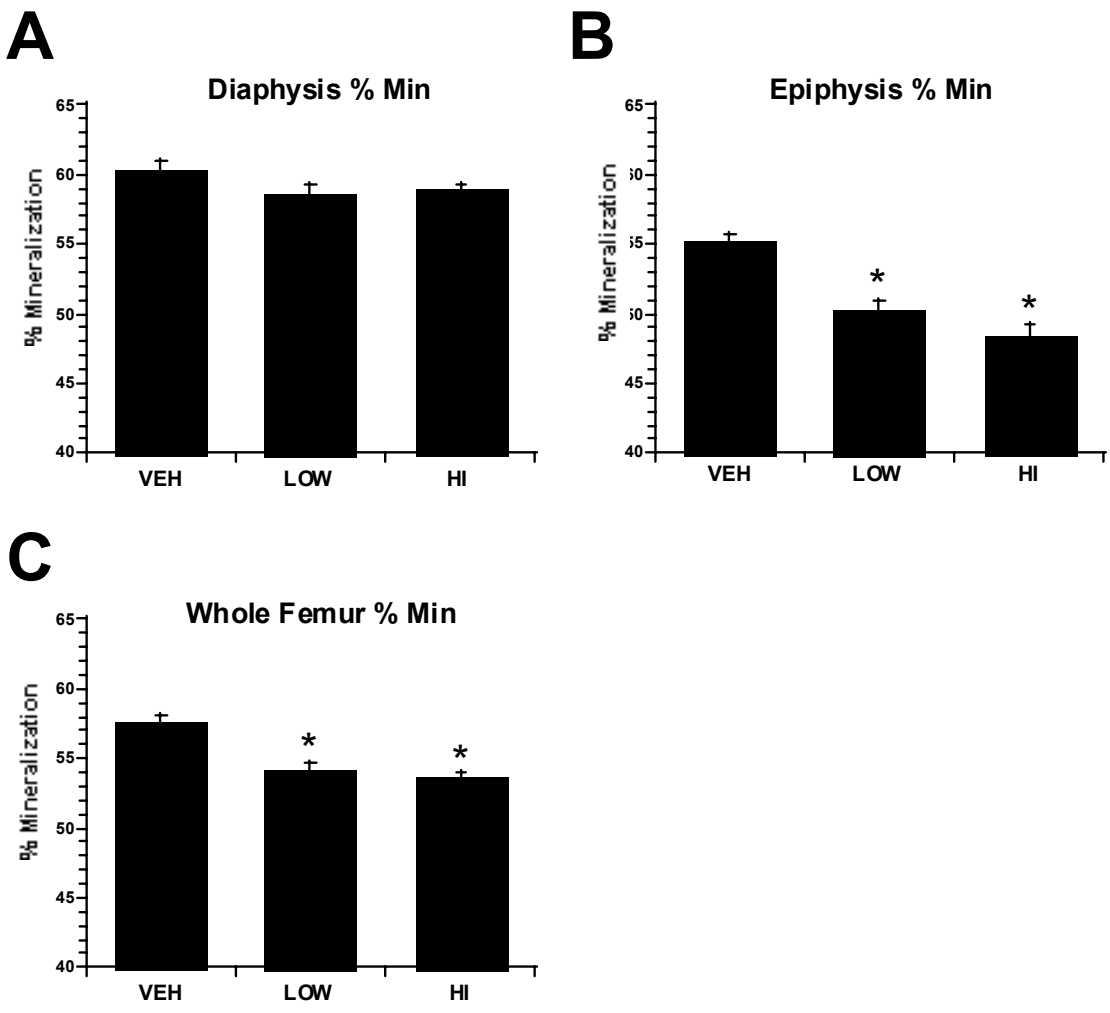

Figure 3.11 RANKL reduced percent mineralization in mice femur. (A) No significant difference in percent mineralization was observed at femur diaphysis. (B) Femur epiphysis %Min was decreased by 8.9% and 12.5% in LOW and HI groups ($p<0.001$), respectively. Dose-dependence manner was observed: Higher dose of RANKL induced lower %Min than lower dosage ($p<0.05$). (C) Femur total %Min was decreased by 5.9% and 6.8% ($p<0.05$) by low and hi dose of RANKL. Data are presented as the mean ± SE. * = significant difference compared to VEH.

3.3.5 Bone volumes indicated by MicroCT

Cortical bone parameters were measured and calculated in an 8 mm span of the femur diaphysis. Moment of inertia at the mid-femur remained unchanged between groups (Figure 3.12). Cortical bone volumes from LOW and HI groups were significantly

lower than VEH (12.5% and 9.4% respectively; $p<0.001$, Figure 3.13A). Trabecular parameters were measured from a 0.9 mm thick section of trabecular bone in proximal tibia. Trabecular volume fraction (BV/TV) was decreased drastically, by 85%, in both RANKL groups compared to VEH ($p<0.001$, Figure 3.13B).

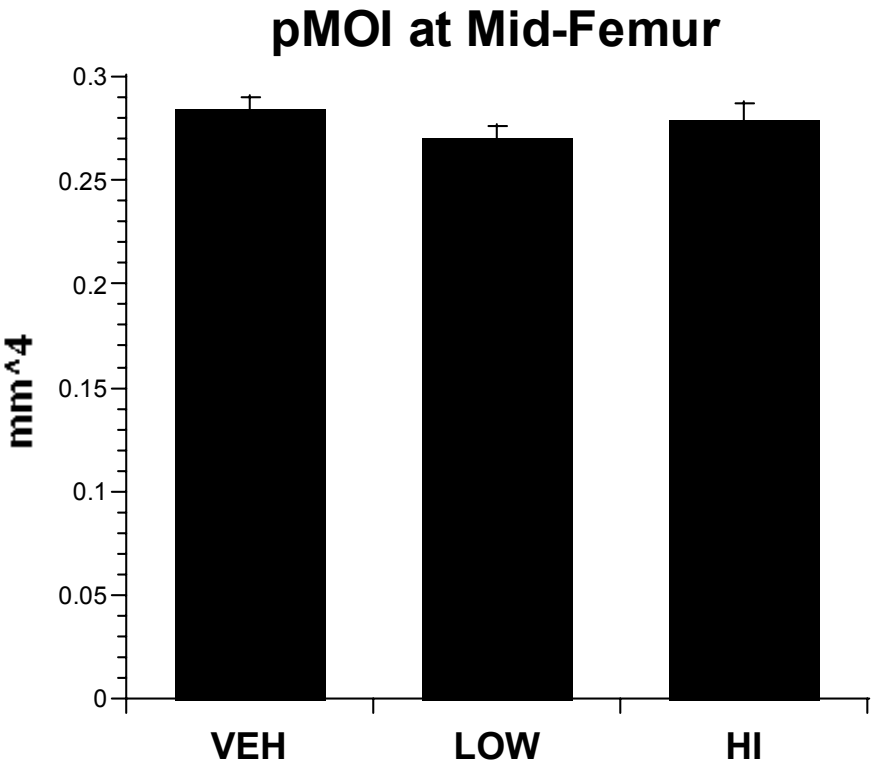

Figure 3.12 No differences were observed in polar moment of inertia at femur mid-diaphysis. Data are presented as the mean ± SE.

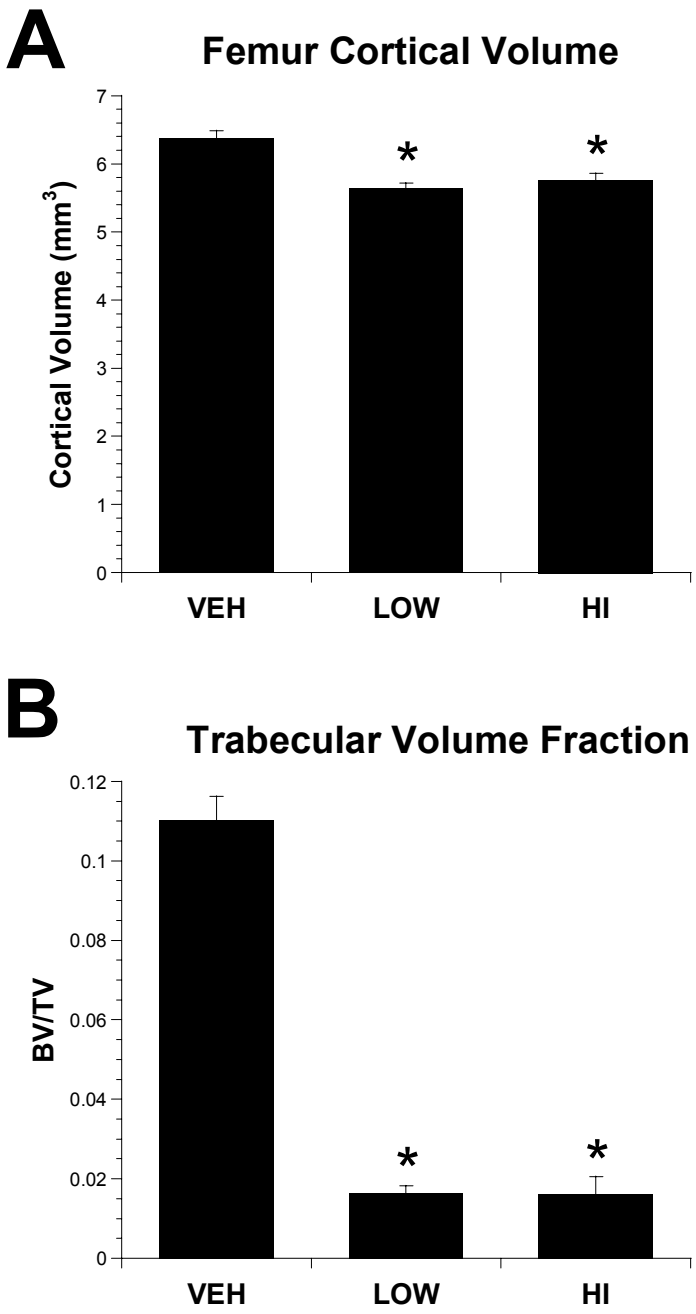

Figure 3.13 RANKL reduced both cortical and trabecular bone volume. (A) Cortical bone volume was measured and calculated in an 8-mm section of femur diaphysis. RANKL significantly reduced cortical bone volume by 13% and 10% in low-and high-dose RANKL groups ($p<0.001$ vs. VEH). (B) Trabecular bone parameters were measured from a 0.9mm section of trabecular bone at proximal tibia. RANKL drastically reduced trabecular bone fraction (BV/TV) in both treatment groups by 85% ($p<0.001$ vs. VEH). Data are presented as the mean ± SE. * = significant difference between VEH.

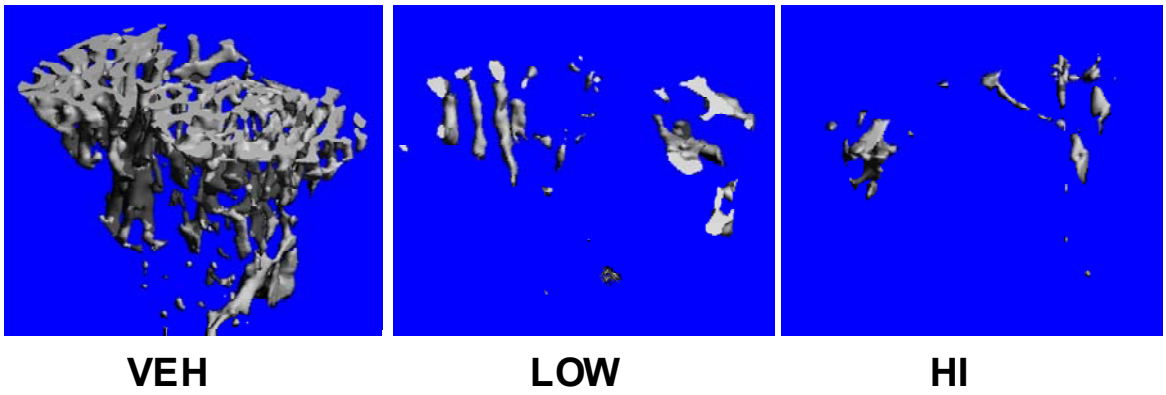

Figure 3.14 3D microCT pictures of 2-mm sections of trabecular bone at proximal tibia illustrate severe bone loss induced by RANKL.

3.3.6 Quantitative histomorphometry

Quantitative histomorphometric analysis (Table 3.1) of the femur mid-diaphysis revealed that endocortical bone resorption was sharply increased in both RANKL treatment groups. Endocortical area was increased by 8.9% and 7.8% ($p<0.05$) in LOW and HI groups, respectively, due to the increase in bone resorption at the endocortical surface; this is evidenced by greater endocortical resorption perimeters of 83% and 79% in LOW and HI groups, respectively. This increase in resorption led to a decrease of cortical area of 6.3% and 7.8% in LOW and HI groups ($p<0.05$), respectively.

RANKL increased cortical bone turnover rate, as evidenced by significant elevations of periosteal bone-formation rate with low-dose (87.3%, $p<0.001$) and high-dose RANKL (63.9%, $p<0.05$) versus VEH. Increases in endocortical bone formation rates were not observed, perhaps because bone resorption on this surface was sufficiently robust to remove the fluorochrome label. Consistently, active mineralizing perimeters were increased for the periosteal surface ($p<0.05$) but decreased at the endocortical surface ($p<0.001$). Similarly, RANKL increased mineral apposition rates in both

periosteal and endocortical surfaces, leading to an increase of 33% ($p<0.001$) and 23% ($p<0.05$) in LOW and HI groups, respectively. Because of the increase in periosteal bone formation and endosteal bone resorption, no significant change was observed in polar moment of inertia of the femur diaphysis.

Table 3.1 Quantitative histomorphometry at femur mid-diaphysis: Measurements were taken from the UV microscope photographs of the mid-diaphysis cross section. Ec = endocortical, Ps = periosteal, Tt = total, Ar = area, B = bone, BFR = bone formation rate, aMPm = active mineralizing perimeter, MAR = mineral apposition rate, Ec.Rs.Pm = endocortical resorption perimeter, pMOI = polar moment of inertia at mid-diaphysis. Data are presented as mean ± SE. *: data are significantly different vs. VEH at $p<0.001$. #: data are significantly different vs. VEH at $p<0.05$. a: $p=0.07$, b: $p=0.06$, c: $p=0.08$.

Measurement	Vehicle	RANKL treated	
		0.4 mg/kg (Low)	2 mg/kg (Hi)
Ec.Ar. (mm^2)	0.90 ± 0.01	0.98 ± 0.02#	0.97 ± 0.01#
Ct. Ar (mm^2)	0.64 ± 0.02	0.60 ± 0.01#	0.59 ± 0.01#
Tt.B.Ar (mm^2)	1.55 ± 0.02	1.57 ± 0.02	1.56 ± 0.01
Ct.Th (mm)	0.151 ± 0.004	0.136 ± 0.002#	0.135 ± 0.002#
Ec.BFR (10^{-3} mm^2/day)	3.76 ± 0.30	2.96 ± 0.14#	3.09 ± 0.32
Ps.BFR (10^{-3} mm^2/day)	1.66 ± 0.18	3.11 ± 0.33*	2.72 ± 0.21#
Tt.BFR (10^{-3} mm^2/day)	5.42 ± 0.36	6.07 ± 0.39	5.81 ± 0.41
Ec.aMPm (mm)	2.24 ± 0.15	1.44 ± 0.05*	1.56 ± 0.13*
Ps.aMPm (mm)	1.14 ± 0.05	1.39 ± 0.10#	1.37 ± 0.05 a
Tt. aMPm (mm)	3.38 ± 0.17	2.83 ± 0.12#	2.93 ± 0.10 b
Ec.MAR (10^{-3} mm/day)	1.68 ± 0.10	2.06 ± 0.07#	1.96 ± 0.11 c
Ps.MAR (10^{-3} mm/day)	1.42 ± 0.11	2.15 ± 0.17*	1.96 ± 0.11#
Tt.MAR (10^{-3} mm/day)	1.60 ± 0.07	2.13 ± 0.09*	1.97 ± 0.10#
Ec.Rs.Pm (mm)	1.12 ± 0.09	2.05 ± 0.09*	2.01 ± 0.12*

3.3.7 Femur diaphysis cortical porosity

Cortical porosity at the femur diaphysis was increased by 25.9% and 45.1% in LOW and HI groups ($p<0.001$) vs. VEH. By separating the femur diaphysis into proximal diaphysis, mid-diaphysis, and distal diaphysis, we found that RANKL had differential effects on these sites (Figure 3.15). Pore size and number at the trochanter (proximal) were increased in both LOW and HI groups, resulting in 54.8% and 82% increase of porosity ($p<0.001$) vs. VEH. In the distal femur, porosity was increased by 38.6% in HI group ($p<0.001$); the change in LOW was not significant. There was a trend towards increased porosity at mid-diaphysis in both RANKL groups ($p=0.08$) compared to VEH.

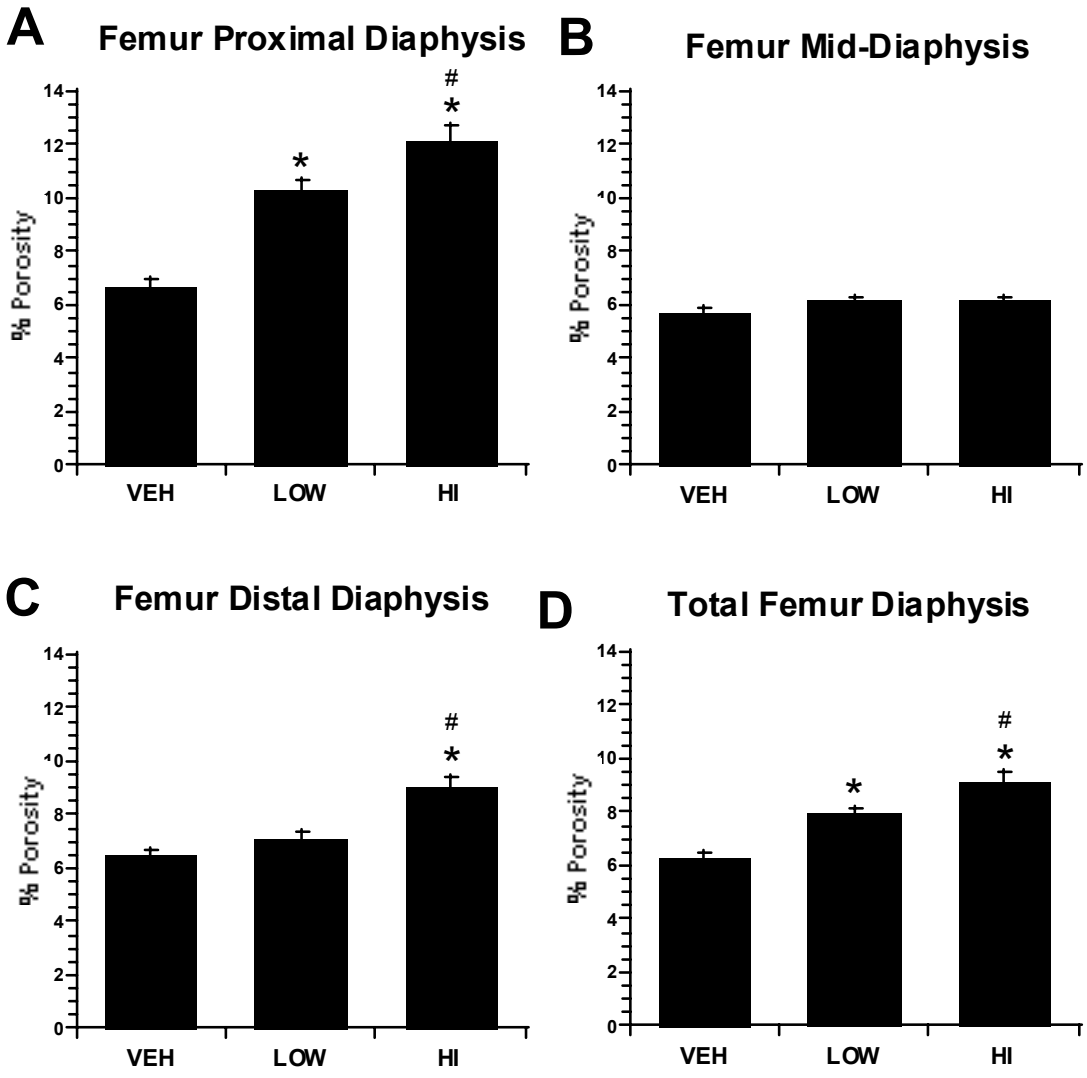

Figure 3.15 RANKL increased cortical porosity at the femur diaphysis. By dividing the femur diaphysis (8mm long scan area) to distal diaphysis (distal 2.5mm), mid-diaphysis (middle 3mm) and proximal diaphysis (proximal 2.5mm), we observed different effects on different sites of femur. (A) At distal femur, high dose RANKL caused an increase of 38.6% in porosity; the change in the low-dose RANKL group was not significant. (B) There was a trend of increased porosity at mid-diaphysis ($p=0.08$) by both doses of RANKL. (C) Both low and hi dose of RANKL increased porosity at the proximal diaphysis (trochanter) by 54.8% and 82% in LOW and HI groups, respectively. (D) Whole femur cortical porosity was increased by 25.9% and 45.1% in LOW and HI groups. Data are presented as mean ± SE. * = $p<0.001$ vs. VEH. # = $p<0.05$ vs. LOW.

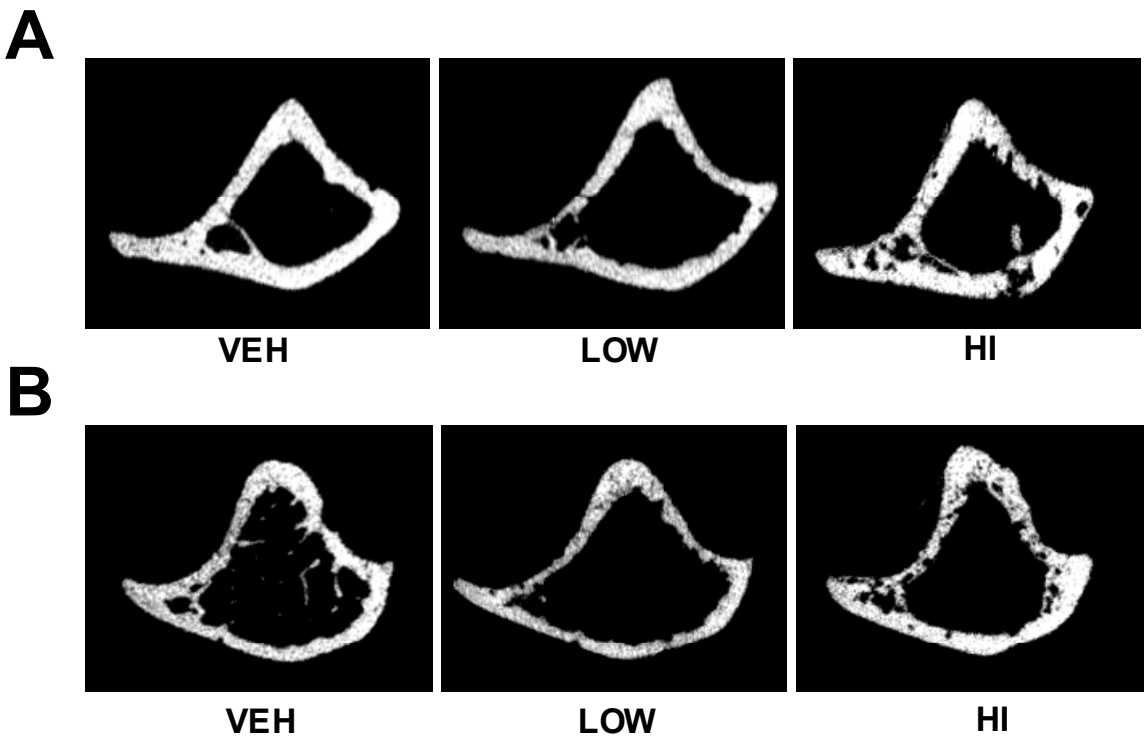

Figure 3.16 2-D microCT images from 4mm to plateau (A) and 2mm to plateau (B) at proximal tibia were taken to demonstrate cortical porosity.

Cortical porosity at the total femur diaphysis was examined for correlations. It was observed to be associated with reduced bone strength, as shown by a negative correlation between porosity in the HI group and the maximum strength of the femur ($R= -0.76$, $p=0.007$, Figure 3.17).

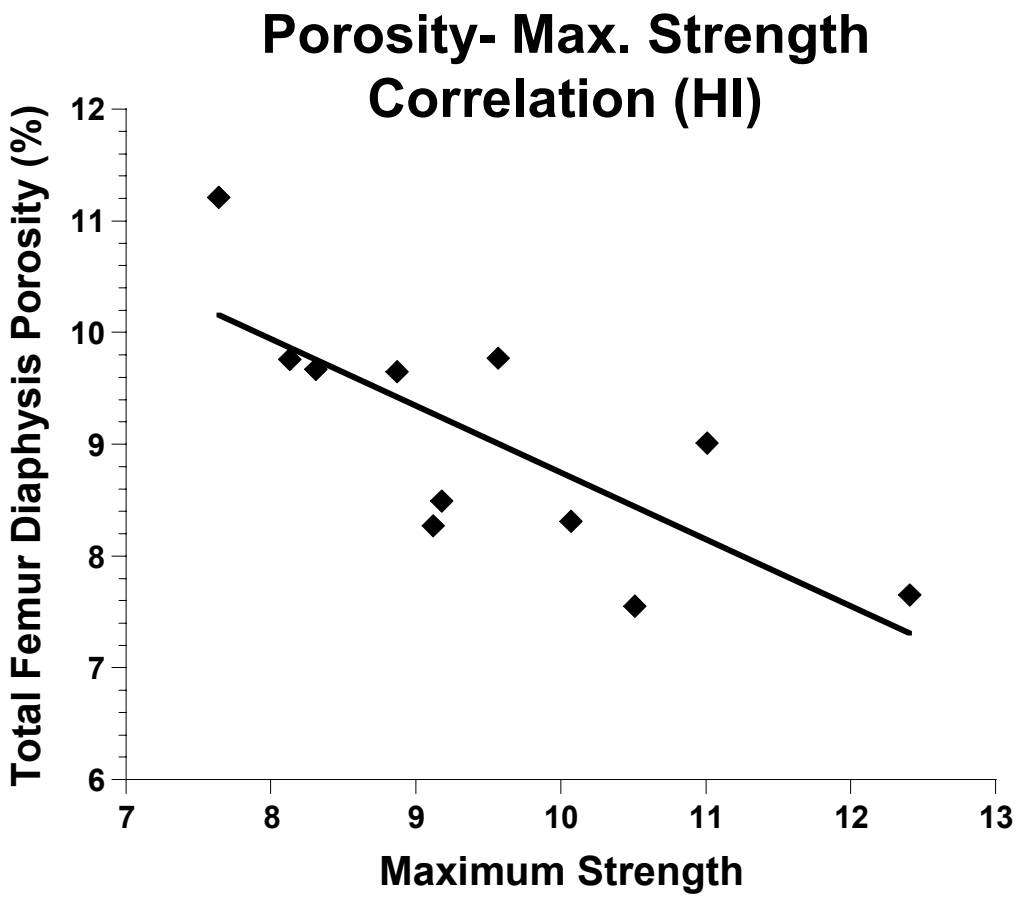

Figure 3.17 In the HI group, whole femur porosity negatively correlated to femur maximum strength with correlation coefficient r= -0.76 (p= 0.007).

3.4 Discussion

High bone turnover is thought to contribute to fracture incidence in postmenopausal osteoporosis subjects (Hochberg, Greenspan et al. 2002). One potential etiological factor in the high turnover state of postmenopausal osteoporosis is RANKL (Eghbali-Fatourechi, Khosla et al. 2003), a TNF family member that is essential for osteoclast formation, function and survival (Lacey, Timms et al. 1998; Lacey, Tan et al. 2000). There are numerous animal models for studying the impact of high-turnover bone disease on bone quality and bone strength, and ovariectomy (OVX) is the most

commonly used. OVX recapitulates many of the important skeletal changes associated with postmenopausal osteoporosis, including increased osteoclast and osteoblast numbers, reduced bone volume and density, and decreased strength of trabecular sites such as the lumbar vertebrae (Kostenuik, Capparelli et al. 2001; Kostenuik, Bolon et al. 2004). While postmenopausal osteoporosis is associated with increased fracture incidence at both cortical and cancellous sites, OVX does not consistently result in reductions in cortical bone strength in mice or rats. We have used soluble RANKL to develop a new animal model of high-turnover bone disease that recapitulates many of the deleterious skeletal changes associated with postmenopausal osteoporosis, including a reduction in the strength of cortical bone. Advantages of this model include its rapidity (10 days) and the lack of surgical intervention.

There are limited data on the direct catabolic effects of RANKL on bone. Short-term (3-day) injection of RANKL resulted in reduced cancellous bone volume and hypercalcemia (Lacey, Timms et al. 1998), but the effects of RANKL injections on bone mineralization, formation, geometry, and strength have not been previously described. In an isolated report, the overexpression of soluble RANKL in transgenic mice was shown to increase bone turnover and reduce bone density and femur strength, suggesting that continuous exposure to excess RANKL can mimic some of the cortical changes associated with postmenopausal osteoporosis (Mizuno, Kanno et al. 2002). However, the skeletal changes in these mice are partially related to overexpression of RANKL during the early growth and development of the skeleton, which would limit the utility of these mice as a model of postmenopausal osteoporosis. In contrast, the direct injection of soluble RANKL can create osteoporosis-like changes that can be monitored over a short

period of time in young or adult animals. An interesting observation with RANKL transgenic mice was that the skeletal phenotype appeared to be less severe than the phenotype associated with OPG knockout mice. This could imply that the local and systemic absence of the endogenous RANKL inhibitor OPG results in skeletal changes that cannot be mimicked by systemic exposure to soluble RANKL. Alternatively, transgene expression may have been too modest in these animals to fully overcome the local inhibitory effects of OPG. The latter possibility is supported by the current data, wherein the direct injection of high doses of soluble RANKL created a skeletal phenotype that was very similar to that associated with the total ablation of OPG (Bucay, Sarosi et al. 1998; Mizuno, Amizuka et al. 1998; Min, Morony et al. 2000; Nakamura, Udagawa et al. 2003). The phenotypic similarities included increased serum alkaline phosphatase, decreased bone volume and density, reduced mineralization, increased cortical porosity and reduced strength.

The ability of soluble RANKL to increase local and systemic bone resorption parameters was shown by increases in endocortical resorption, cortical porosity, and serum TRAP-5b (a specific marker of osteoclasts). While intracortical remodeling is not a common finding in mice, it appears that excessive RANKL activity can lead to this pathologic change. The strong negative correlation between cortical porosity and bone strength suggests a possible mechanism by which excessive RANKL activity might contribute to reduced cortical bone quality and strength.

Increased endocortical bone resorption perimeter was associated with an enlarged medullar cavity and a decrease in cortical area and thickness. These results are consistent with the previous finding that OPG knockout mice have increased endocortical osteoclast

surface, which was reversed by the transgenic overexpression of soluble OPG (Min, Morony et al. 2000). Another negative consequence of high bone turnover is an increase in cortical porosity. Increased cortical porosity appears to account for a substantial age-related decline in bone strength (McCalden, McGeough et al. 1993), and cortical porosity in hip fracture cases shows a distinct regional (non-homogenous) distribution (Bell, Loveridge et al. 1999). In our study, administration of RANKL induced cortical porosity of the femur by increasing both the size and number of pores. Cortical porosity was region-specific, with significant increases observed in the proximal and distal metaphyses of the femoral diaphysis but not the mid-diaphysis. Despite the lack of porosity at the mid-diaphysis, bone strength at this location was reduced by RANKL based on 3-point bending tests that created mid-shaft fractures. This location was associated with increased endocortical area and reduced cortical thickness, area and volume, which were likely contributors to the observed reduction in bone strength. The potential contribution of porosity to reduced bone strength at the distal and proximal femur shaft was not determined, and would be better studied in larger species such as the rat. Compositional analysis data of the femora revealed reduced mineralization with RANKL injections. The dose-dependent reduction in percent mineralization was more significant in trabecular bone than in cortical bone, suggesting changes in materials properties in addition to structural changes described.

Previous studies have shown that markers of bone formation (e.g. serum alkaline phosphatase) tend to increase following periods of bone resorption, due to the normal physiological coupling between osteoblasts and osteoclasts (Bucay, Sarosi et al. 1998; Nakamura, Udagawa et al. 2003). In this study, RANKL injections increased local and

systemic bone formation paramaters, as indicated by a 3- to 4-fold increase in serum ALP levels and a significant increase in periosteal bone formation rate. The increase in bone formation is likely related to normal physiological coupling, a process that is preserved in settings of RANKL inhibition (Nakamura, Udagawa et al. 2003). Our data suggest that excessive RANKL also leads to a coupling-related increase in bone formation. While positive, the compensatory effect of RANKL on periosteal bone formation was apparently insufficient to counteract deleterious effects on endocortical area and cortical thickness, area and volume. These cortical changes are somewhat reminiscent of changes that were recently described in a longitudinal analysis of cortical bone geometry in subjects with postmenopausal osteoporosis (Ahlborg, Johnell et al. 2003). Menopause was accompanied by a progressive decrease in femur BMD and an increase in endocortical diameter, while periosteal diameter increased over time. It was proposed that this periosteal expansion may occur as a naturally reaction to the menopause-related decline in BMD and increase in endocortical resorption (Ahlborg, Johnell et al. 2003). In our study, increased periosteal bone formation may have contributed to the maintenance of a normal polar moment of inertia at the femur diaphysis, despite the increase in endocortical area. This constructive periosteal response may have helped to limit the loss of cortical bone strength associated with RANKL injections, but longer-term follow up would be required to determine if absolute periosteal expansion occurs in association with RANKL injections and if the new bone is of a competent nature with appropriate material properties.

This study has some limitations, including the lack of an obvious dose-response for many of the endpoints. We believe that a lower dose range would have provided a

clearer dose response for the majority of parameters. Dose-dependent weight loss and hypercalcemia are consistent with the notion that the twice-daily injection of RANKL at 2 mg/kg was an excessive dose that resulted in toxicity. It remains possible that a once-daily dose of RANKL at 0.4 mg/kg or lower could recapitulate many of the deleterious skeletal effects we describe with twice-daily dosing, but without signs of the harmful response. Another limitation is that we did not study changes in cancellous bone compartments, primarily because mice have modest cancellous bone volume and the biomechanical testing of mouse vertebrae is challenging. Rat studies would be a preferred model for characterizing the effects of RANKL on cancellous bone, and preliminary data have been recently described (Yuan, Kostenuik et al. 2006 (Abstract)).

3.5 Conclusions

In this study, we have demonstrated that the direct injection of soluble recombinant RANKL levels caused severe and rapid catabolic effects on both trabecular and cortical bone. These effects include increased bone resorption, reduction of cortical and trabecular mineral content, reduction of cortical and trabecular bone volume, increase in cortical bone porosity, and reduction of cortical bone strength. These data establish a new non-surgical model for rapid bone loss in mice, which is characterized by cortical and cancellous changes that are similar to those associated with OPG gene ablation and more severe than those associated with ovariectomy. The ability of systemic RANKL injections to mediate these changes suggests that soluble RANKL could be involved in pathologic bone loss, although further studies are clearly needed to evaluate the relative role of soluble versus membrane RANKL in the regulation of bone resorption. This model may be relevant for bone loss initiated by local and/or systemic changes that are

associated with osteoporosis and joint destruction associated with inflammation (Kong, Feige et al. 1999; Eghbali-Fatourechi, Khosla et al. 2003).

3.6 References

Ahlborg, H. G., O. Johnell, et al. (2003). "Bone loss and bone size after menopause." N Engl J Med **349**(4): 327-34.

Ammann, P. and R. Rizzoli (2003). "Bone strength and its determinants." Osteoporos Int **14 Suppl 3**: S13-8.

Bell, K. L., N. Loveridge, et al. (1999). "Regional differences in cortical porosity in the fractured femoral neck." Bone **24**(1): 57-64.

Broz, J. J., S. J. Simske, et al. (1993). "Effects of rehydration state on the flexural properties of whole mouse long bones." J Biomech Eng **115**(4A): 447-9.

Bucay, N., I. Sarosi, et al. (1998). "osteoprotegerin-deficient mice develop early onset osteoporosis and arterial calcification." Genes Dev **12**(9): 1260-8.

Dufresne, T. (1998). "Segmentation techniques for analysis of bone by three-dimensional computed tomographic imaging." Technol Health Care **6**(5-6): 351-9.

Eghbali-Fatourechi, G., S. Khosla, et al. (2003). "Role of RANK ligand in mediating increased bone resorption in early postmenopausal women." J Clin Invest **111**(8): 1221-30.

Heaney, R. P. (2003). "Is the paradigm shifting?" Bone **33**(4): 457-65.

Hochberg, M. C., S. Greenspan, et al. (2002). "Changes in bone density and turnover explain the reductions in incidence of nonvertebral fractures that occur during treatment with antiresorptive agents." J Clin Endocrinol Metab **87**(4): 1586-92.

Hofbauer, L. C. and A. E. Heufelder (2001). "Role of receptor activator of nuclear factor-kappaB ligand and osteoprotegerin in bone cell biology." J Mol Med **79**(5-6): 243-53.

Kanamaru, F., H. Iwai, et al. (2004). "Expression of membrane-bound and soluble receptor activator of NF-kappaB ligand (RANKL) in human T cells." Immunol Lett **94**(3): 239-46.

Khosla, S. (2001). "Minireview: the OPG/RANKL/RANK system." Endocrinology **142**(12): 5050-5.

Kong, Y. Y., U. Feige, et al. (1999). "Activated T cells regulate bone loss and joint destruction in adjuvant arthritis through osteoprotegerin ligand." Nature **402**(6759): 304-9.

Kostenuik, P. J., B. Bolon, et al. (2004). "Gene therapy with human recombinant osteoprotegerin reverses established osteopenia in ovariectomized mice." Bone **34**(4): 656-64.

Kostenuik, P. J., C. Capparelli, et al. (2001). "OPG and PTH-(1-34) have additive effects on bone density and mechanical strength in osteopenic ovariectomized rats." Endocrinology **142**(10): 4295-304.

Kostenuik, P. J. and V. Shalhoub (2001). "Osteoprotegerin: a physiological and pharmacological inhibitor of bone resorption." Curr Pharm Des **7**(8): 613-35.

Lacey, D. L., H. L. Tan, et al. (2000). "Osteoprotegerin ligand modulates murine osteoclast survival in vitro and in vivo." Am J Pathol **157**(2): 435-48.

Lacey, D. L., E. Timms, et al. (1998). "Osteoprotegerin ligand is a cytokine that regulates osteoclast differentiation and activation." Cell **93**(2): 165-76.

McCalden, R. W., J. A. McGeough, et al. (1993). "Age-related changes in the tensile properties of cortical bone. The relative importance of changes in porosity, mineralization, and microstructure." J Bone Joint Surg Am **75**(8): 1193-205.

Min, H., S. Morony, et al. (2000). "Osteoprotegerin reverses osteoporosis by inhibiting endosteal osteoclasts and prevents vascular calcification by blocking a process resembling osteoclastogenesis." J Exp Med **192**(4): 463-74.

Mizuno, A., N. Amizuka, et al. (1998). "Severe osteoporosis in mice lacking osteoclastogenesis inhibitory factor/osteoprotegerin." Biochem Biophys Res Commun **247**(3): 610-5.

Mizuno, A., T. Kanno, et al. (2002). "Transgenic mice overexpressing soluble osteoclast differentiation factor (sODF) exhibit severe osteoporosis." J Bone Miner Metab **20**(6): 337-44.

Nakamura, M., N. Udagawa, et al. (2003). "Osteoprotegerin regulates bone formation through a coupling mechanism with bone resorption." Endocrinology **144**(12): 5441-9.

Nakashima, T., Y. Kobayashi, et al. (2000). "Protein expression and functional difference of membrane-bound and soluble receptor activator of NF-kappaB ligand: modulation of the expression by osteotropic factors and cytokines." Biochem Biophys Res Commun **275**(3): 768-75.

Parfitt, A. M., M. K. Drezner, et al. (1987). "Bone histomorphometry: standardization of nomenclature, symbols, and units. Report of the ASBMR Histomorphometry Nomenclature Committee." J Bone Miner Res **2**(6): 595-610.

Roodman, G. D. and J. J. Windle (2005). "Paget disease of bone." J Clin Invest **115**(2): 200-8.

Ruegsegger, P., B. Koller, et al. (1996). "A microtomographic system for the nondestructive evaluation of bone architecture." Calcif Tissue Int **58**(1): 24-9.

Simonet, W. S., D. L. Lacey, et al. (1997). "Osteoprotegerin: a novel secreted protein involved in the regulation of bone density." Cell **89**(2): 309-19.

Suda, T., N. Takahashi, et al. (1999). "Modulation of osteoclast differentiation and function by the new members of the tumor necrosis factor receptor and ligand families." Endocr Rev **20**(3): 345-57.

Suzuki, J., T. Ikeda, et al. (2004). "Regulation of osteoclastogenesis by three human RANKL isoforms expressed in NIH3T3 cells." Biochem Biophys Res Commun **314**(4): 1021-7.

Takahashi, N., N. Udagawa, et al. (1999). "A new member of tumor necrosis factor ligand family, ODF/OPGL/TRANCE/RANKL, regulates osteoclast differentiation and function." Biochem Biophys Res Commun **256**(3): 449-55.

Turner, C. H. (2002). "Biomechanics of bone: determinants of skeletal fragility and bone quality." Osteoporos Int **13**(2): 97-104.

Yasuda, H., N. Shima, et al. (1998). "Osteoclast differentiation factor is a ligand for osteoprotegerin/osteoclastogenesis-inhibitory factor and is identical to TRANCE/RANKL." Proc Natl Acad Sci U S A **95**(7): 3597-602.

Yuan, Y. Y., P. J. Kostenuik, et al. (2006 (Abstract)). "RANKL infusion as a disease model: Implications for bone and vascular systems." J Bone Min Res **21**: S163.

CHAPTER 4

RANKL INFUSION AS A DISEASE MODEL: INDICATIONS ON SKELETAL DETERIORATION

Data related to this chapter has been submitted as a manuscript to *Journal of Bone and Mineral Research.* Contents presented here are the manuscript formatted following dissertation requirements.

4.1 Introduction

Bone remodeling is a continuous lifelong process that plays an important role in regulating bone structure and function. Bone remodeling is homeostatic when the amount of bone resorbed during each remodeling cycle is matched by subsequent bone formation and refilling of the remodeling site. Bone resorption exceeds bone formation in many pathological states, leading to net bone loss, inferior bone architecture, and increased fracture risk (Coleman 1997; Hofbauer and Schoppet 2004; Blair, Zhou et al. 2006). The bone remodeling process is regulated by a variety of hormones and cytokines (Teitelbaum 2000; Boyle, Simonet et al. 2003), including parathyroid hormone (PTH), interleukin-1 (IL-1), tumor necrosis factor α (TNF-α), transforming growth factor β (TGF-β), vitamin D3, and macrophage colony stimulating factor (M-CSF) (Suda, Takahashi et al. 1999; Teitelbaum 2000; Boyle, Simonet et al. 2003; Zaidi, Blair et al. 2003). The initiation of bone remodeling requires the presence and activity of RANKL (Receptor Activator of Nuclear Factor κB Ligand) (Morony, Capparelli et al. 1999).

RANKL is a member of TNF superfamily that is expressed by osteoblasts (Fuller, Wong et al. 1998), bone marrow stromal cells (Eghbali-Fatourechi, Khosla et al. 2003), and activated T-cells (Anderson, Maraskovsky et al. 1997). RANKL stimulates bone resorption by binding to its receptor, RANK, on the surface of osteoclasts and their precursors, thereby promoting osteoclast formation, function and survival (Lacey, Timms et al. 1998; Yasuda, Shima et al. 1998). OPG is a soluble decoy receptor for RANKL, and its binding to RANKL inhibits bone resorption and prevents bone loss by preventing RANKL-RANK interactions (Simonet, Lacey et al. 1997; Tsuda, Goto et al. 1997).

The RANKL:OPG ratio might represent a potentially important determinant of bone remodeling (Nagai and Sato 1999; Fazzalari, Kuliwaba et al. 2001), and an increased RANKL:OPG ratio is evident in various bone diseases (Haynes, Crotti et al. 2001; Grimaud, Soubigou et al. 2003; Stilgren, Rettmer et al. 2004). Estrogen deficiency in postmenopausal women is associated with enhanced RANKL expression by stromal cells and T cells, and low bone mineral density (Eghbali-Fatourechi, Khosla et al. 2003). In an inflammatory environment, such as in rheumatoid arthritis, cytokines released by the immune cells increase the RANKL/OPG ratio and lead to joint destruction and bone loss (Kong, Feige et al. 1999; Lubberts, van den Bersselaar et al. 2003; Stolina, Adamu et al. 2005). RANKL also plays an important role in malignant diseases, such as multiple myeloma and osteolytic bone metastases. Myeloma cells enhance RANKL release and down-regulate OPG expression, thereby increasing bone resorption and promoting bone loss (Giuliani, Bataille et al. 2001; Standal, Seidel et al. 2002). In osteolytic bone metastases, such as breast and lung cancer, tumor cells directly express RANKL and/or

indirectly increase RANKL levels through expression of PTH related peptide (PTHrP), resulting in bone lesions (Michigami, Ihara-Watanabe et al. 2001; Mundy 2002).

There are at least 3 isoforms of RANKL, including membrane-bound and soluble forms. The membrane-bound form is the likely candidate for mediating osteoclastogenic responses that require cell-cell contact in certain co-culture systems (Fuller, Gallagher et al. 1991). The soluble forms of RANKL are either directly secreted, or enzymatically cleaved from the cell surface (Ikeda, Kasai et al. 2001; Suzuki, Ikeda et al. 2004). The relative contribution of soluble versus membrane-bound RANKL to bone turnover is unclear, and may differ with normal versus pathological bone remodeling. Increased soluble RANKL was observed in the serum of animals with high-turnover bone disease associated with inflammatory arthritis (Stolina, Adamu et al. 2005). Increased serum RANKL was also reported in patients with high-turnover bone disease (Franchimont, Reenaers et al. 2004; Morabito, Gaudio et al. 2004; Avbersek-Luznik, Balon et al. 2005; Geusens, Landewe et al. 2006; Kim, Kim et al. 2006). Reports of upregulated membrane RANKL are sporadic, perhaps due to the more cumbersome nature of such analyses compared to ELISA-based serum assays. In one example, postmenopausal subjects showed higher levels of RANKL on the surface of bone marrow cells compared to premenopausal subjects, while no menopause-related differences in soluble RANKL were observed in peripheral blood(Eghbali-Fatourechi, Khosla et al. 2003). Circulating levels of soluble RANKL are very low, and are frequently below the detection limits of presently available ELISA assays (Abrahamsen, Hjelmborg et al. 2005). It remains unclear as to whether changes in serum RANKL are reflective of changes found within

bone, which further confounds attempts to deduce from observational studies the potential consequences of excessive RANKL on bone.

To study the skeletal pathologies associated with increased RANKL levels, we created an animal model using normal rats exposed to four-week continuous administration of soluble human RANKL via osmotic pumps. We hypothesized that excessive RANKL levels would create a spectrum of skeletal changes that are typically associated with high-turnover bone loss conditions, including reduced bone mass, density and strength in association with the deterioration of cancellous bone architecture and cortical bone geometry. The RANKL/OPG system has also been implicated in vascular disease, as evidenced by the development of arterial calcification in OPG deficient mice (Min, Morony et al. 2000). We therefore harvested aortas at the end of the study to evaluate mineral content as a surrogate for vascular calcification.

4.2 Materials and Methods

4.2.1 Study design

The form of human RANKL used in all studies comprised amino acids 143-317, a region that includes the entire active ligand moiety distal to the extracellular cleavage site, as previously described (Lacey, Timms et al. 1998). This construct, which lacks transmembrane and intracellular domains, was expressed in Chinese hamster ovary (CHO) cells and purified at Amgen. The purified protein had a molecular weight of 27 kD. A pilot study was performed to determine safe, effective doses for continuous RANKL administration to rats. Twenty Sprague-Dawley (SD, Harlan, Indianapolis) rats six months of age were assigned to five groups of four rats per group. Alzet osmotic pumps (2ML2) implanted subcutaneously in the rats for 14 days administered RANKL at

10, 50, 100, 200, and 400 μg/kg/day dosages. Blood was collected daily from each specimen via the saphenous vein to examine ionized calcium levels. The two highest doses of RANKL led to significant and dose-dependent hypercalcemia (Figure 4.1), with the 200 μg/kg/day rats recovering weight loss relatively quickly (data not shown), indicating that this dosage has less toxicity. We therefore selected a lower dose of 175 ug/kg/day as the highest dose to study skeletal catabolism, as well as a 5-fold lower one (35 ug/kg/day) to examine the lowest effective dosage .

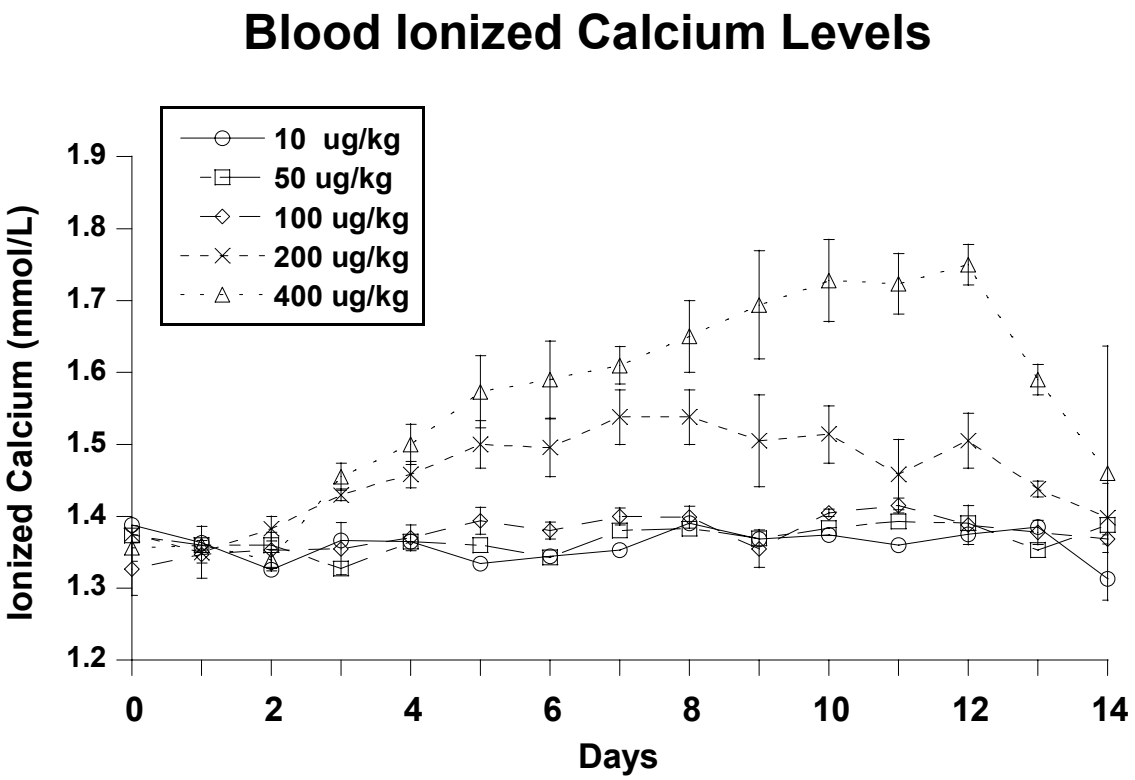

Figure 4.1 Five groups of SD rats (n=4) received 14 days RANKL infusion at 10, 50, 100, 200 and 400 μg/kg/day dosages in the pilot study. Blood was collected daily, and ionized-calcium levels were examined as the efficacy indicator for RANKL administration. Rats treated with 200 and 400 μg/kg/day RANKL experienced a significant hypercalcemia, which recovered to baseline level at the end of the study. Data are presented as the mean ± SE.

For the main study, 36 male SD rats approximately 6 months of age were assigned to 3 groups: VEH (Vehicle control, phosphate buffered saline, n=12), LOW (low dose RANKL, 35 μg/kg/day, n=12) and HI (high dose RANKL, 175 μg/kg/day, n=12). On Day 0, surgeries were performed to insert the osmotic pumps (Alzet 2ML4) subcutaneously (dorsal region) into the rats (Figure 4.2). Treatments were delivered at a constant rate of 2.5 μl per hour in the body environment for 28 days. Injection of 20 mg/kg calcein (*i.p.*) at days 2 and 26 provided fluorescent labels to monitor new bone growth. To achieve serial serum data, blood was collected intermittently at Days 0, 3, 7, 14, and 21 from the saphenous vein and at Day 28 via cardiac puncture and exsanguination.

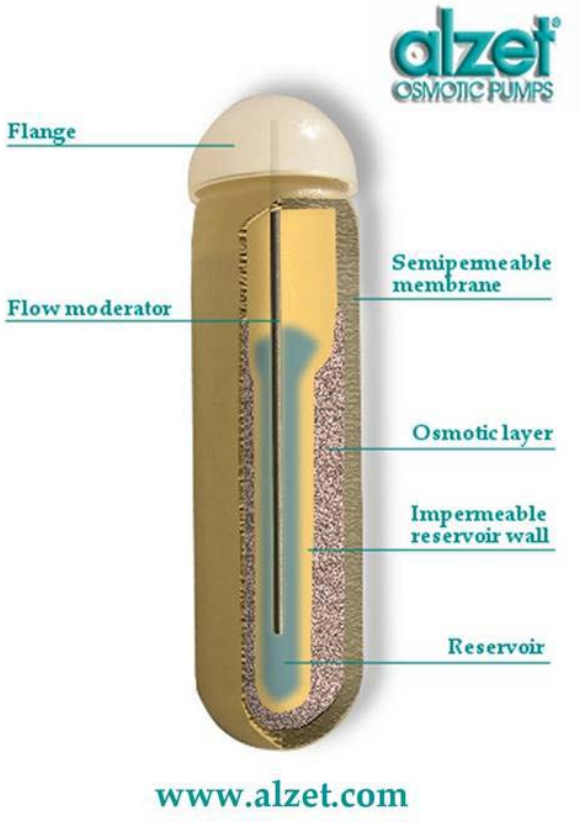

Figure 4.2 Diagram of Alzet osmotic pumps for drug delivery

At sacrifice, pumps were removed and residual drug volumes were checked to ensure drug delivery. Hind limbs were collected and cleaned of all non-osseous tissue; and the arterial trunks dissected. Throughout the experiment, all procedures conformed to the guidelines of Clemson University's Institutional Animal Care and Use Committee (Figure 4.3).

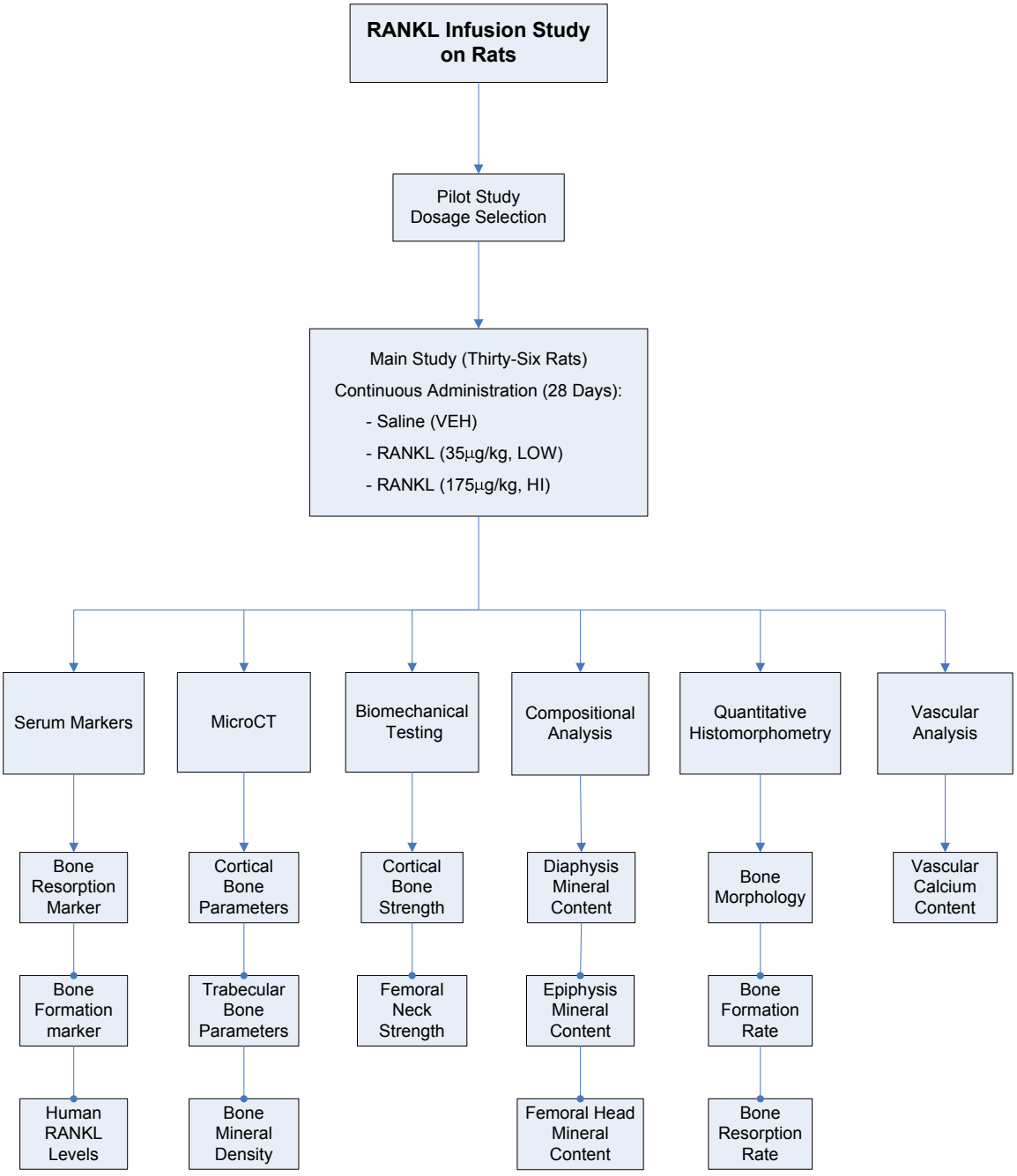

Figure 4.3 Flowchart illustrating the study design of the RANKL infusion study

4.2.2 Serum bone-turnover markers

Serum was collected at the time points identified. Osteocalcin and TRAP-5b were measured by ELISA (SBA Science/IDS Inc.) as bone formation and resorption markers, respectively. Human RANKL levels were quantified via ELISA on Day 28, using an ELISA kit (SBA Science/IDS Inc.).

4.2.3 Micro CT

A Scanco micro CT system (μCT20, Scanco Medical AG, Bassersdorf, Switzerland) was used to obtain both trabecular (11 μm voxel size) and cortical parameters (13 μm voxel size). Right tibiae were separated and fixed in 10% neural buffered formalin for 48 hours, then stored in 70% ethanol. Trabecular bone parameters were obtained by analyzing 1.65mm (150 slices) trabecular bone immediately distal to the growth plate at the proximal end of the tibia. These parameters include total volume (TV), trabecular bone volume (BV), percent connectivity of trabecular struts, and trabecular volume fraction (BV/TV). Bone mineral density data were also obtained from the CT scans. A phantom (Scanco) with increasing density hydroxyapatite columns was scanned by microCT; the linear curve of hydroxyapatite content was used as the standard curve to obtain the mineral content of the bones. Bone density data were calibrated to milligrams of hydroxyapatite per cubic centimeter.

Left femora were air-dried and scanned for cortical parameters. A 24 mm length of femoral diaphysis was analyzed with a total of 49 slices at 500 μm increments between slices (13 μm voxel size with 487 μm void space between slices). Cortical volume and polar moment of inertia (pMOI) data were obtained using IPL-Moment-of-Inertia software (Scanco).

4.2.4 Biomechanical testing

Mechanical properties were determined from femoral diaphyses and necks. After the cortical bone was scanned, left femora were rehydrated in phosphate buffered saline (PBS) for 90 min prior to testing to mimic *in vivo* properties (Broz, Simske et al. 1993). Three-point bending tests were performed using an Instron 5582 (Merlin, Series IX software); femora were tested to failure with a 24 mm span length and 5mm/min deflection rate. The force-deflection curves were analyzed to determine the strengths and deflections at the elastic, maximum, and failure limits. Stiffness was calculated by dividing elastic strength by elastic deflection.

Right femora were air-dried and sectioned at the middle of the third trochanter. The proximal portions were embedded vertically in noninfiltrating Epo-Kwick epoxy (Buehler, Lake Bluff, IL) from the mid-trochanter to 2 mm distal to the base of the femoral neck (Ross, Bateman et al. 2001). Disks were rehydrated in PBS for 90 minutes prior to testing and then placed firmly in the Instron 5582. Loads were applied on the heads of the femora with a rate of 5mm/min until failure (Figure 4.4). Strengths, deflections, and stiffness were analyzed as previously described.

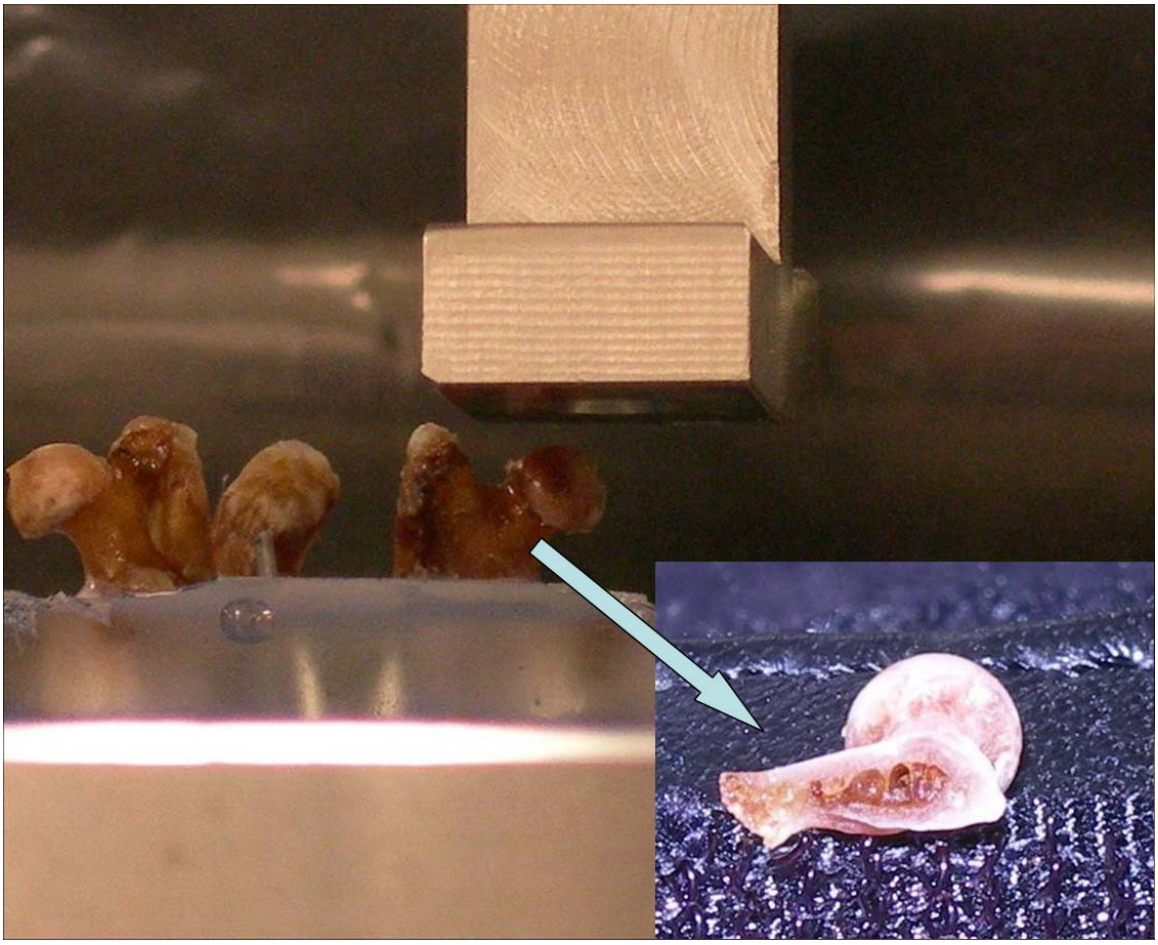

Figure 4.4 Photograph of mechanical test on femoral neck

4.2.5 Mineral content analysis

Distal epiphyses, femoral diaphyses and femoral head were separated from the fractured left femur. Mineral content data were obtained separately from each of these parts. Dry mass (Dry-M) was measured after heating the bones for 24 h at 105 ºC. Mineral mass (Min-M) was measured after the bones had been ashed by baking for another 24h at 800 ºC. Organic mass (Org-M) was calculated as Dry-M minus Min-M. Percent mineralization (%Min) was calculated by the formula % Min = Min-M/Dry-M * 100%.

4.2.6 Quantitative histomorphometry

The distal portions of the right femora were placed in 10% neutral-buffered formalin for 48 hours, rinsed with distilled water, and stored in ethanol. Bones were then air-dried for 96 hours and embedded with noninfiltrating Epo-Kwick epoxy (Buehler). Disks were sectioned using a low-speed saw (Buehler, 12.7cm x 0.5mm diamond blade) at the mid-diaphysis. The distal sections were wheel-polished to a flat, smooth surface using 600-, 800- and 1200-grit carbide paper followed by polishing with a cloth impregnated with 6 μm diamond paste. This allowed micrographs (25X magnification) of the bone cross-sections under a far blue light (400nm wavelength). Calcein labels in bone fluoresce green, identifying bone formation sites during the period of the study. Quantitative histomorphometric analyses were performed using SigmaScan Pro software (SPSS, San Rafael, CA) on these photographs.

Measurements of bone morphology included total bone area (T.B.Ar) enclosed by periosteal perimeter and endocortical area (Ec.Ar) (Parfitt, Drezner et al. 1987). Cortical area was calculated as T.B.Ar – Ec.Ar. At the periosteal surface, area between labels was measured as periosteal bone formation area (Ps.BFA); linear content of the labeled area was defined as active mineralizing perimeter (Ps.AMPm). Periosteal bone formation rates were calculated by dividing the 24 days between the two injected labels by periosteal bone formation area (Ps. BFR = Ps. BFA/24) and mineral apposition rate as Ps.MAR = Ps.BFR/Ps.AMPm. At the endosteal surface, endocortical bone resorption perimeter (Ec.Rs.Pm) was measured by quantifying the portion of the nonlabeled surface with rough border. Bone formation was not quantified on the endocortical surface because a

significant portion of the calcein labels was clearly eroded in many of the rats, making accurate measurements not possible.

4.2.7 Vascular analysis

At sacrifice, after removal of hind limbs, the entire arterial trunk from the aortic arch to the bifurcation of the iliac arteries was dissected manually from each rat. After being rinsed in saline, the abdominal aorta segment (1-1.5 cm length) was processed for calcium analysis. Tissues were lyophilized, weighed, and dry weight was recorded. Dry samples were placed in 1 ml 6 N HCl and completely hydrolyzed in a boiling water bath for 8 hours. Samples were evaporated under a continuous stream of nitrogen gas; residual material was dissolved in 1 ml 0.01 N HCl. Calcium content was determined with an atomic absorption spectrophotometer (Perkin-Elmer Model 3030, Perkin-Elmer, Norwalk, CT). Values are expressed as μg calcium/mg dry aorta (Analysis above was performed by Dan Simionescu and Dina Basalyga).

4.2.8 Statistics

Statistical comparisons were performed using repeated measures of analysis of variance (ANOVA) with SigmaStat software. One-way ANOVAs, with a Tukey test for follow-up comparisons, were used. A 95% level of significance (type I error) was used for each of these tests. The correlation between serum TRAP-5b levels and bone strength was obtained from Pearson Product Moment Correlation test with SigmaStat. Data are presented as mean $\pm$ standard error (SE).

4.3 Results

4.3.1 Serum markers

Expected residue drug volume was observed in each osmotic pump, indicating the successful delivery. Serum bone turnover marker levels were greatly enhanced in the rats treated with high-dose RANKL. TRAP-5b levels increased steeply during the first week of the study, peaking on day 7 with a five-fold increase ($p<0.001$ HI vs. VEH). TRAP-5b levels gradually declined after day 7 and eventually returned to baseline levels at sacrifice (Figure 4.5).

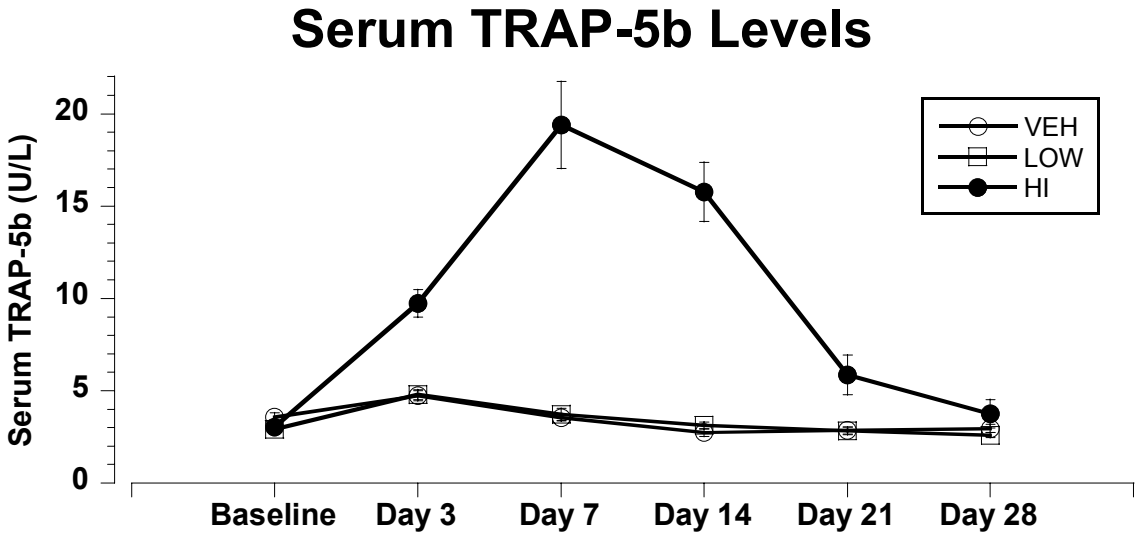

Figure 4.5 TRAP-5b (bone resorption marker) levels in HI increased steeply during the first week of the study, peaking on day 7 with a five-fold increase, and gradually declined to baseline at sacrifice. Data are presented as the mean ± SE. *: $p<0.001$ vs. VEH.

Similarly, serum osteocalcin levels for the HI group gradually increased and peaked on day 14 at 82% higher ($p<0.001$) than VEH, then decreased over the course of the following two weeks, ending at 40% higher than the VEH ($p<0.05$) at sacrifice (Figure 4.6).

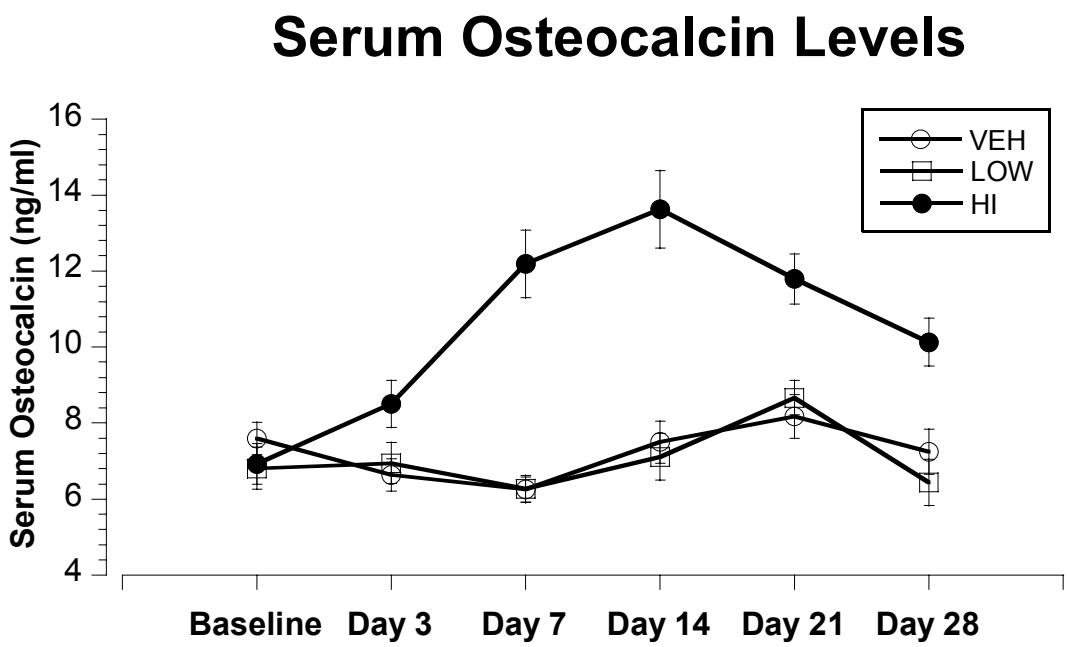

Figure 4.6 Serum osteocalcin (bone formation marker) levels in HI gradually increased and peaked at day 14 with an 82% higher than the VEH, then decreased and ending at 40% higher than VEH. Data are presented as the mean ± SE. *: $p<0.001$ vs. VEH.

Serum levels of human RANKL were measured from samples taken at sacrifice. Human RANKL was detectable in all animals, including vehicle controls, consistent with modest cross-reactivity of the assay's human polyclonal RANKL antisera with endogenous murine RANKL. Human RANKL levels in the high dose group were 5-fold higher than levels found in VEH controls (Figure 4.7); consistent with the notion that drug delivery was maintained for the study duration. Neither dose of RANKL caused significant changes in body weight throughout the study.

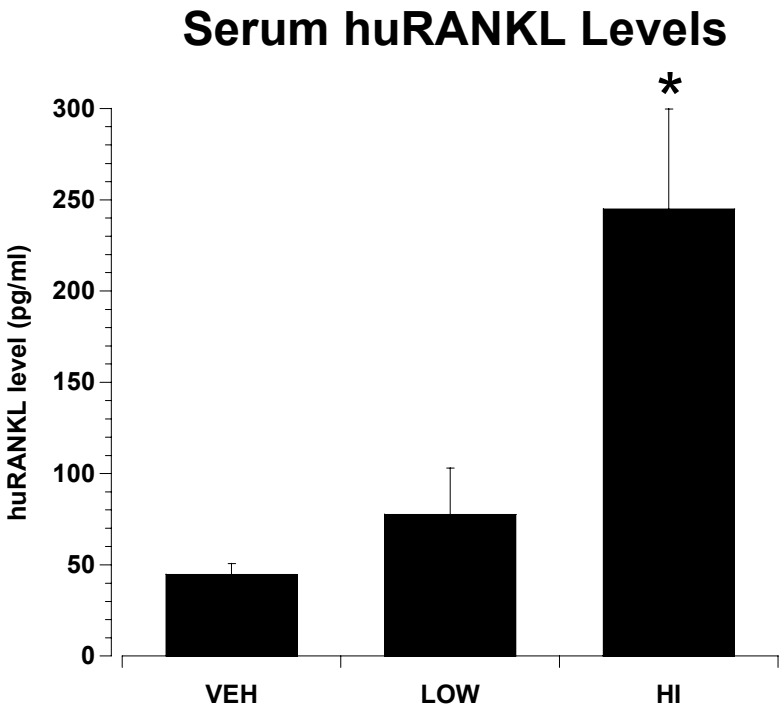

Figure 4.7 huRANKL levels at sacrifice were five-fold higher in HI than in VEH. Data are presented as the mean ± SE. *: $p<0.001$ vs. VEH.

4.3.2 MicroCT analysis

The low dose of RANKL was generally associated with few skeletal changes that reached statistical significance. However, analysis of trabecular bone at the proximal tibia revealed trends towards significant reductions in trabecular bone volume (-11%, $p= 0.126$) and trabecular connectivity (-17%., $p = 0.054$) compared to VEH. For the HI group, RANKL treatment induced significant decreases in microCT-derived measures of cortical and trabecular bone mass. High-dose RANKL treatment resulted in 7.6% reduction in cortical bone volume ($p<0.05$, Figure 4.8) and 64% reduction in trabecular volume fraction (BV/TV, $p<0.001$, Figure 4.9) compared to VEH. No differences were observed in polar moment of inertia (pMOI) at mid-femur diaphysis (Figure 4.8).

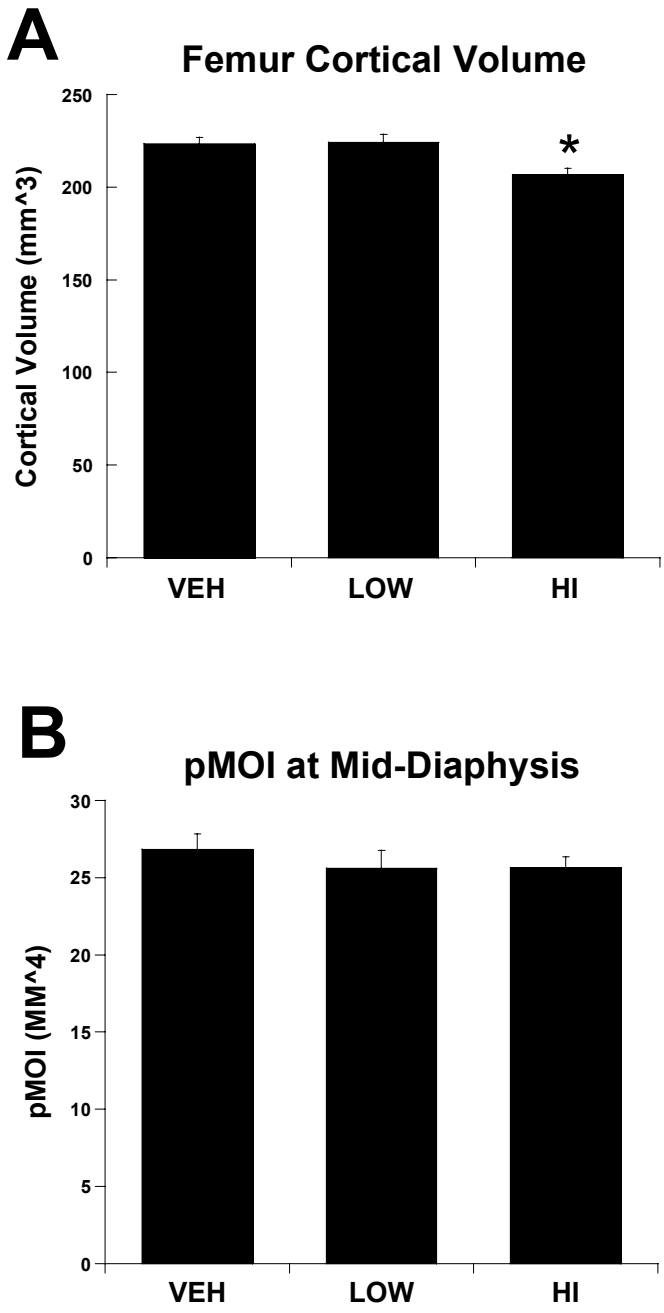

Figure 4.8 Cortical bone properties were obtained via MicroCT analysis from the femoral diaphyses. (A) Cortical volume reduced by 7.6% in the HI group ($p<0.05$ vs. VEH), no change was observed in the LOW. (B) No significance differences were observed in Polar Moment of Inertia (pMOI) at mid-femoral diaphyses. Data are presented as the mean ± SE. *: Significant different vs. VEH.

Trabecular connectivity density was affected by RANKL at a relatively higher degree: Rats treated with high dose RANKL decreased in Conn-Dens. by 86% ($p<0.001$, HI vs. VEH, Figure 4.9). Bone density values were calibrated to milligrams of hydroxyapatite per cubic centimeter. Rats in the HI group exhibited a 1.5% decrease in bone density compared to VEH ($p=0.002$, Figure 4.11).

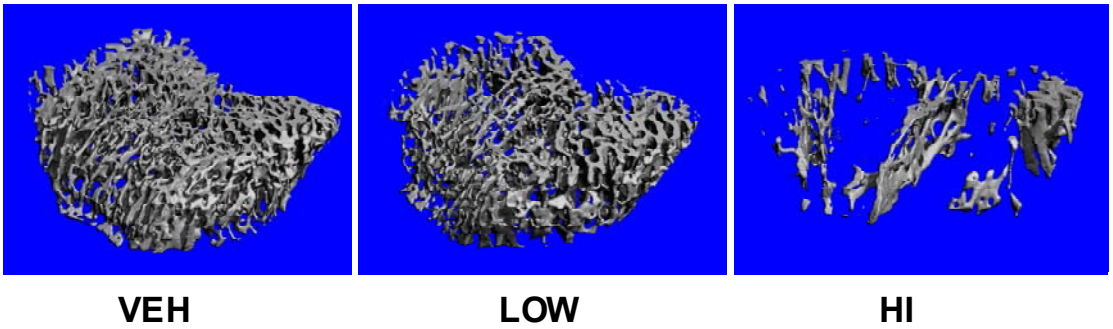

Figure 4.9 MicroCT pictures of trabecular bone at proximal tibia.

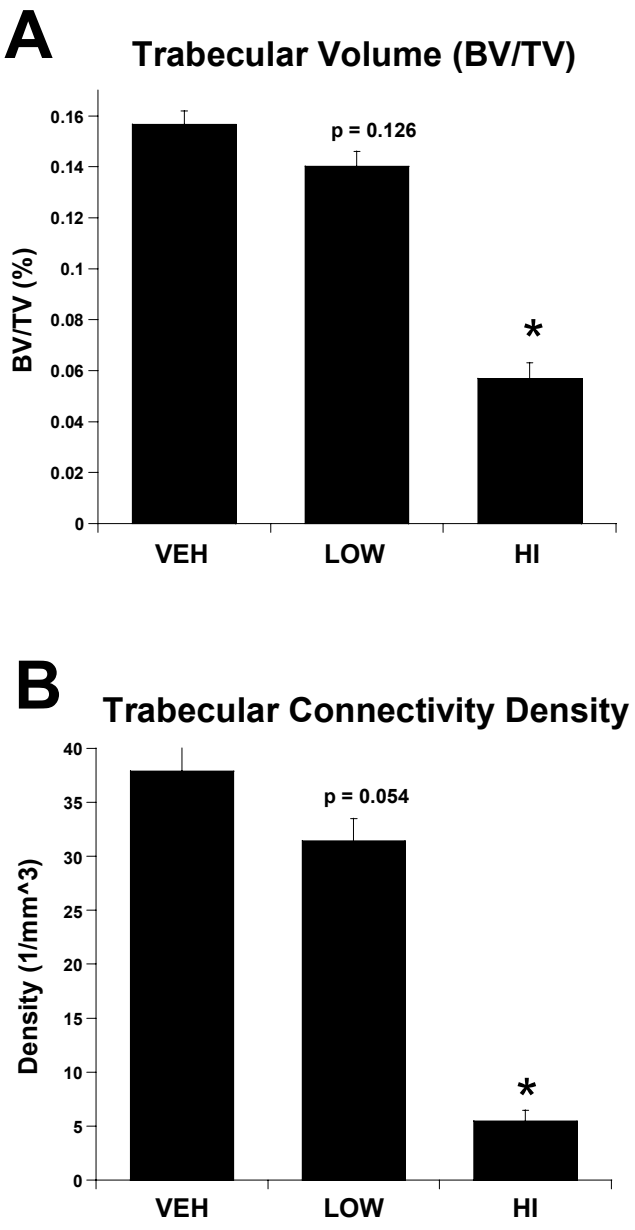

Figure 4.10 Trabecular bone properties were obtained via MicroCT analysis from the proximal tibias. (A) Trabecular volume fraction (BV/TV) decreased by 64% in HI ($p<0.001$ vs. VEH), trend of decrease was observed in LOW ($p= 0.126$ vs. VEH). (B) Connectivity density (Conn-Dens.) decreased by 86% ($p<0.001$) in HI, trend of decrease by 17% was observed in LOW ($p=0.054$). Data are presented as the mean ± SE. *: Significant different vs. VEH.

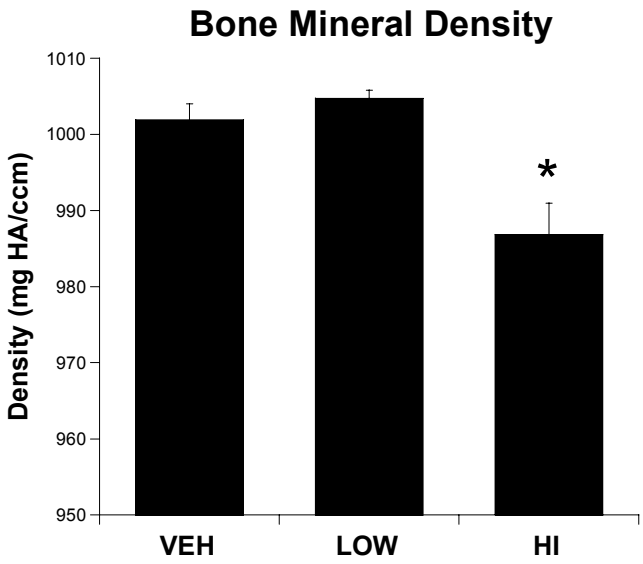

Figure 4.11 Bone mineral density data obtained from the trabecular bone at proximal tibia showed a 1.5% decrease in HI compared to VEH ($p<0.05$. Data are presented as the mean ± SE. *: Significantly different vs. VEH.

4.3.3 Bone strength

Low-dose RANKL did not result in any functional changes in bone strength for either the femoral diaphysis or neck. However, high-dose RANKL treatment caused significant reductions in parameters of bone strength. Rats treated with 175μg/kg/day RANKL exhibited parallel declines in mechanical properties for both femoral diaphyses and femoral necks (Figure 4.12). For the femoral diaphyses, elastic, maximum, fracture-strength and elastic-stiffness of the rats in the HI group decreased by 18%, 21%, 22%, and 13% ($p<0.05$) compared to VEH, respectively. In the femoral necks, high-dose RANKL treatment decreased elastic and maximum strength by 20% and 17% ($p<0.05$) compared to VEH. In HI group rats, elastic stiffness and fracture strength exhibited trends of decrease by 18% ($p=0.061$) and 17% ($p=0.11$) compared to VEH, respectively (Figure 4.12).

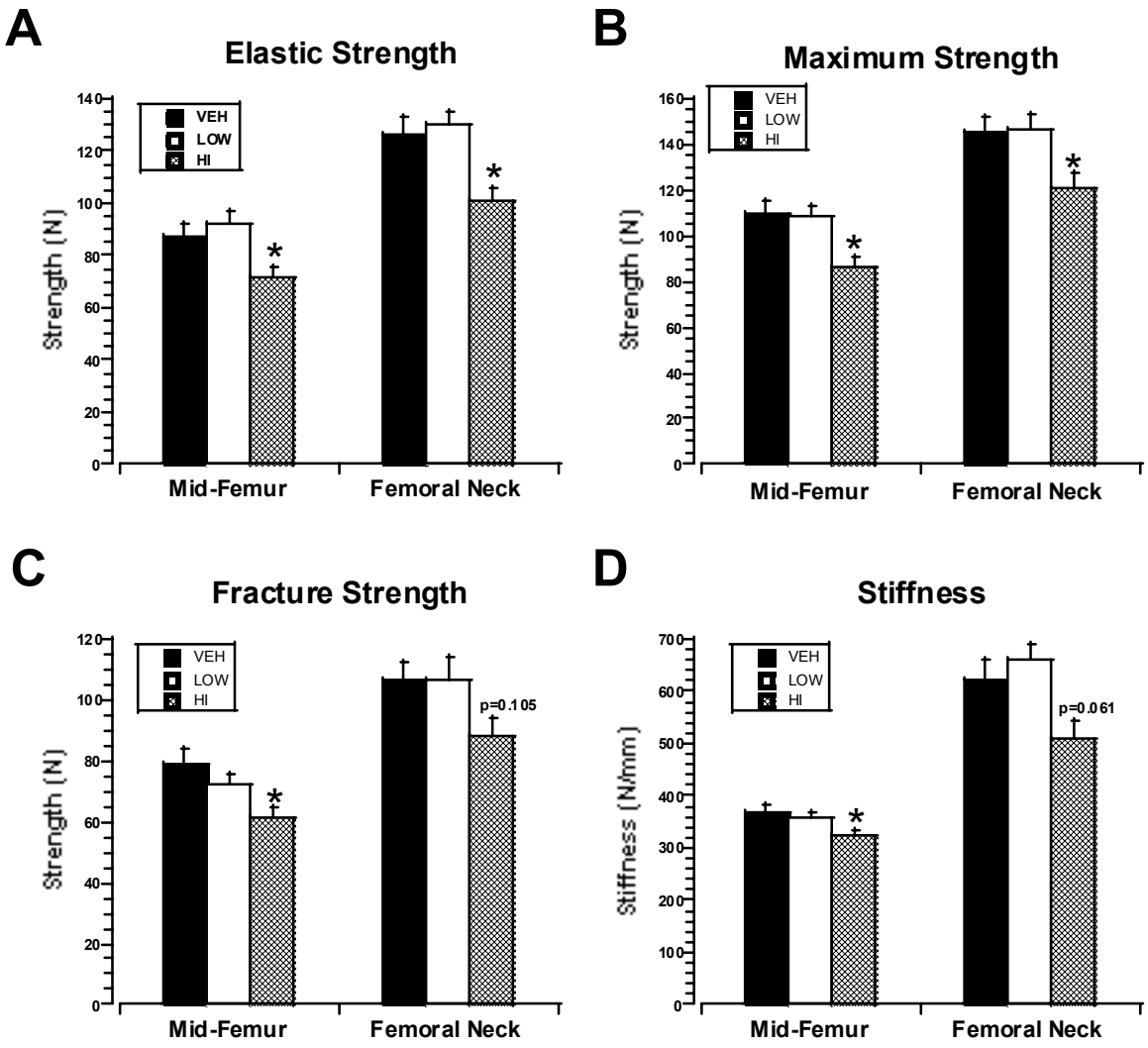

Figure 4.12 In femur mechanical properties, no differences were observed in the rats treated with low-dose RANKL. However, High-dose RANKL infusion degraded femur mechanical properties in both diaphyses and necks with a similar manner (A-D). Decreased mechanical parameters were observed from elastic strength (A, 18%), maximum strength (B, 21%), fracture strength (C, 22%) and elastic stiffness (D, 13%, vs. VEH) at femoral diaphyses though three-point bending tests. Similarly, high-dose RANKL treatment decreased elastic, maximum strength by 20% (A) and 17% (B, $p<0.05$) and fracture strength, elastic stiffness, by 17% (C, $p=0.105$) and 18% (D, $p=0.061$), respectively, at the femoral neck region compared to VEH. Data are presented as the mean ± SE. *: $p<0.05$ vs. VEH.

4.3.4 Bone compositional Analysis

For the LOW group, no differences were observed for Dry-M, Min-M, Org-M, or %Min at any testing site compare to VEH. However, rats in the HI group exhibited a 2.7% ($p<0.05$) lower whole-femur %Min compared to VEH, and site-specific effects in the changes of %Min were observed: Distal epiphyses and femoral heads exhibited 8.0% and 3.0% lower %Min, respectively ($p<0.001$ vs. VEH); changes in femoral diaphyses were not significant (Table 4.1).

Table 4.1 Mineral content analysis data were collected separately from femoral diaphyses, distal epiphyses and femoral heads. No differences in dry mass (Dry-M), mineral mass (Min-M), organic mass (Org-M) or percent mineralization (%Min = Min-M/Dry-M) were observed in any site of the LOW group. However, rats in HI decreased 2.7% ($p<0.05$) whole femur %Min and exhibited site specific effects: Distal epiphyses and femoral heads exhibited 8.0% and 3.0% lower %Min ($p<0.001$ vs. VEH), while %Min in femoral diaphyses remained unchanged. Data are presented as the mean ± SE. a, b: $p<0.05$, a, c: $p<0.001$, #: $p=0.055$ vs. LOW.

Measurement	VEH	LOW (35μg/kg RANKL)	HI (175μg/kg RANKL)
Dry-M (mg)	664 ± 13	676 ± 13	634 ± 12$^{\#}$
Min-M (mg)	422 ± 9^{a,b}	430 ± 9^{a}	393 ± 9^{b}
Org-M (mg)	242 ± 5	247 ± 5	242 ± 4
%Min Whole Femur	63.5 ± 0.3^{a}	63.5 ± 0.4^{a}	61.8 ± 0.4^{b}
%Min Diaphysis	68.1 ± 0.5	68.7 ± 0.3	67.9 ± 0.4
%Min Distal Epiphysis	55.3 ± 0.4^{a}	54.1 ± 0.6^{a}	50.9 ± 0.6^{c}
%Min Head	65.6 ± 0.3^{a}	65.2 ± 0.3^{a}	63.6 ± 0.3^{c}

4.3.5 Quantitative Histomorphometry

There were no morphometric, formation, or resorption-related changes in the cortical bone of LOW rats as identified by quantitative histomorphometry. For the HI group, analysis of the femur mid-diaphysis revealed the deleterious effects of RANKL on cortical bone structure (Table 4.2). High-dose RANKL significantly increased

endocortical bone resorption, as evidenced by a 50% increase in endocortical resorption perimeter (Ec.Rs.Pm) compared to VEH. This resulted in the endocortical area (Ec.Ar) being significantly greater in the HI group than in the LOW group ($p<0.05$), though the difference versus VEH did not reach statistical difference. Periosteal bone formation rate (Ps.BFR) was accelerated by high-dose RANKL administration, with the HI group exhibiting a 35% higher periosteal bone formation rate than the LOW ($p<0.05$). Additionally, there were trends in periosteal active mineralizing perimeter ($p=0.051$) and mineral apposition rate ($p=0.088$) with high-dose RANKL: Both increased compared to LOW.

Table 4.2 Quantitative histomorphometric data were obtained from cross-sections of femoral diaphyses. No differences were observed in LOW. For HI, endocortical resorption perimeter (Ec.Rs.Pm) increased by 50% ($p<0.05$ vs. VEH), leading to 20% greater endocortical area (Ec.Ar) compared to LOW ($p<0.05$). Periosteal bone formation rate (Ps.BFR) was accelerated by 35% ($p<0.05$ vs. LOW) by high-dose RANKL administration. There were trends in periosteal active mineralizing perimeter (Ps.AMPm) and mineral apposition rate (Ps.MAR) being increased by high-dose RANKL compared to LOW. Bone formation was not quantified on the endocortical surface due to a significant portion of the calcein labels being eroded. Data are presented as the mean ± SE. a, b: $p<0.05$, #: P=0.066 vs. LOW; *: p = 0.051 vs. LOW; §: P=0.088 vs. LOW.

Measurement	VEH	RANKL treated	
		LOW (35 μg/kg)	HI (175 μg/kg)
Ec.Ar. (mm^2)	$4.64 \pm 0.13^{a,b}$	4.28 ± 0.18^{a}	5.13 ± 0.22^{b}
Tt.B.Ar (mm^2)	14.08 ± 0.16	13.76 ± 0.34	14.06 ± 0.25
Ct. Ar (mm^2)	9.44 ± 0.13	9.48 ± 0.21	$8.93 \pm 0.19^{\#}$
Ps.BFR (10^{-3} mm^2/day)	$10.8 \pm 0.7^{a,b}$	9.5 ± 1.0^{a}	12.8 ± 1.0^{b}
Ps.AMPm (mm)	12.21 ± 0.41	10.80 ± 0.66	$12.51 \pm 0.37^{*}$
Ps.MAR (10^{-3} mm/day)	0.89 ± 0.04	0.86 ± 0.04	$1.01 \pm 0.06^{\S}$
Ec.Rs.Pm (mm)	1.62 ± 0.12^{a}	1.54 ± 0.15^{a}	2.43 ± 0.25^{b}

4.3.6 Vascular calcification

Atomic absorption spectrophotometry was used to assess calcium content in abdominal aortas, and neither dose of RANKL caused any significant changes in calcium content (Table 4.3).

Table 4.3 No differences were observed in the calcium content levels of the abdominal aorta. Data are presented as the mean ± SE.

Measurement	VEH	LOW (35 μg/kg RANKL)	HI (175 μg/kg RANKL)
Abdominal aorta Ca (μg/mg dry)	0.22 ± 0.02	0.22 ± 0.03	0.23 ± 0.02

4.4 Discussion

Numerous studies have identified the critical physiological and pathological roles of the RANK/RANKL/OPG pathway in a variety of skeletal diseases. The RANKL:OPG ratio may be central to the regulation of bone remodeling in postmenopausal osteoporosis, rheumatoid arthritis, bone metastases, and other skeletal disease states. It has been shown that postmenopausal women express higher levels of RANKL in bone marrow preosteoblasts and T and B lymphocytes than premenopausal women or postmenopausal women receiving estrogen replacement therapy (Eghbali-Fatourechi, Khosla et al. 2003). Interestingly, serum RANKL levels were not different among these patient populations, which is consistent with the possibility that serum RANKL levels do not reflect the levels found within bone. RANKL levels in serum are typically very low and frequently below the detection limits of current assays (Abrahamsen, Hjelmborg et al. 2005). These limitations have made it difficult to identify the effects of RANKL on aspects of bone mass, density, microarchitecture, geometry and quality.

We attempted to elucidate these relationships by creating a new animal model of high-turnover bone disease that is driven by the continuous infusion of soluble recombinant RANKL. In rats treated with high-dose RANKL, microCT scans revealed an overall loss of bone volume in both trabecular and cortical sites, as well as the a loss of trabecular connectivity, which are commonly seen in skeletal diseases (Coleman 1997; Hofbauer and Schoppet 2004). Although there were no significant differences in bone microarchitecture in the LOW group, there were trends in both trabecular volume fraction and trabecular connectivity with no changes in other parameters. It is interesting to note that, for this group, there were no corresponding changes in serum markers for bone resorption or formation at any time point during the study. Furthermore, serum levels of human RANKL were not significantly greater than the background levels found in vehicle-treated mice. These results suggest that RANKL may be capable of causing deleterious changes in bone mass in the absence of marked changes in circulating levels of RANKL itself, or biochemical markers of bone turnover. This possibility is consistent with clinical observational studies, wherein serum RANKL concentrations failed to correlate with bone disease despite observed increases in the levels of RANKL within bone (Stilgren, Hegedus et al. 2003; Stilgren, Rettmer et al. 2004).

Bone turnover had been identified as one of the major factors determining bone quality and skeletal fragility (Turner 2002; Heaney 2003). OPG-deficient mice (OPG-/-) produce a high bone-turnover osteoporotic phenotype with significant decreases in bone mineral density and strength (Bucay, Sarosi et al. 1998). The analysis of sequential serum markers for the current rat study demonstrated that bone turnover responded to increased circulating RANKL levels with a coupled increase in both bone formation and resorption.

RANKL injections led to a maximal 5-fold increase in serum TRAP-5b, which exceeded the maximal increase in serum osteocalcin (~2-fold). These changes, in addition to the clear loss of bone mass, density and strength, indicate that the catabolic actions of RANKL are not effectively countered by the observed increases in bone formation. These effects were observed in growing gonad-intact rats, which would otherwise exhibit a positive bone remodeling balance. These observations indicate that RANKL-mediated bone remodeling might result in bone loss independent of age, sex hormone levels, age, or baseline levels of bone turnover or density.

The accelerated bone resorption resulted in hypercalcemia as described in the pilot study, which is a common metabolic complication of malignant diseases associated with morbidity (Coleman 1997). Due to the coupling effect between osteoclasts and osteoblasts, bone formation markers increased accordingly with a delay relative to the increase in resorption, peaking on Day 14, and remained at high levels through the end of the study. This sequential stimulation of bone resorption and formation correlates with the activation sequence in normal skeleton remodeling cycle. Most osteolytic metastases demonstrate similar changes in bone resorption and formation, with the dominant lesion being lytic and destructive but coupled by elevated formation (Mundy 2002).

In this study, we observed that serum TRAP-5b levels returned to baseline after 28 days of RANKL infusion. To test whether this decline was related to premature exhaustion of the osmotic pumps, we measured human RANKL levels from serum collected at sacrifice. Significant levels of human RANKL were observed at the end of the study in the high-dose group, which indicates that drug delivery was maintained throughout the study. However, RANKL concentrations were relatively low at the end of

the study (~250 pg/ml in the high-dose group) and it is possible that immune responses against human RANKL led to lower drug exposure during the latter phase of the infusion period. Nonetheless, the high-dose infusion regimen was shown to cause significant bone loss over a 4 week period, which establishes this as a useful model of high-turnover bone disease for future studies. It is also possible that the gradual recovery of serum TRAP-5b levels during the latter phase of RANKL infusion was related to a homeostatic response that attempts to minimize the severity of bone loss. The osteoporotic phenotype of OPG-deficient mice shows that even a lifetime of unopposed RANKL activity does not lead to complete resorption of the skeleton (Bucay, Sarosi et al. 1998). It is therefore likely that compensatory mechanisms eventually defend the skeleton against the extremes of bone loss, perhaps via a feedback increase in bone formation.

A direct consequence of this high bone turnover model was degraded bone quality, which includes poor material properties and inferior bone architecture. Bone mineralization status can be indicated as material properties. When calibrated with hydroxyapatite content, bone density on trabecular bone showed a 1.5 % decrease in the HI compared to VEH as revealed by MicroCT . The changes in mineralization status were also indicated by the decrease of percent mineralization at bone cortical and trabecular regions. Both techniques demonstrate that high-dose RANKL infusion resulted in poor mineralization, which is probably a consequence of the increased turnover.

Quantitative histomorphometric analysis of the femoral mid-diaphyses revealed the effects of RANKL on cortical bone. The decreased femoral cortical volume, as identified by microCT, was caused by stimulation of endocortical bone resorption, which resulted in thinning of the cortex. This observation correlates with a previous study

demonstrating that OPG reverses osteoporosis by inhibiting activation of endosteal osteoclasts (Min, Morony et al. 2000). Correlated to the high osteocalcin levels observed in serum, periosteal bone formation rate increased in the HI group. However, this positive effect on bone strength was counteracted by greater endocortical resorption, as confirmed by the three-point bending test.

Strength of the femoral neck is a composite of both cortical and trabecular bone properties. Extrapolating the cortical and trabecular changes observed at other sites, it is clear that the combination of reduced trabecular architecture, poor trabecular mineralization, and inferior cortical structure resulting from high-dose RANKL infusion compromised strength at the femoral neck. These observations in gonad-intact rats are consistent with data showing that the ratio of RANKL:OPG is elevated in postmenopausal women with prevalent hip fractures (Abdallah, Stilgren et al. 2005). The ability of RANKL inhibitor to improve femoral neck BMD and geometry in postmenopausal women appears to confirm that RANKL plays a role in bone turnover at this clinically important skeletal site (Beck, Miller et al. 2006).

Vascular calcification has been indicated to be closely related to RANK/RANKL/OPG pathway; OPG knock-out mice develop arterial calcification of the renal arteries and aorta (Min, Morony et al. 2000). However, analysis of the calcium content from abdominal aortas indicated that continuous RANKL administration did not cause vascular calcification. It is possible that systemic exposure to RANKL does not induce or exacerbate vascular disease. Alternatively, RANKL-related changes in the vasculature might require a longer infusion period or the presence of additional vascular insults or challenges. This study utilized healthy rats, and it remains possible that

RANKL could have deleterious effects on the vasculature in animals that are more susceptible to vascular disease.

4.5 Conclusions

In summary, high-dose RANKL infusion resulted in systemic bone loss and decline in bone quality and structural integrity that were comparable to the skeletal complications caused by diseases such as osteoporosis. Thus, therapies targeting inhibition of RANKL may be a viable approach in treating skeletal complications of these bone diseases (Body, Facon et al. 2006; McClung, Lewiecki et al. 2006). Continuous administration of RANKL resulted in low bone mass and reduced bone strength without obvious complications or toxicities. Modification of RANKL administration (local to a joint rather than systemic) could possibly mimic the peri-articular bone loss and/or focal bone erosions that are associated with rheumatoid arthritis. The model presented here (and variations thereof) could have utility as a model of high-turnover bone disease, and for characterizing the potential role of the RANKL/RANK/OPG pathway for multiple skeletal diseases.

4.6 References

Abdallah, B. M., L. S. Stilgren, et al. (2005). "Increased RANKL/OPG mRNA ratio in iliac bone biopsies from women with hip fractures." Calcif Tissue Int **76**(2): 90-7.

Abrahamsen, B., J. V. Hjelmborg, et al. (2005). "Circulating amounts of osteoprotegerin and RANK ligand: genetic influence and relationship with BMD assessed in female twins." Bone **36**(4): 727-35.

Anderson, D. M., E. Maraskovsky, et al. (1997). "A homologue of the TNF receptor and its ligand enhance T-cell growth and dendritic-cell function." Nature **390**(6656): 175-9.

Avbersek-Luznik, I., B. P. Balon, et al. (2005). "Increased bone resorption in HD patients: is it caused by elevated RANKL synthesis?" Nephrol Dial Transplant **20**(3): 566-70.

Beck, T. J., P. D. Miller, et al. (2006). "Denosumab improves the structural geometry of the proximal femur in postmenopausal women with low bone mass." J Bone Min Res **21:S71 (Abstract)**.

Blair, J. M., H. Zhou, et al. (2006). "Mechanisms of disease: roles of OPG, RANKL and RANK in the pathophysiology of skeletal metastasis." Nat Clin Pract Oncol **3**(1): 41-9.

Body, J. J., T. Facon, et al. (2006). "A Study of the Biological Receptor Activator of Nuclear Factor-{kappa}B Ligand Inhibitor, Denosumab, in Patients with Multiple Myeloma or Bone Metastases from Breast Cancer." Clin Cancer Res **12**(4): 1221-8.

Boyle, W. J., W. S. Simonet, et al. (2003). "Osteoclast differentiation and activation." Nature **423**(6937): 337-42.

Broz, J. J., S. J. Simske, et al. (1993). "Effects of rehydration state on the flexural properties of whole mouse long bones." J Biomech Eng **115**(4A): 447-9.

Bucay, N., I. Sarosi, et al. (1998). "osteoprotegerin-deficient mice develop early onset osteoporosis and arterial calcification." Genes Dev **12**(9): 1260-8.

Coleman, R. E. (1997). "Skeletal complications of malignancy." Cancer **80**(8 Suppl): 1588-94.

Eghbali-Fatourechi, G., S. Khosla, et al. (2003). "Role of RANK ligand in mediating increased bone resorption in early postmenopausal women." J Clin Invest **111**(8): 1221-30.

Fazzalari, N. L., J. S. Kuliwaba, et al. (2001). "The ratio of messenger RNA levels of receptor activator of nuclear factor kappaB ligand to osteoprotegerin correlates with bone remodeling indices in normal human cancellous bone but not in osteoarthritis." J Bone Miner Res **16**(6): 1015-27.

Franchimont, N., C. Reenaers, et al. (2004). "Increased expression of receptor activator of NF-kappaB ligand (RANKL), its receptor RANK and its decoy receptor osteoprotegerin in the colon of Crohn's disease patients." Clin Exp Immunol **138**(3): 491-8.

Fuller, K., A. C. Gallagher, et al. (1991). "Osteoclast resorption-stimulating activity is associated with the osteoblast cell surface and/or the extracellular matrix." Biochem Biophys Res Commun **181**(1): 67-73.

Fuller, K., B. Wong, et al. (1998). "TRANCE is necessary and sufficient for osteoblast-mediated activation of bone resorption in osteoclasts." J Exp Med **188**(5): 997-1001.

Geusens, P. P., R. B. Landewe, et al. (2006). "The ratio of circulating osteoprotegerin to RANKL in early rheumatoid arthritis predicts later joint destruction." Arthritis Rheum **54**(6): 1772-7.

Giuliani, N., R. Bataille, et al. (2001). "Myeloma cells induce imbalance in the osteoprotegerin/osteoprotegerin ligand system in the human bone marrow environment." Blood **98**(13): 3527-33.

Grimaud, E., L. Soubigou, et al. (2003). "Receptor activator of nuclear factor kappaB ligand (RANKL)/osteoprotegerin (OPG) ratio is increased in severe osteolysis." Am J Pathol **163**(5): 2021-31.

Haynes, D. R., T. N. Crotti, et al. (2001). "Osteoprotegerin and receptor activator of nuclear factor kappaB ligand (RANKL) regulate osteoclast formation by cells in the human rheumatoid arthritic joint." Rheumatology (Oxford) **40**(6): 623-30.

Heaney, R. P. (2003). "Is the paradigm shifting?" Bone **33**(4): 457-65.

Hofbauer, L. C. and M. Schoppet (2004). "Clinical implications of the osteoprotegerin/RANKL/RANK system for bone and vascular diseases." Jama **292**(4): 490-5.

Ikeda, T., M. Kasai, et al. (2001). "Determination of three isoforms of the receptor activator of nuclear factor-kappaB ligand and their differential expression in bone and thymus." Endocrinology **142**(4): 1419-26.

Kim, H. R., H. Y. Kim, et al. (2006). "Elevated serum levels of soluble receptor activator of nuclear factors-kappaB ligand (sRANKL) and reduced bone mineral density in patients with ankylosing spondylitis (AS)." Rheumatology (Oxford) **45**(10): 1197-200.

Kong, Y. Y., U. Feige, et al. (1999). "Activated T cells regulate bone loss and joint destruction in adjuvant arthritis through osteoprotegerin ligand." Nature **402**(6759): 304-9.

Lacey, D. L., E. Timms, et al. (1998). "Osteoprotegerin ligand is a cytokine that regulates osteoclast differentiation and activation." Cell **93**(2): 165-76.

Lubberts, E., L. van den Bersselaar, et al. (2003). "IL-17 promotes bone erosion in murine collagen-induced arthritis through loss of the receptor activator of NF-kappa B ligand/osteoprotegerin balance." J Immunol **170**(5): 2655-62.

McClung, M. R., E. M. Lewiecki, et al. (2006). "Denosumab in postmenopausal women with low bone mineral density." N Engl J Med **354**(8): 821-31.

Michigami, T., M. Ihara-Watanabe, et al. (2001). "Receptor activator of nuclear factor kappaB ligand (RANKL) is a key molecule of osteoclast formation for bone metastasis in a newly developed model of human neuroblastoma." Cancer Res **61**(4): 1637-44.

Min, H., S. Morony, et al. (2000). "Osteoprotegerin reverses osteoporosis by inhibiting endosteal osteoclasts and prevents vascular calcification by blocking a process resembling osteoclastogenesis." J Exp Med **192**(4): 463-74.

Morabito, N., A. Gaudio, et al. (2004). "Osteoprotegerin and RANKL in the pathogenesis of thalassemia-induced osteoporosis: new pieces of the puzzle." J Bone Miner Res **19**(5): 722-7.

Morony, S., C. Capparelli, et al. (1999). "A chimeric form of osteoprotegerin inhibits hypercalcemia and bone resorption induced by IL-1beta, TNF-alpha, PTH, PTHrP, and 1, 25(OH)2D3." J Bone Miner Res **14**(9): 1478-85.

Mundy, G. R. (2002). "Metastasis to bone: causes, consequences and therapeutic opportunities." Nat Rev Cancer **2**(8): 584-93.

Nagai, M. and N. Sato (1999). "Reciprocal gene expression of osteoclastogenesis inhibitory factor and osteoclast differentiation factor regulates osteoclast formation." Biochem Biophys Res Commun **257**(3): 719-23.

Parfitt, A. M., M. K. Drezner, et al. (1987). "Bone histomorphometry: standardization of nomenclature, symbols, and units. Report of the ASBMR Histomorphometry Nomenclature Committee." J Bone Miner Res **2**(6): 595-610.

Ross, A. B., T. A. Bateman, et al. (2001). "The effects of osteoprotegerin on the mechanical properties of rat bone." J Mater Sci Mater Med **12**(7): 583-8.

Simonet, W. S., D. L. Lacey, et al. (1997). "Osteoprotegerin: a novel secreted protein involved in the regulation of bone density." Cell **89**(2): 309-19.

Standal, T., C. Seidel, et al. (2002). "Osteoprotegerin is bound, internalized, and degraded by multiple myeloma cells." Blood **100**(8): 3002-7.

Stilgren, L. S., L. M. Hegedus, et al. (2003). "Osteoprotegerin levels in primary hyperparathyroidism: effect of parathyroidectomy and association with bone metabolism." Calcif Tissue Int **73**(3): 210-6.

Stilgren, L. S., E. Rettmer, et al. (2004). "Skeletal changes in osteoprotegerin and receptor activator of nuclear factor-kappab ligand mRNA levels in primary hyperparathyroidism: effect of parathyroidectomy and association with bone metabolism." Bone **35**(1): 256-65.

Stolina, M., S. Adamu, et al. (2005). "RANKL is a marker and mediator of local and systemic bone loss in two rat models of inflammatory arthritis." J Bone Miner Res **20**(10): 1756-65.

Suda, T., N. Takahashi, et al. (1999). "Modulation of osteoclast differentiation and function by the new members of the tumor necrosis factor receptor and ligand families." Endocr Rev **20**(3): 345-57.

Suzuki, J., T. Ikeda, et al. (2004). "Regulation of osteoclastogenesis by three human RANKL isoforms expressed in NIH3T3 cells." Biochem Biophys Res Commun **314**(4): 1021-7.

Teitelbaum, S. L. (2000). "Bone resorption by osteoclasts." Science **289**(5484): 1504-8.

Tsuda, E., M. Goto, et al. (1997). "Isolation of a novel cytokine from human fibroblasts that specifically inhibits osteoclastogenesis." Biochem Biophys Res Commun **234**(1): 137-42.

Turner, C. H. (2002). "Biomechanics of bone: determinants of skeletal fragility and bone quality." Osteoporos Int **13**(2): 97-104.

Yasuda, H., N. Shima, et al. (1998). "Osteoclast differentiation factor is a ligand for osteoprotegerin/osteoclastogenesis-inhibitory factor and is identical to TRANCE/RANKL." Proc Natl Acad Sci U S A **95**(7): 3597-602.

Zaidi, M., H. C. Blair, et al. (2003). "Osteoclastogenesis, bone resorption, and osteoclast-based therapeutics." J Bone Miner Res **18**(4): 599-609.

CHAPTER 5

CHARACTERIZATION OF M-CSF AS AN ANABOLIC AGENT FOR BONE BIOMECHANICS

5.1 Introduction

Macrophage colony-stimulating factor (M-CSF, also named CSF-1) was defined originally by its ability to stimulate the growth and development of macrophage colonies from bone marrow precursors (Stanley, Guilbert et al. 1983). Subsequent studies showed that M-CSF is a haematopoietic growth factor that stimulates the proliferation, differentiation, and survival of cells from the mononuclear phagocytes lineage, including macrophages and osteoclasts (Hume, Pavli et al. 1988; Rettenmier and Sherr 1989; Hattersley, Owens et al. 1991). M-CSF is produced primarily by connective tissue cells, including stromal cells and osteoblasts. Through alternative mRNA splicing of a unique gene, these cells synthesize three mature isoforms of M-CSF, including a membrane-bound glycoprotein, an extracellular matrix-anchored proteoglycan, and a soluble glycoprotein that is rapidly secreted into the circulation (Stanley, Berg et al. 1994). These M-CSF isoforms act on target cells through a specific cell-surface tyrosine kinase receptor (CSF-1R) that is encoded by the *c-fms* proto-oncogene (Pixley and Stanley 2004).

In bone, M-CSF acts as a key regulator of osteoclastogenesis both *in vitro* and *in vivo*. Previous studies showed that M-CSF is necessary for both proliferation and differentiation of osteoclast progenitors as well as for their survival (Fuller, Owens et al.

1993; Tanaka, Takahashi et al. 1993). In a coculture system of mouse osteoblasts and spleen cells, osteoclast formation induced by $1,25(OH)_2$ Vitamin D_3 was inhibited when the coculture system was incubated with either anti-M-CSF or anti-M-CSF receptor antibodies during the proliferation or differentiation phase (Tanaka, Takahashi et al. 1993). The role of M-CSF in osteoclastogenesis *in vivo* has been confirmed using M-CSF-deficient osteopetrotic (*op/op*) mouse model. Transgenic mice with specific knock-out of the M-CSF gene developed profound osteopetrotic phenotypes with little or no osteoclast activity (Wiktor-Jedrzejczak, Bartocci et al. 1990; Yoshida, Hayashi et al. 1990). Subsequent studies demonstrated that systemic administration of recombinant human M-CSF to *op/op* mice increased the number of osteoclasts and led to partial or complete resolution of the osteopetrotic defect (Kodama, Yamasaki et al. 1991; Abboud, Woodruff et al. 2002).

It is clear that M-CSF stimulates osteoclastogenesis by promoting early entry of progenitors into the osteoclast lineage. However, there is no evidence that M-CSF stimulates the later stages of osteoclastogenesis, such as fusion and activation, or subsequent bone resorption (Biskobing, Fan et al. 1995; Udagawa, Takahashi et al. 1999). In fact, several studies have reported that high concentrations of M-CSF can suppress osteoclast formation and activation in vitro (Hattersley, Dorey et al. 1988; Fuller, Owens et al. 1993; Perkins and Kling 1995). For example, Perkins et al. showed that exogenous M-CSF caused a dose-dependent 98% decrease in tartrate-resistant acid phosphatase (TRAP)-positive multinucleated cells in a coculture system of ST-2 stromal cells and murine bone marrow cells (Perkins and Kling 1995). In studies using isolated mature rat osteoclasts, Hattersley and Fuller demonstrated that M-CSF inhibited bone

resorption by reducing the proportion of osteoclasts that were resorbing bone (Hattersley, Dorey et al. 1988; Fuller, Owens et al. 1993). Furthermore, addition of M-CSF has been shown to down-regulate the expression of its receptor *c-fms* on macrophages and isolated osteoclasts (Panterne, Zhou et al. 1993; Amano, Hofstetter et al. 1995; Fan, Biskobing et al. 1997).

These findings suggest a complex action of M-CSF in bone physiology: It stimulates the proliferation and differentiation of osteoclast progenitors but exhibits antiresorptive effects by inhibiting formation of mature osteoclasts and their functional activities. Recently, studies showed that mice over-expressing M-CSF or receiving daily M-CSF injections increased cortical bone formation and improved cortical bone material and biomechanical properties (Hermann 2000; Abboud, Ghosh-Choudhury et al. 2003).

Osteoblasts play an integral role in regulating osteoclastogenesis through both cell-cell interactions and release of cytokines (Takahashi, Akatsu et al. 1988; Teitelbaum 2000). These bone formation responses, possibly induced by the coupling phenomena between osteoclasts and osteoblasts (Nishino, Amizuka et al. 2001), demonstrate the potential of M-CSF as an anabolic agent for osteolytic bone diseases, such as osteoporosis. However, many important anabolic indicators of the skeleton, such as bone turnover rates and trabecular bone formation and geometry, have not been examined. In the present study, we explored a series of functional changes of the skeleton in response to different doses of M-CSF, with the aim of further characterizing its potential as an anabolic agent.

5.2 Materials and Methods

5.2.1 Study design

Prior to the main study, two pilot studies were performed using lower doses of M-CSF. In study I, seven-week-old C57BL/6J male mice (Jackson Laboratory, Bar Harbor, ME) received two different doses of M-CSF (0.01 mg/kg/day, 0.1 mg/kg/day) via daily injections for 3 weeks. In study II, mice of the same strain and age received a 4-week administration of two higher doses of M-CSF (0.5 mg/kg/day, 1 mg/kg/day) via both daily injections and continuous administrations using osmotic pumps. At sacrifice, hind limbs were removed and analyzed; no differences in bone volume, geometry, mineralization, or strength were observed. Therefore, a higher dose of M-CSF (5mg/kg/day) was selected in this study to examine its in vivo effects on bone biomechanics.

In the main study, twenty-four male C57BL/6J mice aged 7 weeks were assigned to one of two groups, VEH (placebo control, phosphate buffered saline, n=12) or M-CSF (5 mg/kg/day, n=12). The protein used in this project was donated by Chiron (Emeryville, CA); it was an unglycosylated 49-kDa homodimer (a truncated form of native M-CSF) that was expressed in *Escherichia coli* and stored as a lyophilized powder. All mice received daily subcutaneous injections (0.2 ml per injection) for 21 days. Body weights were monitored every three days, and drug concentrations were adjusted accordingly. Calcein (20 mg/kg) was injected (*i.p.*) as a fluorescent label at Day 2 to monitor new bone growth. On Day 21, animals were anesthetized with isoflurane and euthanized by exsanguination followed by cervical dislocation. Both hind limbs were removed and cleaned of all nonosseous tissue; spleens were also collected and weighted.

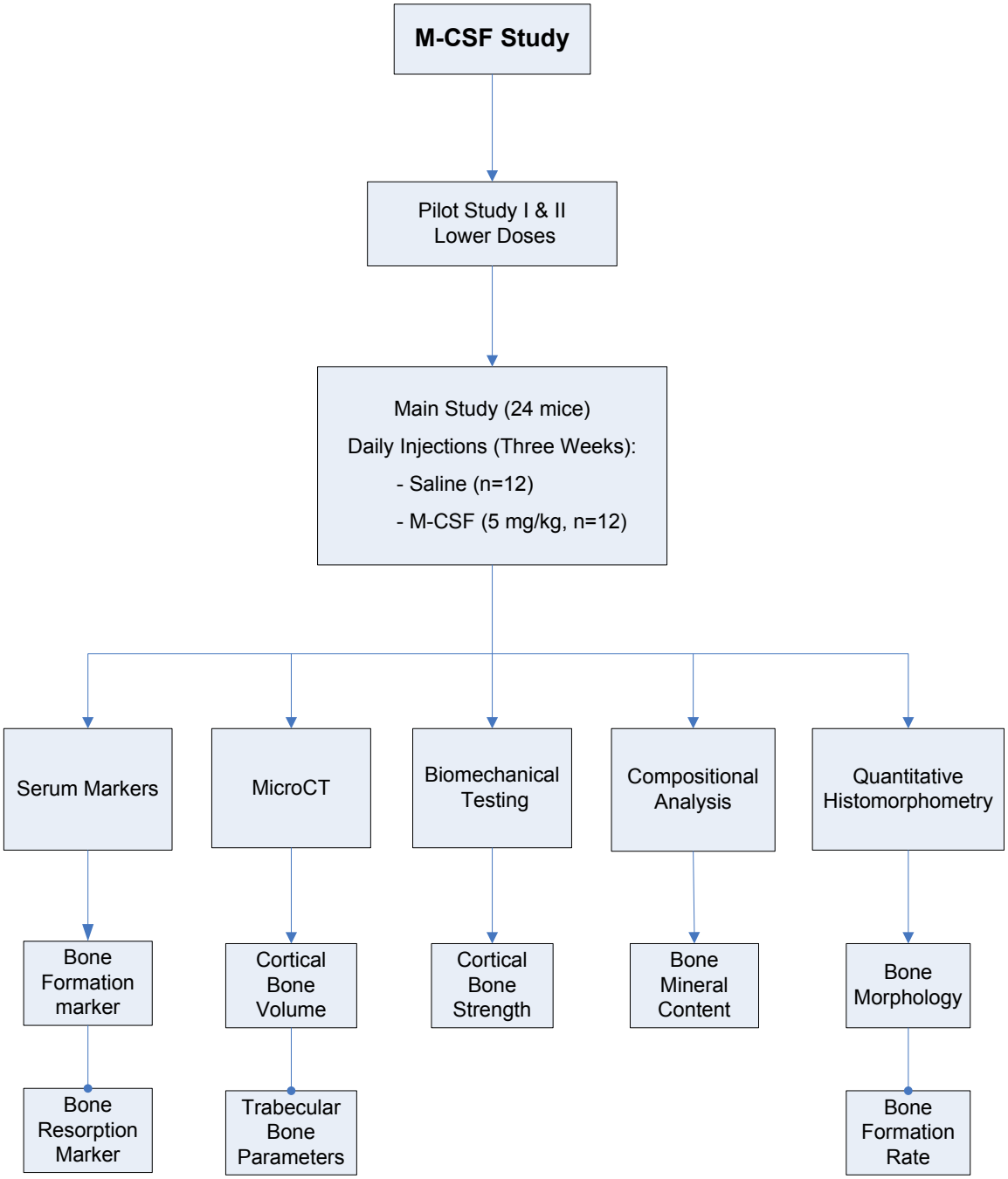

Figure 5.1 Flowchart illustrating the study design of the M-CSF study

All procedures performed throughout the experiment conformed to the guidelines of Clemson University's Institutional Animal Care and Use Committee (Figure 5.1).

5.2.2 Serum bone-turnover markers

Serum was obtained at sacrifice, and markers for bone formation and resorption were measured. Serum osteocalcin and TRAP-5b levels were measured as markers of bone formation and bone resorption by ELISA (SBA Science/IDS Inc.), respectively.

5.2.3 Micro CT

Left tibiae and femurs were fixed in 10% neural buffered formalin for 2 days, rinsed with distilled water, and stored in 70% ethanol. Cortical and trabecular parameters were obtained from the microcomputed tomography analysis (*μCT20*, Scanco Medical AG, Bassersdorf, Switzerland) with a voxel size of 9 μm in all three spatial dimensions (Ruegsegger, Koller et al. 1996; Dufresne 1998). Left femoral diaphyses were scanned, and a total of 75 slices, with 100μm increments between slices, were analyzed for cortical bone parameters. To determine bone volume and polar moment of inertia, contours were traced at the periosteal surface and calculated by Scanco IPL-Moment software.

Trabecular bone parameters were obtained from the microCT scans of 0.9 mm trabecular bone sections at the proximal end of tibiae, immediately distal to the growth plate. These parameters included trabecular bone volume (BV), total volume (TV), connectivity density (Conn. Dens.) of trabecular struts, trabecular number (Tb.N), and trabecular separation (Tb.Sp). BV was normalized with TV to obtain trabecular volume fraction (BV/TV). Trabecular number was calculated by taking the inverse of the mean distance between the middle axes of the trabeculae; trabecular separation was calculated

by measuring 3D distances directly in the trabecular network and taking the mean over all voxels. A phantom (Scanco) with increasing density hydroxyapatite columns was scanned by microCT; the linear curve of hydroxyapatite content was used as the standard curve to obtain the mineral content of the bones. Bone density data were obtained and calibrated to milligrams of hydroxyapatite per cubic centimeter.

5.2.4 Biomechanical testing

Mechanical properties of left femora were tested following microCT analysis. All bones were removed from ethanol, rinsed with distilled water, and rehydrated in phosphate-buffered saline (PBS) for 1.5 hours prior to mechanical testing. Three-point bending tests were performed using an Instron 5582 (Merlin, Series IX software). Femora were tested to failure with an 8 mm span length and deflection rate of 5mm/min. Force (N) and deflection (mm) were measured at the elastic limit (P_e, δ_e), maximum force, and failure for all mechanically tested bones. Stiffness (S) was calculated from P_e/δ_e.

5.2.5 Mineral content analysis

Mineral content analysis was performed on the fractured femur. Prior to analysis, epiphyses at both proximal and distal ends were separated. Mineral-content data were obtained separately from epiphyses and diaphysis. Dry mass (Dry-M) was measured after heating the bones for 24 h at 105ºC. Mineral mass (Min-M) was measured after the bones had been ashed by baking for another 24 h at 800ºC. Percent mineralization (%Min) was calculated by the formula % Min = Min-M/Dry-M * 100%.

5.2.6 Quantitative histomorphometry

Left femora were air-dried and embedded with noninfiltrating Epo-Kwick epoxy (Buehler, Lake Bluff, IL). The formed disks were sectioned with a low-speed saw (Buehler, 12.7cm x 0.5mm diamond blade) at the mid-diaphysis of the femur. The sections were wheel-polished to a flat, smooth surface using 600-, 800-, and 1200-grit carbide paper followed by polishing with a cloth impregnated with 6 μm diamond paste. This allowed micrographs at 50X magnification to be taken of the bone cross-sections under a far blue light (400 nm). Green calcein labels were visualized, indicating the bone formation sites during the period of the study. Quantitative histomorphometric analysis was performed using these photographs and SigmaScan Pro software (SPSS, San Rafael, CA).

Measurements of bone morphology (Parfitt, Drezner et al. 1987) included total bone area (Tt.B.Ar) and endocortical area (Ec.Ar), cortical area was calculated as Tt.B.Ar – Ec.Ar. Bone formation area (BFA) was obtained by measuring the area between the labels and the cortical perimeter, and linear content of the labeled perimeter was defined as active mineralizing perimeter (aMPm). Bone-formation rates were calculated as BFR = BFA/19 days, and mineral apposition rate was calculated as MAR = BFR/aMPm separately in the periosteal (Ps.BFR, Ps.MAR) and endocortical (Ec.BFR, Ps.MAR) areas.

5.2.7 Statistics

Statistical comparisons were performed using unpaired *t*-tests with SigmaStat software. A 95% level of significance (type I error) was used for each of these tests. Data are presented as mean $\pm$ standard error (SE).

5.3 Results

5.3.1 Body and spleen mass

Animal mass in both groups increased during the 21-day study. Mice in the VEH group increased body mass from 19.5 grams at Day 0 to 21.5 grams at Day 21, while those treated with M-CSF experienced a 55% higher net body mass gain than the VEH mice ($p=0.001$); average body mass increased from 19.3 grams at Day 0 to 22.4 grams at sacrifice. Significant differences in the net increases of body mass between VEH and M-CSF groups were observed from Day 3 ($p<0.001$) and continued to the end of the study (Figure 5.2). At sacrifice, spleens were removed and weighed; mice treated with M-CSF increased in spleen mass by 80% compared to the VEH group ($p<0.001$).

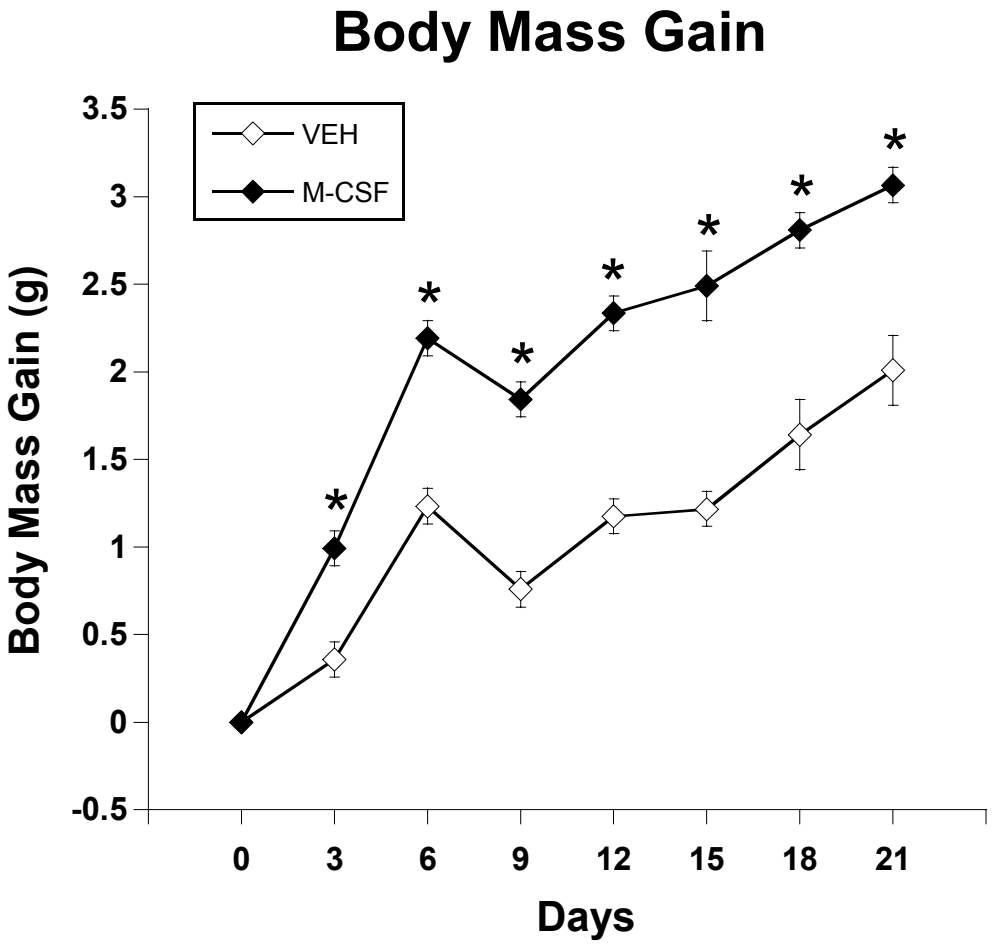

Figure 5.2 Animal mass in both groups increased during the 21-day study. Mice in the VEH group increased body mass from 19.5 grams at Day 0 to 21.5 grams at Day 21. Significant difference in net increases of body mass between VEH and M-CSF groups were observed from Day 3 ($p<0.001$) and remained to the end of the study. At sacrifice, mice treated with M-CSF gained an average of 3.1 gram body mass, increased from 19.3 grams at Day 0 to 22.4 grams, which was 55% higher than those in the VEH mice ($p=0.001$). Data are presented as the mean ± SE. * = significantly different from VEH.

5.3.2 Bone turnover

Daily administration of M-CSF stimulated general bone turnover in mice, as evidenced by significantly increased bone formation and resorption rates. Serum osteocalcin levels (marker of bone formation) in M-CSF group increased 44% compared

to VEH ($p<0.001$). Meanwhile, the bone specific resorption marker, serum TRAP-5b levels, increased by 57% relative to VEH ($p<0.001$, Figure 5.3).

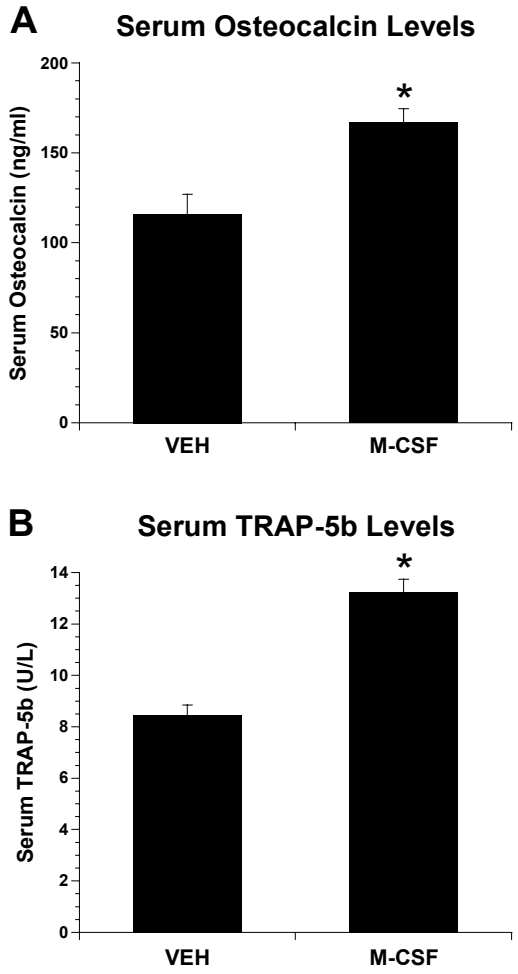

Figure 5.3 M-CSF increased both bone formation and resorption rates. (A) Serum osteocalcin exhibited 44% higher in the M-CSF group (167ng/ml) than VEH (116ng/ml, $p<0.001$). (B) Serum TRAP-5b levels in the M-CSF group (13.2 U/L) increased by 57% compared to VEH (8.4U/L, $p<0.001$). Data are presented as the mean ± SE. * = significantly different from VEH.

5.3.3 Cortical Strength

Mechanical properties of the cortical bone were obtained from femur diaphyses. Between the groups of M-CSF and VEH, significant differences were not observed in any of the elastic, maximum, fracture strength or energy (Table 5.1).

Table 5.1 Three point bending tests were performed on femur diaphyses to obtain mechanical properties data of the cortical bone. Significant differences were not observed in any of the elastic, maximum, fracture strength or stiffness. Data are presented as the mean ± SE.

Measurements	VEH	M-CSF
Stiffness (N/mm)	39.2 ± 2.1	41.5 ± 4.5
Elastic force (N)	9.05 ± 0.31	8.89 ± 0.21
Maximum force (N)	11.8 ± 0.4	11.7 ± 0.3
Fracture force (N)	6.17 ± 0.30	6.62 ± 0.38

5.3.4 Bone mineral content

Bone mineral data were obtained separately from femoral diaphyses and epiphyses. No differences in dry mass (Dry-M), mineral mass (Min-M), organic mass (Org-M) were observed in the M-CSF group compared to VEH. Data in percent mineralization in sites of diaphyses, epiphyses or whole femur between groups were similar and not significant different (Table 5.2).

Table 5.2 Mineral content analysis data were collected separately from femoral diaphyses and epiphyses. In the M-CSF group, no differences in dry mass (Dry-M), mineral mass (Min-M), organic mass (Org-M) were observed compared to VEH. Differences in percent mineralization (%Min = Min-M/Dry-M) in sites of diaphyses, epiphyses or whole femur were also not observed (vs. VEH). Data are presented as the mean ± SE.

Measurement	VEH	M-CSF
Dry-M (mg)	33.0 ± 0.6	32.3 ± 0.9
Min-M (mg)	20.0 ± 0.4	19.7 ± 0.5
Org-M (mg)	13.0 ± 0.2	12.7 ± 0.4
%Min Whole Femur	60.6 ± 0.1	60.8 ± 0.2
%Min Diaphysis	62.6 ± 0.3	62.6 ± 0.3
%Min Epiphysis	59.1 ± 0.3	59.1 ± 0.3

5.3.5 Bone volumes indicated by MicroCT

M-CSF caused differential effects in mouse cortical and trabecular bone. Cortical bone volumes were measured and calculated in a 7.4 mm span of the femur diaphysis. M-CSF caused a trend of decrease in cortical volume by 2.9% compared to VEH ($p=0.095$, Figure 5.4A), though data did not reach statistical difference. Similar trends were observed in the average polar moment of inertia (pMOI) data; M-CSF treatment resulted in a trend of decrease by 5.8% in pMOI value of the femur diaphysis ($p=0.074$ vs. VEH, Figure 5.4B).

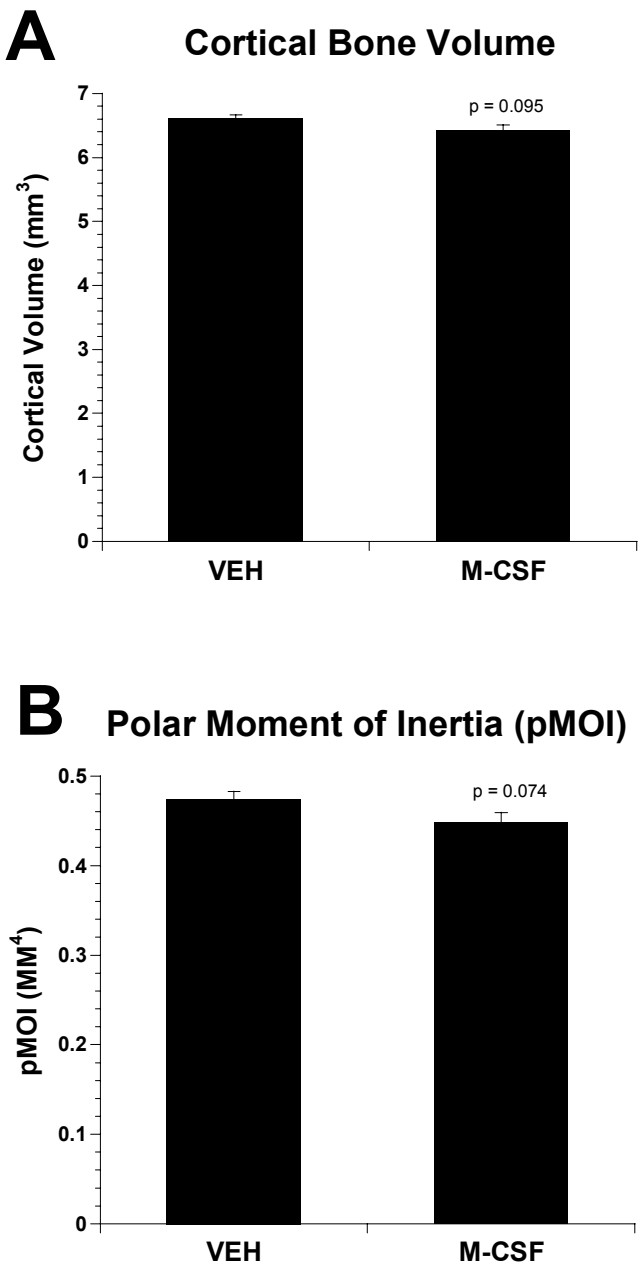

Figure 5.4 No significant differences were observed in cortical bone parameters between M-CSF and VEH groups. However, trends of decreased cortical volume (A) by 2.9% (p=0.095) and mean polar moment of inertia (pMOI) of femur diaphyses (B) by 5.8% were observed in the M-CSF group compared to VEH. Data are presented as the mean ± SE. * = significantly different from VEH.

Trabecular parameters were measured from a 0.9 mm thick section of trabecular bone in proximal tibia. In contrast, average trabecular volume fraction (BV/TV) increased by 35% in the mice treated with M-CSF ($p<0.001$ vs. VEH, Figure 5.5A). M-CSF significantly increased trabecular connectivity by 79% ($p<0.001$, Figure 5.5B) compared to the VEH group.

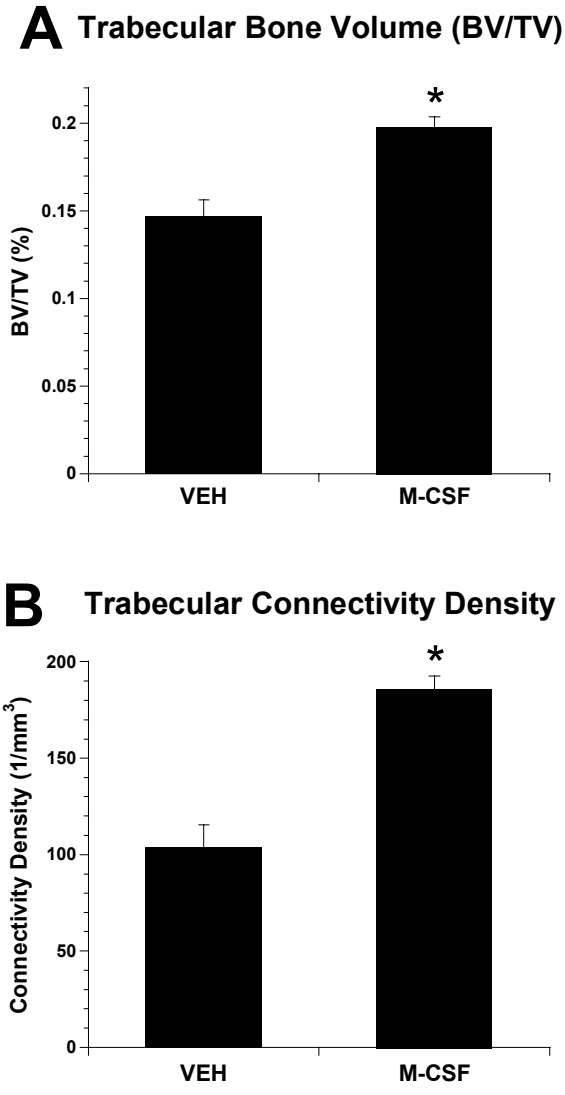

Figure 5.5 M-CSF stimulated trabecular bone formation. (A) Average trabecular volume fraction (BV/TV) increased by 35% ($p<0.001$ vs. VEH) in mice treated with M-CSF. (B) M-CSF significantly increased trabecular connectivity by 79% ($p<0.001$) compared to the VEH group. Data are presented as the mean ± SE. * = significantly different from VEH.

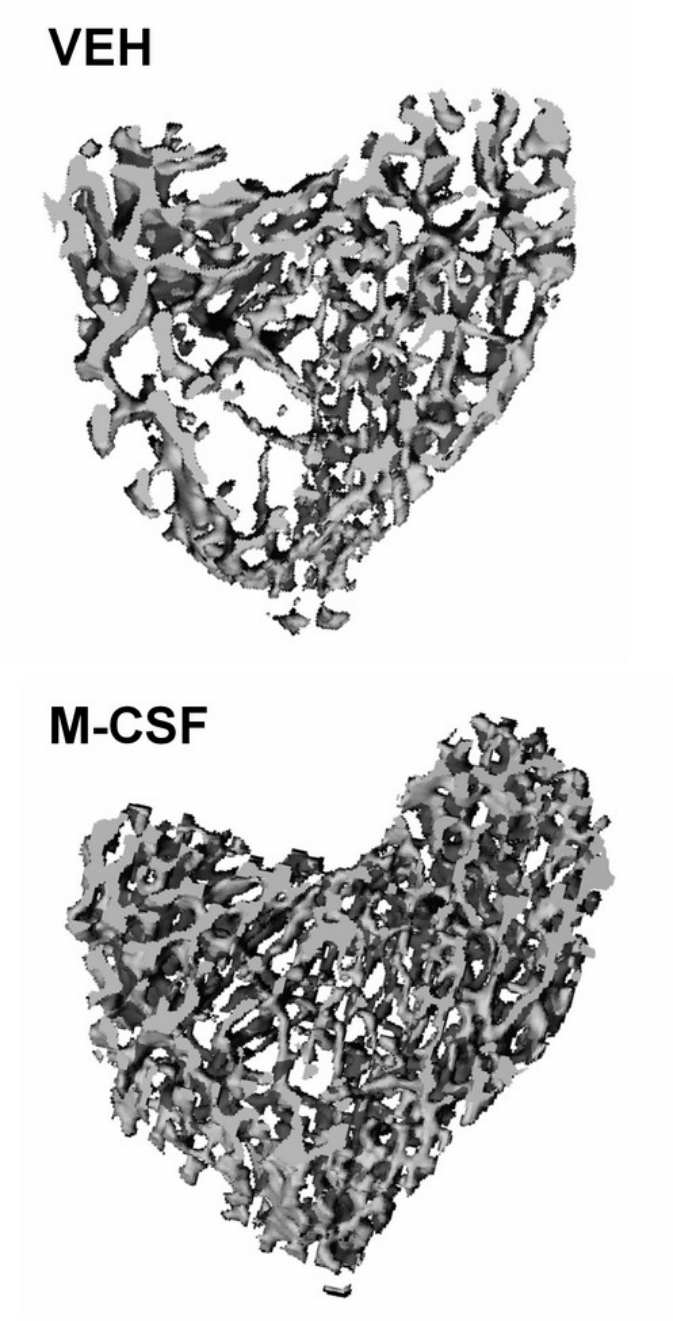

Figure 5.6 Trabecular parameters were measured with microCT from a 0.9 mm thick trabecular bone section at proximal tibia. 3-D trabecular pictures showed the mouse treated with M-CSF has a thicker and denser trabecular bone than that in VEH. Both pictures were obtained from mice with median bone volume of individual groups.

Significant differences were also observed in other trabecular parameters: M-CSF increased trabecular number by 17.7% ($p<0.001$, Figure 5.7A), and lower trabecular spacing by 17.8% ($p<0.001$, Figure 5.7B) compared to VEH. Bone density values were calibrated to milligrams of hydroxyapatite per cubic centimeter. Mice in the M-CSF group exhibited a 3.5% lower bone density than VEH ($p=0.007$, Figure 5.8).

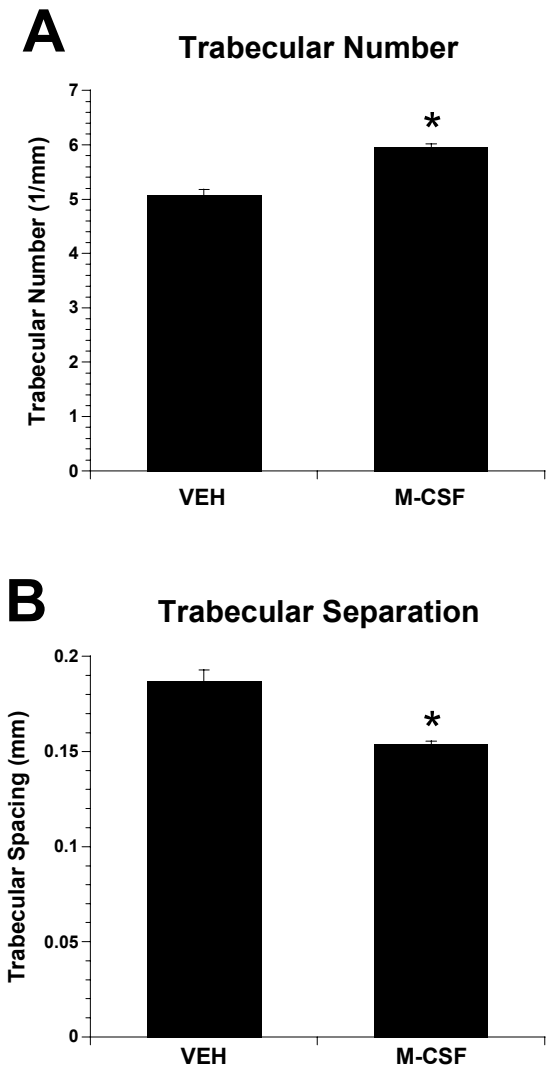

Figure 5.7 M-CSF also affected other trabecular bone parameter, such as increased trabecular number (A) by 17.7% ($p<0.001$), and lower trabecular separation (B) by 17.8% ($p<0.001$ vs. VEH). Data are presented as the mean ± SE. * = significantly different from VEH.

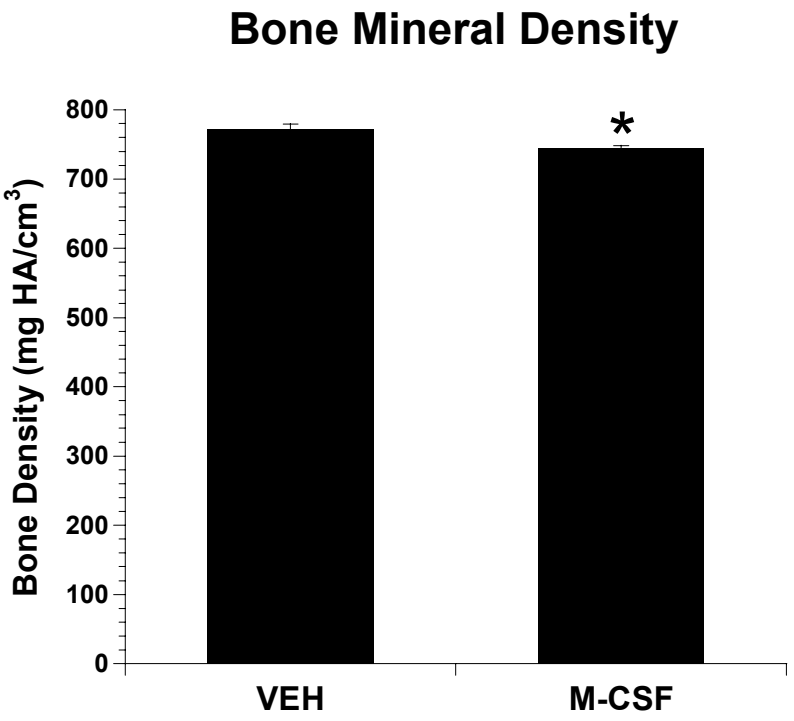

Figure 5.8 The newly formed trabecular bone induced by M-CSF administration exhibited a 3.5% lower bone density than those in VEH (p=0.007). Data are presented as the mean ± SE. * = significantly different from VEH.

5.3.6 Quantitative histomorphometry

As indicated by quantitative histomorphometry, M-CSF administration did not cause significant changes in cortical geometry (Table 5.3). However, trends of increase in periosteal mineral apposition rate (Ps.MAR, p=0.12) and total mineral apposition rate (Tt.MAR, p=0.14) were observed in the M-CSF group when compared to VEH.

Table 5.3 Quantitative histomorphometry measurements were taken from the UV microscope photographs of the femur mid-diaphysis cross-sections. Ec = endocortical, Ps = periosteal, Tt = total, Ar = area, B = bone, BFR = bone formation rate, AMPm = active mineralizing perimeter, MAR = mineral apposition rate. Data are presented as mean ± SE.

Measurement	VEH	M-CSF
Ec.Ar. (mm^2)	0.85 ± 0.03	0.82 ± 0.03
Ct. Ar (mm^2)	0.81 ± 0.02	0.80 ± 0.02
Tt.B.Ar (mm^2)	1.66 ± 0.03	1.63 ± 0.01
Ec.BFR (10^{-3} mm^2/day)	2.11 ± 0.36	2.03 ± 0.21
Ps.BFR (10^{-3} mm^2/day)	5.60 ± 0.34	6.44 ± 0.54
Tt.BFR (10^{-3} mm^2/day)	5.42 ± 0.36	5.42 ± 0.36
Ec.AMPm (mm)	1.87 ± 0.17	1.80 ± 0.13
Ps.AMPm (mm)	3.39 ± 0.29	3.37 ± 0.30
Tt. AMPm (mm)	5.26 ± 0.31	5.17 ± 0.31
Ec.MAR (10^{-3} mm/day)	1.09 ± 0.12	1.12 ± 0.07
Ps.MAR (10^{-3} mm/day)	1.72 ± 0.11	1.96 ± 0.10 $^{p=0.12}$
Tt.MAR (10^{-3} mm/day)	1.49 ± 0.07	1.65 ± 0.07 $^{p=0.14}$

5.4 Discussion

Bone remodeling, a lifetime process that includes bones being continuously broken down (bone resorption) and reformed (bone formation), allows the maintenance of bone mass and quality. Activities of osteoblasts and osteoclasts are tightly linked and balanced under normal conditions, a phenomenon often referred to as coupling (Howard, Bottemiller et al. 1981; Martin 1993). In this study, we observed an increase of osteoclastogenesis, as evidenced by the 57% increase in serum TRAP-5b levels. Meanwhile, bone formation activities (serum osteocalcin) also increased, indicating M-

CSF indirectly stimulated bone formation through coupling of osteoblasts and osteoclasts. The mechanism of the coupling phenomena, though not fully understood, is generally considered to be the result of direct communication between osteoclasts and osteoblasts by cell-cell interaction and by cytokines released to the bone microenvironment during bone resorption (Howard, Bottemiller et al. 1981; Centrella, McCarthy et al. 1991; Rodan 1991; Martin 1993). Previous studies have indicated that these coupling factors might include insulin-like growth fact-1 (IGF-1), transforming growth factor-β (TGF-β), and bone morphogenetic factor (BMP) (Centrella, McCarthy et al. 1991; Rodan 1991; Martin 1993).

Although both bone turnover rates increased, the most evident changes in bone came from the markedly increased trabecular volume, indicating that M-CSF dissociated bone remodeling and functioned as an anabolic agent. Mice treated with high doses of M-CSF showed increased trabecular volume (35%), connectivity density (79%), and trabecular number (17.7%) and reduced separation (-17.8%). The newly formed trabecular bone was less mineralized due to the high bone turnover rates, as revealed by the microCT data. Anabolic effects of M-CSF also came from the increased body mass observed in this study; mice treated with M-CSF gained significantly higher body weight from Day 3 and remained throughout the whole course of this study.

Anabolic effects of M-CSF were not reflected in cortical bone. Data obtained in this study showed that M-CSF induced a nonsignificant trend of decreasing cortical volume and polar moment of inertia. However, these probably catabolic effects on cortical bone did not cause significant changes in bone strength. In fact, the presence of both anabolism and catabolism is common in most bone anabolic agents (Lacey, Timms

et al. 1998; Poole and Reeve 2005). Other cortical bone parameters, including geometry and mineralization, remained unchanged. Interestingly, these observations on cortical bone are opposite compared to previous findings of increased cortical thickness or improved mineral and mechanical properties in studies with either transgenic models or lower-dose M-CSF administrations (Hermann 2000; Abboud, Ghosh-Choudhury et al. 2003).

The clear increases in trabecular bone parameters and the trend of decrease in cortical bone volume indicated that M-CSF exhibits both anabolic and catabolic effects with site-specific differences. Similar results are known in anabolic agents for osteoporosis, such as PTH (Poole and Reeve 2005). Anabolic effects of intermittent PTH injections were observed primarily in trabecular bone through increasing trabecular bone volume, connectivity density and trabecular number and decreasing separation (Jiang, Zhao et al. 2003). Along with these strong anabolic actions on trabecular bone, PTH stimulates endocortical bone remodeling and increases cortical porosity, a catabolic effect that has led to concern that the increases in trabecular bone parameters may be obtained at the expense of cortical bone (Horwitz, Stewart et al. 2000; Neer, Arnaud et al. 2001; Rubin, Cosman et al. 2002). Such site-specific anabolic and catabolic changes in bones are similar to those induced by M-CSF in this study.

However, PTH acts anabolically by directly stimulating bone formation through promoting differentiation of committed osteoblast precursors and inhibiting apoptosis of osteoblasts (Dobnig and Turner 1995; Jilka, Weinstein et al. 1999) In contrast, M-CSF targets osteoclast lineage and stimulates the proliferation and early differentiation of osteoclast progenitors but not mature osteoclasts (Tanaka, Takahashi et al. 1993), thus

indirectly promoting osteoblast formation via coupling. These two seemingly radically different mechanisms may not be fully independent. Recent studies have indicated that the resorptive action of PTH might be necessary for its anabolic effect. In a study using ovariectomized rats treated with PTH, bone formation was partially inhibited with a combined treatment of antiresorptive therapies (Wronski, Yen et al. 1993). Transgenic mice with *c-fos* gene knock-out exhibit osteopetrotic symptoms due to defects on osteoclast development and fail to show an anabolic response to PTH (Demiralp, Chen et al. 2002).

In vivo studies targeting the effects of M-CSF on the skeleton system are sparse; however, complicated action of M-CSF has been seen. In vitro studies demonstrated divergent effects of M-CSF on osteoclast formation and bone resorption in varying concentrations (Perkins and Kling 1995). The importance of protein concentrations was also reflected in the pilot studies for this project. In these in vivo studies, we examined a series of lower doses of M-CSF (0.01mg, 0.1mg., 0.5mg, and 1mg per kilogram body mass per day) given to mice of the same strain and age as the current 5mg/kg/day M-CSF study, and neither anabolic nor catabolic effects on the skeleton were observed in the mice receiving lower doses. This might indicate that M-CSF causes dose-dependent bone functional changes. In addition, administration routes and periods might also cause different bone reactions. An *in vivo* study using transgenic mice that overexpressed soluble M-CSF showed no changes in bone parameters at 5 weeks but had increased cortical bone thickness at 14 weeks (Abboud, Ghosh-Choudhury et al. 2003). One possible explanation for this observation might be the variety of the M-CSF-receptor expression. Earlier studies by other groups showed that M-CSF receptors could be

expressed at variable levels under different populations of monocyte cells and local cytokine environments (Kreipe, Radzun et al. 1988; Gusella, Ayroldi et al. 1990). As a stimulator of circulating monocytes and macrophages, M-CSF can influence the local environments of its receptor. In addition, M-CSF itself can down-regulate its receptor expression in macrophages and isolated osteoclasts (Amano, Hofstetter et al. 1995).

5.5 Conclusions

In summary, this study demonstrates the anabolic actions of M-CSF on trabecular bone formation. These anabolic effects, probably through coupling between osteoclasts and osteoblasts, suggest the potential of M-CSF as an anabolic agent to stimulate new bone formation and improve bone strength. In vitro studies have shown that M-CSF in higher concentrations exhibits unique antiresorptive effects on bone resorption; however, these antiresorptive effects were not observed in this in vivo study. Future studies examining changes in skeleton exposed to different dosages, administration routes, and periods or effects in larger and skeletally mature animals like rats will be necessary to elucidate the mechanism and utilize its anabolic potential. In addition, since soluble M-CSF exhibits a relatively short clearance time in the circulation (Bauer, Gibbons et al. 1994), further modifications on molecular structures or drug delivery methods aiming to improve the pharmacokinetics and pharmacodynamics of this protein would be valuable in developing its unique potential as an anabolic and antiresorptive therapy for osteoporosis.

5.6 References

Abboud, S. L., N. Ghosh-Choudhury, et al. (2003). "Osteoblast-specific targeting of soluble colony-stimulating factor-1 increases cortical bone thickness in mice." J Bone Miner Res **18**(8): 1386-94.

Abboud, S. L., K. Woodruff, et al. (2002). "Rescue of the osteopetrotic defect in op/op mice by osteoblast-specific targeting of soluble colony-stimulating factor-1." Endocrinology **143**(5): 1942-9.

Amano, H., W. Hofstetter, et al. (1995). "Downregulation of colony-stimulating factor-1 (CSF-1) binding by CSF-1 in isolated osteoclasts." Calcif Tissue Int **57**(5): 367-70.

Bauer, R. J., J. A. Gibbons, et al. (1994). "Nonlinear pharmacokinetics of recombinant human macrophage colony-stimulating factor (M-CSF) in rats." J Pharmacol Exp Ther **268**(1): 152-8.

Biskobing, D. M., X. Fan, et al. (1995). "Characterization of MCSF-induced proliferation and subsequent osteoclast formation in murine marrow culture." J Bone Miner Res **10**(7): 1025-32.

Centrella, M., T. L. McCarthy, et al. (1991). "Transforming growth factor-beta and remodeling of bone." J Bone Joint Surg Am **73**(9): 1418-28.

Demiralp, B., H. L. Chen, et al. (2002). "Anabolic actions of parathyroid hormone during bone growth are dependent on c-fos." Endocrinology **143**(10): 4038-47.

Dobnig, H. and R. T. Turner (1995). "Evidence that intermittent treatment with parathyroid hormone increases bone formation in adult rats by activation of bone lining cells." Endocrinology **136**(8): 3632-8.

Dufresne, T. (1998). "Segmentation techniques for analysis of bone by three-dimensional computed tomographic imaging." Technol Health Care **6**(5-6): 351-9.

Fan, X., D. M. Biskobing, et al. (1997). "Macrophage colony stimulating factor down-regulates MCSF-receptor expression and entry of progenitors into the osteoclast lineage." J Bone Miner Res **12**(9): 1387-95.

Fuller, K., J. M. Owens, et al. (1993). "Macrophage colony-stimulating factor stimulates survival and chemotactic behavior in isolated osteoclasts." J Exp Med **178**(5): 1733-44.

Gusella, G. L., E. Ayroldi, et al. (1990). "Lipopolysaccharide, but not IFN-gamma, down-regulates c-fms mRNA proto-oncogene expression in murine macrophages." J Immunol **144**(9): 3574-80.

Hattersley, G., E. Dorey, et al. (1988). "Human macrophage colony-stimulating factor inhibits bone resorption by osteoclasts disaggregated from rat bone." J Cell Physiol **137**(1): 199-203.

Hattersley, G., J. Owens, et al. (1991). "Macrophage colony stimulating factor (M-CSF) is essential for osteoclast formation in vitro." Biochem Biophys Res Commun **177**(1): 526-31.

Hermann, L., Ferguson, VL, Bateman, TA, Simske, SJ (2000). "Combined treatment effects of IGF-I and M-CSF on mouse bone composition, mechanical properties and quantitative histomorphometry." J Bone Miner Res **15Sup**: S369.

Horwitz, M., A. Stewart, et al. (2000). "Sequential parathyroid hormone/alendronate therapy for osteoporosis--robbing Peter to pay Paul?" J Clin Endocrinol Metab **85**(6): 2127-8.

Howard, G. A., B. L. Bottemiller, et al. (1981). "Parathyroid hormone stimulates bone formation and resorption in organ culture: evidence for a coupling mechanism." Proc Natl Acad Sci U S A **78**(5): 3204-8.

Hume, D. A., P. Pavli, et al. (1988). "The effect of human recombinant macrophage colony-stimulating factor (CSF-1) on the murine mononuclear phagocyte system in vivo." J Immunol **141**(10): 3405-9.

Jiang, Y., J. J. Zhao, et al. (2003). "Recombinant human parathyroid hormone (1-34) [teriparatide] improves both cortical and cancellous bone structure." J Bone Miner Res **18**(11): 1932-41.

Jilka, R. L., R. S. Weinstein, et al. (1999). "Increased bone formation by prevention of osteoblast apoptosis with parathyroid hormone." J Clin Invest **104**(4): 439-46.

Jimi, E., T. Shuto, et al. (1995). "Macrophage colony-stimulating factor and interleukin-1 alpha maintain the survival of osteoclast-like cells." Endocrinology **136**(2): 808-11.

Kodama, H., M. Nose, et al. (1991). "Essential role of macrophage colony-stimulating factor in the osteoclast differentiation supported by stromal cells." J Exp Med **173**(5): 1291-4.

Kodama, H., A. Yamasaki, et al. (1991). "Congenital osteoclast deficiency in osteopetrotic (op/op) mice is cured by injections of macrophage colony-stimulating factor." J Exp Med **173**(1): 269-72.

Kreipe, H., H. J. Radzun, et al. (1988). "Multinucleated giant cells generated in vitro. Terminally differentiated macrophages with down-regulated c-fms expression." Am J Pathol **130**(2): 232-43.

Lacey, D. L., E. Timms, et al. (1998). "Osteoprotegerin ligand is a cytokine that regulates osteoclast differentiation and activation." Cell **93**(2): 165-76.

Li, W. and E. R. Stanley (1991). "Role of dimerization and modification of the CSF-1 receptor in its activation and internalization during the CSF-1 response." Embo J **10**(2): 277-88.

Martin, T. J. (1993). "Hormones in the coupling of bone resorption and formation." Osteoporos Int **3 Suppl 1**: 121-5.

Neer, R. M., C. D. Arnaud, et al. (2001). "Effect of parathyroid hormone (1-34) on fractures and bone mineral density in postmenopausal women with osteoporosis." N Engl J Med **344**(19): 1434-41.

Nishino, I., N. Amizuka, et al. (2001). "Histochemical examination of osteoblastic activity in op/op mice with or without injection of recombinant M-CSF." J Bone Miner Metab **19**(5): 267-76.

Panterne, B., Y. Q. Zhou, et al. (1993). "CSF-1 control of C-FMS expression in normal human bone marrow progenitors." J Cell Physiol **155**(2): 282-9.

Parfitt, A. M., M. K. Drezner, et al. (1987). "Bone histomorphometry: standardization of nomenclature, symbols, and units. Report of the ASBMR Histomorphometry Nomenclature Committee." J Bone Miner Res **2**(6): 595-610.

Perkins, S. L. and S. J. Kling (1995). "Local concentrations of macrophage colony-stimulating factor mediate osteoclastic differentiation." Am J Physiol **269**(6 Pt 1): E1024-30.

Pixley, F. J. and E. R. Stanley (2004). "CSF-1 regulation of the wandering macrophage: complexity in action." Trends Cell Biol **14**(11): 628-38.

Poole, K. E. and J. Reeve (2005). "Parathyroid hormone - a bone anabolic and catabolic agent." Curr Opin Pharmacol **5**(6): 612-7.

Rettenmier, C. W. and C. J. Sherr (1989). "The mononuclear phagocyte colony-stimulating factor (CSF-1, M-CSF)." Hematol Oncol Clin North Am **3**(3): 479-93.

Rodan, G. A. (1991). "Mechanical loading, estrogen deficiency, and the coupling of bone formation to bone resorption." J Bone Miner Res **6**(6): 527-30.

Rubin, M. R., F. Cosman, et al. (2002). "The anabolic effects of parathyroid hormone." Osteoporos Int **13**(4): 267-77.

Ruegsegger, P., B. Koller, et al. (1996). "A microtomographic system for the nondestructive evaluation of bone architecture." Calcif Tissue Int **58**(1): 24-9.

Shinar, D. M., M. Sato, et al. (1990). "The effect of hemopoietic growth factors on the generation of osteoclast-like cells in mouse bone marrow cultures." Endocrinology **126**(3): 1728-35.

Stanley, E. R., K. L. Berg, et al. (1994). "The biology and action of colony stimulating factor-1." Stem Cells **12 Suppl 1**: 15-24; discussion 25.

Stanley, E. R., L. J. Guilbert, et al. (1983). "CSF-1--a mononuclear phagocyte lineage-specific hemopoietic growth factor." J Cell Biochem **21**(2): 151-9.

Sundquist, K. T., M. E. Jackson, et al. (1995). "Osteoblasts from the toothless (osteopetrotic) mutation in the rat are unable to direct bone resorption by normal osteoclasts in response to 1,25-dihydroxyvitamin D." Tissue Cell **27**(5): 569-74.

Takahashi, N., T. Akatsu, et al. (1988). "Osteoblastic cells are involved in osteoclast formation." Endocrinology **123**(5): 2600-2.

Tanaka, S., N. Takahashi, et al. (1993). "Macrophage colony-stimulating factor is indispensable for both proliferation and differentiation of osteoclast progenitors." J Clin Invest **91**(1): 257-63.

Teitelbaum, S. L. (2000). "Bone resorption by osteoclasts." Science **289**(5484): 1504-8.

Udagawa, N., N. Takahashi, et al. (1999). "Osteoblasts/stromal cells stimulate osteoclast activation through expression of osteoclast differentiation factor/RANKL but not macrophage colony-stimulating factor: receptor activator of NF-kappa B ligand." Bone **25**(5): 517-23.

Wiktor-Jedrzejczak, W., A. Bartocci, et al. (1990). "Total absence of colony-stimulating factor 1 in the macrophage-deficient osteopetrotic (op/op) mouse." Proc Natl Acad Sci U S A **87**(12): 4828-32.

Wronski, T. J., C. F. Yen, et al. (1993). "Parathyroid hormone is more effective than estrogen or bisphosphonates for restoration of lost bone mass in ovariectomized rats." Endocrinology **132**(2): 823-31.

Yoshida, H., S. Hayashi, et al. (1990). "The murine mutation osteopetrosis is in the coding region of the macrophage colony stimulating factor gene." Nature **345**(6274): 442-4.

Yuan, Y., V. L. Ferguson, et al. (2004). "Low dose administration of macrophage colony-stimulating factor in mice." Biomed Sci Instrum **40**: 93-8.

CHAPTER 6

CONCLUSIONS AND RECOMMENDATIONS

This dissertation has examined two key cytokines for osteoclastogenesis regulation (RANKL and M-CSF) and their opposing effects on bone biomechanics. This concluding chapter will highlight the novel findings from the three major animal studies and their pilots studies detailed in the previous three chapters, and propose suggestions on future direction based on these findings.

6.1 Conclusions

Studies in this project have characterized the *in vivo* catabolic effects of RANKL as the late stage regulator and final effector for osteoclastogenesis on bone biomechanics; examined and proposed RANKL-induced skeletal deterioration model as a novel animal model for osteolytic skeletal diseases; and characterized the *in vivo* anabolic effects of M-CSF as the early stage regulator for osteoclastogenesis and its potential of acting as an innovative anabolic therapy for osteoporosis. During the above explorations, a series of novel findings has been concluded in which the details are described as below.

1. Daily injections of soluble RANKL directly activated osteoclastogenesis and stimulated general bone turnover rates, resulting in hypercalcemia.
2. Soluble recombinant RANKL caused severe catabolic effects on both cortical and trabecular bone in a short period of time. These effects include: increases in bone resorption, reduces in both cortical and trabecular bone volume, decreases in both

cortical and trabecular bone mineralization, impairments in cortical bone architecture and reduces in cortical bone strength.

3. Excessive RANKL levels led to a coupling-related increase in bone formation at the periosteal surface of cortical bone. However, these increased bone formations were insufficient to counteract deleterious effects on other areas.
4. Therapies targeting inhibition of RANKL might be a viable approach in treating skeletal complications of high-turnover bone diseases like osteoporosis.
5. The RANKL injection study on mice has some limitations, including the lack of an obvious dose-response for many of the endpoints. We believe that a lower dose range would have provided a clearer dose response for the majority of parameters. Dose-dependent weight loss and hypercalcemia indicated that RANKL administration at 2 mg/kg was an excessive dose that resulted in toxicity.
6. In the RANKL infusion study, we have used soluble RANKL to develop a new animal model for high-turnover bone diseases without obvious complications or toxicities. This novel animal model recapitulates many of the deleterious skeletal changes associated with postmenopausal osteoporosis in which details are compared and listed below:

Table 6.1 Comparisons of bone functional changes between postmenopausal women and RANKL induced bone loss model

Postmenopausal women	RANKL induced bone loss model
• Bone mineral density decreases	• Cortical and trabecular bone volume lost • Trabecular bone mineralization reduced
• Integrity of trabecular bone geometry reduces	• Trabecular bone volume decreased • Trabecular connectivity density reduced
• Medullary cavity increases	• Endocortical bone resorption rate increased • Endocortical bone area increased
• Periosteal diameter (bone size) increases	• Periosteal bone formation rate increased
• Fracture risk increases	• Bone strength at femur mid-diaphysis and femoral neck reduced

7. Bone turnover rates responded to increased circulating RANKL levels with a coupled increase in both bone formation and resorption. Due to the coupling phenomena, bone formation markers increased accordingly with a delay relative to the increase in resorption, and correlates with the activation sequence in normal skeleton remodeling cycle.
8. The lower dosage of RANKL infusion induced trends of decrease in trabecular bone parameters without corresponding changes in serum bone turnover markers and circulating RANKL levels. These results suggested that RANKL may be capable of causing deleterious effects in bone volume and structure in the absence of changes in circulating levels of RANKL itself, or biochemical markers of bone turnover.
9. RANKL administrations induced a homeostatic response that attempts to minimize the severity of bone loss. The osteoporotic phenotype of OPG-deficient mice shows that even a lifetime of unopposed RANKL activity does not lead to

complete resorption of the skeleton (Bucay, Sarosi et al. 1998). It is therefore likely that compensatory mechanisms eventually defend the skeleton against the extremes of bone loss, perhaps via a feedback increase in bone formation.

10. Analysis of the calcium content from abdominal aortas indicated that continuous RANKL administration did not cause vascular calcification. It is possible that systemic exposure to RANKL does not induce or exacerbate vascular disease. Alternatively, RANKL-related changes in the vasculature might require a longer infusion period or the presence of additional vascular insults or challenges. This study utilized healthy rats, and it remains possible that RANKL could have deleterious effects on the vasculature in animals that are more susceptible to vascular diseases.
11. High dose M-CSF administration resulted in marked increases in trabecular bone formation and general bone turnover rates. These novel findings indicated that M-CSF dissociated bone remodeling which favored bone resorption, and have demonstrated the potential of M-CSF as a potent anabolic agent for bone strength.
12. Systemic anabolic effects of M-CSF were reflected by the increases in body mass. Mice treated with M-CSF gained significantly higher body weight from Day 3 and remained throughout whole course of the study.
13. In this study, we observed increases in both osteoclastogenesis and bone formation activities. M-CSF receptors exist on surfaces of osteoclasts and their progenitors but not osteoblasts. These findings indicated that M-CSF indirectly stimulated bone formation through coupling of osteoblasts and osteoclasts.

14. M-CSF induced trends of decrease in cortical bone parameters without changes in bone strength. These observations on cortical bone were contradictory to previous findings of increased cortical thickness in transgenic models over expressing M-CSF (Abboud, Ghosh-Choudhury et al. 2003).
15. The evident increases in trabecular bone parameters and trend of decrease in cortical bone volume indicated that M-CSF exhibits both anabolic and catabolic effects with site-specific differences. These region specific observations are similar to those induce by PTH.
16. Pilot studies of the M-CSF study indicated a dose dependent effect of M-CSF on bone biomechanics. Analysis of the data also indicated that there is a dose threshold for M-CSF to induce bone functional changes.
17. In summary, activations of later and early stages of osteoclastogenesis, through *in vivo* administration of RANKL and M-CSF, induced general opposing changes on bone volume, structure, mineralization and strength. RANKL directly stimulated bone resorption and degraded bone biomechanical properties. The bone loss animal model induced by RANKL exhibited a series of skeletal complications similar to those observed in high-turnover osteolytic skeletal diseases such as osteoporosis. On the other hand, administrations of M-CSF markedly stimulated trabecular bone formation and had less of an influence on cortical bone. These changes demonstrated the potential of M-CSF as an anabolic agent for osteoporosis.
18. Findings in this project, such as the creation of a RANKL induced bone loss model and characterization of M-CSF as an innovative anabolic agent for bone

biomechanics, could provide a useful tool and information for further explorations on the battles with human skeletal diseases.

6.2 Recommendations

6.2.1 RANKL Induced Bone Loss Model

Studies in this project have created an animal bone loss model induced by RANKL administrations. To make this novel model a practical tool for future studies on the field of skeletal diseases, further studies on optimizing this model are recommended:

1. In our studies, we administrated RANKL at high dosages via daily injections on mice and long-term continuous administrations with lower dosages on rats, to ensure the fully catabolic consequences. The amount of RANKL administered to animals appeared excessive. Future studies examining the minimal dosage and administration periods of RANKL on mice or rats will be helpful to lower the toxicity, expense, studies period and increase the practicality of the model. It is recommended to further examine the duration of the bone destructive status in this model which is the body's natural recovery response after RANKL induced bone loss.
2. It will be of further interest to examine the expression levels of up-stream cytokines, such as PTHrP, IL-1, IL-6, M-CSF and TGF-β in this RANKL induced bone loss model. These cytokine expression levels will provide valuable information on the mechanisms of cytokine interaction, indications of skeletal homeostasis from the protein level and predict the skeletal responses.

3. Future studies are recommended to examine the therapeutic agents for skeletal diseases, such as OPG, PTH, and bisphosphonates with this model. These studies may provide further information on therapeutic efficacy and disease mechanisms that were not captured by other models.

6.2.2 Development of M-CSF as a Novel Anabolic Agent for Osteoporosis

In this project, M-CSF showed good potential as an innovative anabolic agent for bone biomechanics. However, due to the limited *in vivo* data available in the literature, the detailed mechanism and functional effects of M-CSF on the skeletal system require further examination. Future recommended studies are:

1. Lower efficacious doses and optimum administration periods and routes of M-CSF, with the capability to induce anabolic response without causing toxicity or immune responses, remain to be characterized.
2. Mechanisms of coupling, such as signal transductions through osteoclasts-osteoblasts direction interaction, and changes in cytokine levels in bone microenvironment after coupling is triggered by M-CSF, are also recommended for further examination.
3. Examinations of M-CSF efficacy on disease models, such as OVX and RANKL induced bone loss model as described in this study, will provide further information on this anabolic agent in addition to those observed in healthy mice of this project.
4. Soluble M-CSF exhibited a relatively short clearance time in the circulation (Bauer, Gibbons et al. 1994). Modifications on molecular structures or drug

delivery methods, aiming to improve the pharmacokinetic and pharmacodynamics of this protein remain to be developed.

5. The antiresorptive potential of M-CSF indicated by *in vitro* studies was not observed in current *in vivo* studies. These antiresorptive effects, if observed in future studies in vivo, will greatly enhance the potential of M-CSF being a therapeutic agent for osteolytic skeletal diseases with both anabolic and antiresorptive effects.

6.3 References

Abboud, S. L., N. Ghosh-Choudhury, et al. (2003). "Osteoblast-specific targeting of soluble colony-stimulating factor-1 increases cortical bone thickness in mice." J Bone Miner Res **18**(8): 1386-94.

Bauer, R. J., J. A. Gibbons, et al. (1994). "Nonlinear pharmacokinetics of recombinant human macrophage colony-stimulating factor (M-CSF) in rats." J Pharmacol Exp Ther **268**(1): 152-8.

Bucay, N., I. Sarosi, et al. (1998). "osteoprotegerin-deficient mice develop early onset osteoporosis and arterial calcification." Genes Dev **12**(9): 1260-8.

APPENDICES

Appendix A: Examination of M-CSF Protein Degradation

The M-CSF protein used in this project was donated by Chiron, manufactured 15 years ago. To examine potential protein degradation, SDS-PAGE and Western Blot analyses were performed.

Materials and Methods

The protein sample (3.9 mg/ml) was serial diluted (10%, 1%, and 0.2%) then mixed with an equal volume of loading buffer. For the SDS-PAGE gels (Piece), 10μl of each concentration was loaded. Thus, 19500ng, 1950ng, 195ng and 39ng of M-CSF were loaded per lane. The molecular weight marker, Kaleidascope (Biomad) was loaded (5 μl). A voltage of 120V for 60 minutes was used. The SDS-PAGE gel was then stained with Coomassie Blue to visualize the protein. Western blot were used to confirm that the protein bands observed on the SDS-PAGE gels were M-CSF and its degraded isoforms. The primary antibody to M-CSF was a rabbit monoclonal from Genetex. A goat anti-rabbit IgG antibody was used as the secondary antibody. All procedures for Western Blot followed the instructions from Bio-Rad.

Results

The serially diluted samples of M-CSF resulted in multiple bands on the gels. Based on comparison of the loaded samples, approximately 2-8% of the protein was degraded. The antibodies detected the lower molecular weight bands on the western blots, indicating that both the primary band and the degraded bands were M-CSF (Figure A.1).

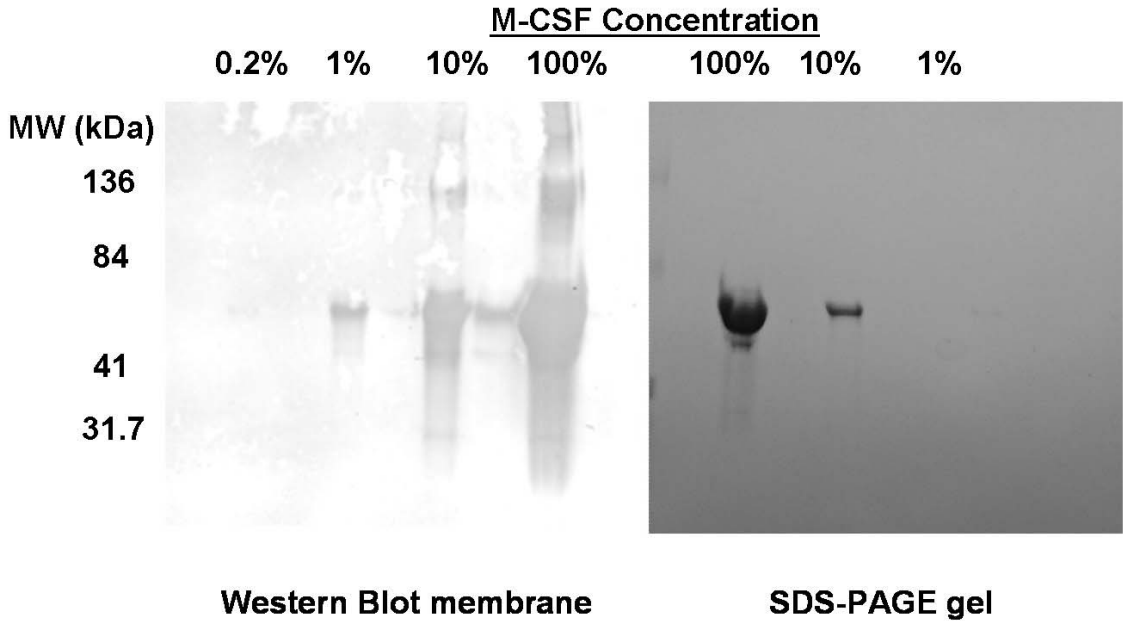

Figure A.1 SDS-PAGE gel and Western blot membrane analysis of the recombinant M-CSF used in these studies confirmed the degradation. The lanes labeled 100%, 10%, 1% and 0.2% contained 19500ng, 1950ng, 195ng and 39ng of M-CSF, respectively. The observed degradation is between 2 to 8% of the total protein in the sample. MW: Molecular weight.

Appendix B: Low Dose Administration of Macrophage-Colony Stimulating Factor in Mice

Part of the M-CSF pilot study I data submitted to Rocky Mountain Bioengineering Symposium as a conference article in 2004: "Low dose administration of macrophage colony-stimulating factor in mice." **Biomed Sci Instrum**. **2004;40:93-8.**

Yuyu Yuan, Virginia L. Ferguson*, Steven J. Simske*, Ted A. Bateman

Department of Bioengineering, Clemson University, Clemson, SC 29634
*BioServe Space Technologies, University of Colorado, Boulder 80309

ABSTRACT

Keywords: M-CSF, CSF-1, bone, mice, anabolic, osteoblast, osteoclast

Macrophage-Colony Stimulating Factor (M-CSF) is critical for osteoclast differentiation and development. It has been previously observed that M-CSF administration and over-expression in mice causes an increase in cortical bone formation. We hypothesize that M-CSF increases osteoblast activity indirectly via coupling of these two bone cells. In this study, we examined the impact on bone properties of relatively low doses of M-CSF in mice. Four groups of seven-week old C57BL/6J mice were used: (1) baseline (age) controls, (2) placebo controls, (3) 10µg/kg/day M-CSF, (4) 100µg/kg/day M-CSF. Injections were administered daily for the 21-day study. Three bone labels of calcein and tetracycline were alternately administrated (days 0, 9 and 18) to allow quantification of new bone formation. MicroCT scans (15 micron resolution) were performed on the proximal end of the right tibiae (1.0 mm section of trabecular bone) and left femur mid-diaphysis (0.25 mm cortical section). Dry mass, mineral content and percent mineral composition were obtained from the left tibiae. Functional changes were not detected in the bone of these mice receiving low doses of M-CSF. In particular, as previous studies have reported in mice receiving high doses of M-CSF or transgenic mice overexpressing bone specific M-CSF, changes to cortical bone did not occur with the lower doses. This may indicate that high doses of M-CSF and/or longer periods of administration may be required to observe the anabolic effect of M-CSF on mouse cortical bone.

INTRODUCTION

Macrophage-Colony Stimulating Factor (M-CSF or CSF-1) is a haematopoietic growth factor that is produced mainly by connective tissue cells, including osteoblasts (Felix, Halasy-Nagy et al. 1996). M-CSF is essential for the cells from the mononuclear

phagocytes lineage, from which osteoclasts are derived (Kodama, Nose et al. 1991). It is known that M-CSF facilitates monocyte survival, monocyte-to-macrophage conversion, and macrophage proliferation (Corboz, Cecchini et al. 1992; Fixe and Praloran 1997). In vitro, it has been shown to promote osteoclastogenesis in bone (Corboz, Cecchini et al. 1992; Sundquist, Jackson et al. 1995; Sarma and Flanagan 1996). The ability of M-CSF to stimulate osteoclast in vivo has been confirmed by using the M-CSF-deficient osteopetrotic (op/op) mouse model (Kodama, Yamasaki et al. 1991; Sundquist, Jackson et al. 1995; Abboud, Woodruff et al. 2002). Repeated injections of M-CSF increased the number of osteoclast, which lead to partial or complete correction of the osteopetrotic defect. A dose-dependent relationship was observed during these treatments. These studies demonstrate the ability of M-CSF to increase bone resorption in mice deficient in osteoclasts.

However, recent studies on transgenic mice targeted expression of M-CSF showed increased cortical thickness and bone mineral density (Abboud, Ghosh-Choudhury et al. 2003). This osteoblast specific expression of soluble M-CSF greatly increased levels of M-CSF in the bone, resulting in increased bone formation rates at the endocortical surface. Our group has observed similar results with the administration of M-CSF improving material and mechanical properties of cortical bone (Hermann 2000). The increase in strength was mediated by a greater percent mineral composition, rather than an accelerated bone formation. An increase in percent mineral composition is observed with the administration of anti-resorptive therapies (Bateman, Lacey et al. 1999; Bateman, Dunstan et al. 2000).

These findings highlight the complex and important role of M-CSF in bone physiology, and demonstrated its potential as an unconventional therapy for osteoporosis. Less clear evidence suggests that M-CSF actually inhibits mature osteoclast activity, potentially acting as an agent that promotes bone formation via coupling by promoting immature osteoclasts, but limiting the amount of bone resorption by mature osteoclasts. This unique role in osteoclast development and survival may have a positive effect on both osteoblast's and osteoclast's increasing bone mass rather than inhibiting bone formation as current anti-resorptive therapies do. To explore this hypothesis and to determine the optimum M-CSF dose for increasing cortical strength, we are examining two different doses of M-CSF (100 μg/kg/day and 100μg/kg/day). These doses are 10% and 1% of the high dose previously examined by our group (Hermann 2000), and more similar to the dose of teriparatide (parathyroid hormone amino acids 1-34) that produces an anabolic effect (Andreassen, Ejersted et al. 1999).

METHODS

In this study, 75 C57BL/6J (Jackson Labs, Bar Harbor, Maine, USA) mice seven-weeks in age were randomly assigned to four groups: (1) baseline (age) controls, (2) placebo controls, (3) 10μg/kg/day M-CSF, and (4) 100μg/kg/day M-CSF. The baseline control group was sacrificed at the beginning of the study, the placebo, M-CSF (10μg/kg) and M-CSF (100μg/kg) groups were administered saline, 10μg/kg M-CSF and 100μg/kg M-CSF through this 21-day study (i.p.). The initial weights of all mice ranged from 18-22 gram,

the weights were monitored daily. During this experiment, Calcein (s.c., 20 mg/kg, at days 0 and 18) and Tetracycline (s.c., 20 mg/kg, at day 9) were administered to all mice to allow the quantification of bone formation rates. Clemson University animal care and use committee approved the animal protocol for this study.

At the end of the study, all the mice were sacrificed via exsanguinations and followed by cervical dislocation. Afterwards, the femora and tibiae were removed and cleaned off all non-osseous tissue. The right femora and tibiae were fixed with 10% neutral buffered formalin for 48 hours and then stored in 70% ethanol. The right femora was air dried and embedded in Epo-Quick epoxy (Buehler, Lake Bluff, IL), then sectioned at mid-diaphysis using a low speed saw (Buehler, 300μm diamond blade). Photographs of the bone were taken at 50X under three different filters (FITC, Fs05, DAPI) to view the bone labels. Quantitative histomorphometric analysis will be performed on these cross-sections.

The proximal end of the right tibiae was scanned with MicroCT (SCANCO Medical, μCT20, Zurich, Switzerland); trabecular bone approximately 1.0 mm beneath the growth plate was analysis. The left femora were dried for 48 hours and a MicroCT scan was performed on the mid-diaphysis. A 0.25 mm thick section of cortical bone was analyzed (15 micron resolution, 9 microns per slice, 28 slices); total volume and bone volume were obtained for all groups (Figure 1). Mineral content of the left tibiae was analyzed, dry mass (Dry-M, 105C for 24 hours) and mineral content (Ash-M, 800C for 24 hours) were obtained on the proximal end and the diaphysis. A one-way-ANOVA statistical comparison was used on all these tests, with a Tukey follow-up. Data are reported as mean +/- standard deviation with 95% statistical significance (type I error).

RESULTS

The mice weights increased normally during this 3-week study, the difference between placebo and M-CSF treated groups was not significant. After examining the trabecular volume, trabecular number, trabecular thickness, trabecular spacing and the ratio of bone volume by total volume of the tibiae proximal end, changes between placebo, 10μg/kg M-CSF and 100μg/kg M-CSF groups were not significant, the bone volume/total volume increased with age compared to baseline group. No significant changes were observed of the dry mass and ash mass of the tibiae proximal end and diaphysis. MicroCT scan of the femora mid-diaphyseal cortical bone showed a normal increase of total volume and bone volume with age, but significant changes between placebo and M-CSF treated groups were not observed.

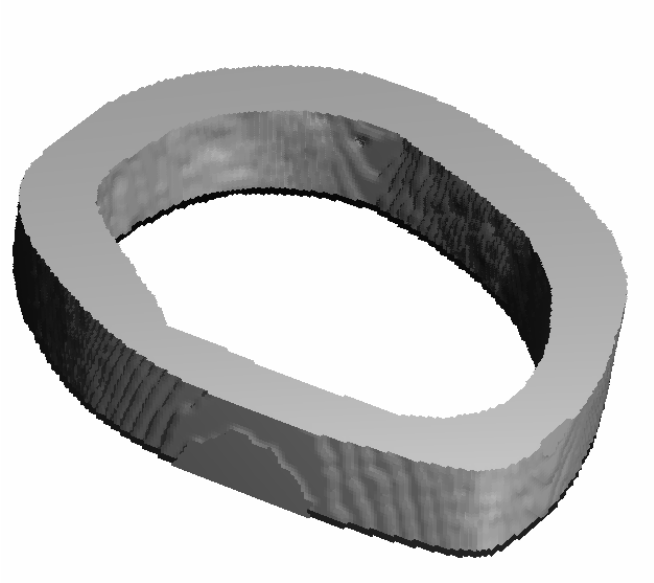

Figure 1. MicroCT scan of cortical bone from the femur mid-diaphysis, 0.25 mm thick. ScanCo Medical, MicroCT 20 Scanner (15 micron resolution, 9 microns per slice, 28 slices).

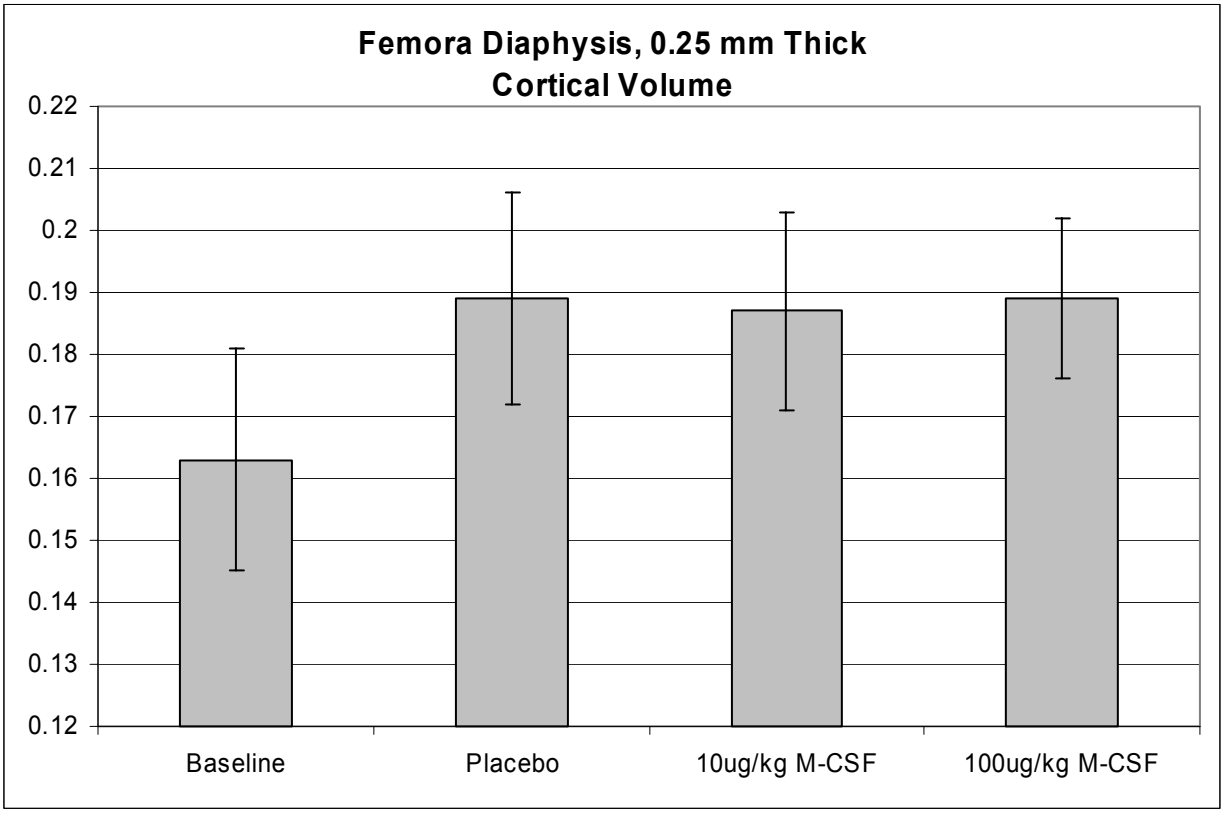

Figure 2. MicroCT scan of Total/Bone Volume (mm^2) of cortical bone in the femur, 0.252mm thick. No significant differences were observed between groups.

DISCUSSION

Previous studies with op/op mice showed increased osteoclasts and macrophages, thus proving that M-CSF is a potent growth and differentiation factor for cells of the mononuclear phagocyte lineage. Discrepancies between the recoveries of osteoclasts and macrophages with respect to locations and dose responsiveness on the op/op mice was reported (Sundquist, Jackson et al. 1995), these suggest different regional sensitivities of these cells and their precursors to M-CSF for survival and differentiation. For this study, low-dose M-CSF administration had no significant on cortical bone, as observed in other studies (Hermann 2000; Abboud, Ghosh-Choudhury et al. 2003). It is important to note that M-CSF administration may have an anabolic effect on cortical bone, but not trabecular. This difference was observed for mice over-expressing M-CSF (but not examined for our previous study administering M-CSF daily) (Hermann 2000; Abboud, Ghosh-Choudhury et al. 2003). But it has been reported in previous study that increased cortical thickness and bone mineral density were showed with high level of M-CSF expression and long period of time [7], this may indicate that higher doses and longer period of administration time may be necessary to induce noticeable effects in cortical bone.

CONCLUSIONS

Daily administration of 10μg/kg and 100μg/kg M-CSF in mice produces no functional changes in cortical bone properties. It is hypothesized that high doses (effectively flooding M-CSF receptors), and potentially longer period of administration, is needed to demonstrate the anabolic effect of M-CSF.

ACKNOWLEDGMENTS

The authors acknowledge the support of NASA cooperative agreement (NCC8-242) and Chiron Corporation (Emeryville, CA) for providing the human recombinant macrophage colony-stimulating factor.

REFERENCES

[1] R. Felix, J. Halasy-Nagy, A. Wetterwald, M. G. Cecchini, H. Fleisch, and W. Hofstetter, "Synthesis of membrane- and matrix-bound colony-stimulating factor-1 by cultured osteoblasts," *J Cell Physiol*, vol. 166, pp. 311-22, 1996.

[2] H. Kodama, M. Nose, S. Niida, and A. Yamasaki, "Essential role of macrophage colony-stimulating factor in the osteoclast differentiation supported by stromal cells," *J Exp Med*, vol. 173, pp. 1291-4, 1991.

[3] P. Fixe and V. Praloran, "Macrophage colony-stimulating-factor (M-CSF or CSF-1) and its receptor: structure-function relationships," *Eur Cytokine Netw*, vol. 8, pp. 125-36, 1997.

[4] V. A. Corboz, M. G. Cecchini, R. Felix, H. Fleisch, G. van der Pluijm, and C. W. Lowik, "Effect of macrophage colony-stimulating factor on in vitro osteoclast generation and bone resorption," *Endocrinology*, vol. 130, pp. 437-42, 1992.

[5] U. Sarma and A. M. Flanagan, "Macrophage colony-stimulating factor induces substantial osteoclast generation and bone resorption in human bone marrow cultures," *Blood*, vol. 88, pp. 2531-40, 1996.

[6] K. T. Sundquist, M. E. Jackson, D. C. Hermey, and S. C. Marks, Jr., "Osteoblasts from the toothless (osteopetrotic) mutation in the rat are unable to direct bone resorption by normal osteoclasts in response to 1,25-dihydroxyvitamin D," *Tissue Cell*, vol. 27, pp. 569-74, 1995.

[7] S. L. Abboud, K. Woodruff, C. Liu, V. Shen, and N. Ghosh-Choudhury, "Rescue of the osteopetrotic defect in op/op mice by osteoblast-specific targeting of soluble colony-stimulating factor-1," *Endocrinology*, vol. 143, pp. 1942-9, 2002.

[8] H. Kodama, A. Yamasaki, M. Nose, S. Niida, Y. Ohgame, M. Abe, M. Kumegawa, and T. Suda, "Congenital osteoclast deficiency in osteopetrotic (op/op) mice is cured by injections of macrophage colony-stimulating factor," *J Exp Med*, vol. 173, pp. 269-72, 1991.

[9] S. L. Abboud, N. Ghosh-Choudhury, L. C. Liu, V. Shen, and K. Woodruff, "Osteoblast-specific targeting of soluble colony-stimulating factor-1 increases cortical bone thickness in mice," *J Bone Miner Res*, vol. 18, pp. 1386-94, 2003.

[10] L. Hermann, Ferguson, VL, Bateman, TA, Simske, SJ, "Combined treatment effects of IGF-I and M-CSF on mouse bone composition, mechanical properties and quantitative histomorphometry.," *J Bone Miner Res*, vol. 15Sup, pp. S369, 2000.

[11] T. A. Bateman, C. R. Dunstan, D. L. Lacey, V. L. Ferguson, R. A. Ayers, and S. J. Simske, "Osteoprotegrin ameliorates sciatic nerve crush induced bone loss," *in press for J. Orthopaedic Research*, 2000.

[12] T. A. Bateman, D. L. Lacey, V. L. Ferguson, C. R. Dunstan, R. A. Ayers, and S. J. Simske, "Comparison of osteoprotegerin, pamidronate and ibandronate in the treatment of suspension disuse osteopenia.," *Journal of Bone and Mineral Research*, vol. 14, pp. S528-S528, 1999.

[13] T. T. Andreassen, C. Ejersted, and H. Oxlund, "Intermittent parathyroid hormone (1-34) treatment increases callus formation and mechanical strength of healing rat fractures," *J Bone Miner Res*, vol. 14, pp. 960-8, 1999.